

University of South Bohemia in České Budějovice  
Faculty of Science



**Kinetic behavior of  
the NAD(P)H: Quinone oxidoreductase WrbA  
from *Escherichia coli*.**

Ph.D. Thesis

**Mgr. Iryna Kishko**

**Supervisor: Assoc. Prof. RNDr. Rüdiger H. Ettrich, PhD**

**Co-supervisor: Professor Jannette Carey**

Institute of Nanobiology and Structural Biology, Global Change Research Center  
Academy of Sciences of the Czech Republic  
Zámek 136, 373 33 Nové Hradky

České Budějovice 2012

This thesis should be cited as: Kishko, I. 2012 Kinetic behavior of the NAD(P)H: Quinone oxidoreductase WrbA from *Escherichia coli*. Ph.D. Thesis. University of South Bohemia, Faculty of Science, School of Doctoral Studies in Biological Sciences, České Budějovice, Czech Republic, 115 pp.

### **Annotation**

This Ph.D. thesis addresses the structure-function relationship of the multimeric oxidoreductase WrbA with the principal aim being the explanation of the unusual kinetics of this enzyme in molecular terms, and thus getting an insight about its physiological role in bacteria.

WrbA is a multimeric enzyme with FMN as a co-factor, catalyzing the oxidation of NADH by a two electrons transfer. Structure and function analysis of WrbA places this enzyme between bacterial flavodoxins and eukaryotic oxidoreductases in terms of its evolutionary relationship. The kinetic activity of WrbA was studied under varying conditions such as temperature, pH etc, and its kinetic mechanism was evaluated from parameters  $K_M$  and  $V_{max}$  and confirmed by product inhibition pattern experiments. Crystallization and proteolytic experiments also underpin the functional importance of the multimeric nature of WrbA and aid the understanding of the physiological role of this enzyme in molecular terms.

### **Declaration [in Czech]**

Prohlašuji, že svoji disertační práci jsem vypracoval samostatně pouze s použitím pramenů a literatury uvedených v seznamu citované literatury.

Prohlašuji, že v souladu s § 47b zákona č. 111/1998 Sb. v platném znění souhlasím se zveřejněním své disertační práce, a to v úpravě vzniklé vypuštěním vyznačených částí archivovaných Přírodovědeckou fakultou elektronickou cestou ve veřejně přístupné části databáze STAG provozované Jihočeskou univerzitou v Českých Budějovicích na jejích internetových stránkách, a to se zachováním mého autorského práva k odevzdanému textu této kvalifikační práce. Souhlasím dále s tím, aby toutéž elektronickou cestou byly v souladu s uvedeným ustanovením zákona č. 111/1998 Sb. zveřejněny posudky školitele a oponentů práce i záznam o průběhu a výsledku obhajoby kvalifikační práce. Rovněž souhlasím s porovnáním textu mé kvalifikační práce s databází kvalifikačních prací Theses.cz provozovanou Národním registrem vysokoškolských kvalifikačních prací a systémem na odhalování plagiátů.

České Budějovice,

.....  
Iryna Kishko

This thesis originated from a partnership of Faculty of Science, University of South Bohemia, and Institute of Nanobiology and Structural Biology, Global Change Research Center, Academy of Sciences of the Czech Republic, supporting doctoral studies in the Biophysics study program.



### **Financial support**

This research was supported from the Ministry of Education, Youth and Sports of the Czech Republic (MSM6007665808, Aktion 64p1), Academy of Sciences of the Czech Republic (AVOZ60870520), Grant Agency of the Czech Republic (P207/10/1934 to R.E.), and joint Czech - US National Science Foundation International Research Cooperation (OISE08-53423 to J.C., and ME09016 to R.E.). Additionally, I.K. was supported by the University of South Bohemia, Grant GAJU 170/2010/P and Grant GAJU 079/2008/P.

*The most exciting phrase to hear in science, the one that heralds new discoveries, is not 'Eureka!' but 'That's funny...'*

*Isaac Asimov*

## **Acknowledgements**

It would not have been possible to write this doctoral thesis without the help and support of the kind people around me, to only some of whom it is possible to give particular mention here.

This thesis would not have been possible without the help and support of my principal supervisor Assoc. Prof. Rudiger H. Ettrich, Ph.D. The good advice, support and friendship of my second supervisor, Prof. Jannette Carey, has been invaluable in both an academic and personal level, for which I am extremely grateful.

I would like to express my deepest gratitude to Dr. Ivana Kuta-Smatanova for support, caring, patience and providing me with excellent atmosphere for doing crystallization research.

I am also indebted to the students I had pleasure to work with. They have been an invaluable support day in, day out, during all these years. Special thanks to Natallia Kulik, Martin Lukes, Jan Urban, Jaroslava Kohoutova, Vitali Bialevich, Katsiaryna Shamaeva, Alina Kevorkova, Mikalai Lapkouski, Žofie Sovová, Tereza Machalova-Lukesova and many others.

I would also like to give a heartfelt, special thanks to my friends in Nove Hradý: Monika Princova, her parents and her grandmother, Jana and Jaroslav Prinzovy and their family, Jaromir and Zanita Cadovy, Ivana Kalatova, Karel Morong, Eva Talirova, Radek Dedina and many many others. Thank them for their encouragement, support and most of all their humor.

In addition, I would like to thank to my friends from Penzion Kamínek, Zdenek Malinka and Hanka Homrova. This thesis never would have been finished without their support, advice, humor and patience. Thank them for a chance to be not only an employee, but a good friend.

Of course no acknowledgements would be complete without thanks to my parents. Both have instilled many admirable qualities in me and given me a good foundation with which to meet life. They've taught me about hard work and self-respect, about

persistence and about how to be independent. They were a great role model of resilience, strength and character. Both have always expressed how proud they are of me and how much they love me. I am proud of them and love them very much. I am grateful for them both and for the “smart genes” they passed on to me.

Last, but certainly not least, I would like to give my deepest thanks to my grandmother, my cousin Sergej, my brother Dimka, his wife Nadya and their daughter Dianka. Their love and patience helped me in my hardest moments. There are no words that can express my gratitude and appreciation for all my family have done and been for me.

### List of papers and author's contribution

The thesis is based on the following papers (listed chronologically):

- **Kishko, I.**, Harish, B., Zayats, V., Reha, D., Tenner, B., Beri, D., Gustavsson, T., Ettrich, R., Carey, J. (2012) Biphasic kinetic behavior of E. coli WrbA an FMN-dependent NAD(P)H:quinone oxidoreductase. In: *PLoS One*. 7(8): e43902. (<http://dx.plos.org/10.1371/journal.pone.0043902>) (IF = 4.09).
- Kishko I, Lapkouski M, Brynda J, Kutty M, Carey J, Kuta Smatanova I, Ettrich R. (2012) Crystallization and diffraction analysis of E.coli WrbA holoprotein with 1.2 Å resolution. *prepared for submission to ACTA CRYST D* (IF = 12.62)

I hereby declare as the senior and corresponding author of the above mentioned papers, that author of this Ph.D. thesis, Iryna Kishko, is the first author of two papers and contributed substantially to these. She carried out most of the experimental work, which included the kinetic activity measurements, sample preparations, protein purification, data assembly, statistical analysis, protein crystallization and participated in writing the manuscript.

On behalf of the co-authors, the above-mentioned declaration was confirmed by:

Assoc. Prof. Rudiger H. Ettrich, Ph.D.

supervisor and co-author of all papers .....

## ABBREVIATIONS

EDTA	Ethylenediaminetetraacetic acid
3D	three dimensional
WrbA	tryptophan repressor-binding protein A
apoWrbA	unliganded form of WrbA
holoWrbA	WrbA in complex with co-factor
TrpR	tryptophan repressor
kDa	kilodalton
DNA	deoxyribonucleic acid
FAD	flavin adenine dinucleotide
FMN	flavin mononucleotide
NAD(P)H	nicotinamide adenine dinucleotide (phosphate) reduced
Nqo	NAD(P)H:quinone oxidoreductase
Nqo1	mammalian NAD(P)H:quinone oxidoreductase
PDB	Protein Data Bank
PDB ID	the Protein Data Bank identification code
NMR	nuclear magnetic resonance
X-ray	Röntgen radiation
R-factor	factor of reliability
MR	molecular replacement
pH	potential of hydrogen
Tris-HCl	2-Amino-2-hydroxymethyl-propane-1,3-diol
Gly	glycine
His	histidine
Thr	threonine
BSA	bovine serum albumin
NAD(P) <sup>+</sup>	nicotinamide adenine dinucleotide (phosphate) oxidized
Acyl-CoA	acyl coenzyme A
V <sub>max</sub>	maximum velocity
K <sub>M</sub>	Michaelis constant
CD	circular dichroism
ESI-MS	electrospray ion source mass spectrometry

GuHCl	guanidine hydrochloride
BQ	1, 4-benzoquinone
AUC	analytical ultracentrifugation
SDS	sodium dodecyl sulfate
SDS-PAGE	SDS polyacrylamide gel electrophoresis
DLS	dynamic light scattering
DCPIP	2, 6 dichlorophenol-indophenol
MS	mass spectrometry
HPLC	high performance liquid chromatography
IPTG	isopropyl $\beta$ -D-1-thiogalactopyranoside
PMSF	phenylmethylsulfonyl fluoride



## CONTENTS

<b>PART I. INTRODUCTION.....</b>	<b>1</b>
<b>1. ELECTRON-TRANSFER PROTEINS.....</b>	<b>1</b>
<b>1.1. Oxidoreductases.....</b>	<b>2</b>
1.1.1. Pyridine Nucleotide-Dependent Dehydrogenases.....	3
1.1.2. Oxidases and Oxygenases.....	4
1.1.3. Flavoproteins.....	5
<b>1.2. Enzyme Kinetic Reaction Mechanism.....</b>	<b>7</b>
1.2.1. One-Substrate Enzyme-Catalyzed Reactions.....	7
1.2.2. Multi-Substrates Enzyme-Catalysed Reactions.....	9
1.2.2.1. Classification.....	9
1.2.3. Inhibition Patterns.....	10
1.2.4. Principles of Allostery.....	13
1.2.5. The Monod-Wyman-Changeux (MWC) Concerted Model.....	15
1.2.6. The Koshland-Némethy-Filmer (KNF) Sequential Model.....	16
<b>2. E.COLI FLAVOPROTEIN WRBA.....</b>	<b>18</b>
<b>2.1. The Structure of the E.Coli Protein WrbA and Its Conjectured Functions.</b>	
.....	18
<b>2.2. Structure of the WrbA Protein.....</b>	<b>19</b>
<b>3. AIMS.....</b>	<b>24</b>
<b>4. REFERENCES.....</b>	<b>26</b>
<b>PART II. METHODS.....</b>	<b>32</b>
<b>1. THEORETICAL ASPECTS.....</b>	<b>32</b>
<b>1.1. Molecular Biology Methods.....</b>	<b>32</b>
1.1.1. Electrophoresis.....	32
1.1.2. Liquid Chromatography.....	33
1.1.3. UV-visible Absorption Spectroscopy.....	33
1.1.4. Enzyme Kinetics.....	34
1.1.5. Circular Dichroism Spectroscopy.....	36

1.1.6. Limited Proteolysis.....	36
<b>1.2. Crystallization.....</b>	<b>38</b>
1.2.1. Vapor Diffusion Methods.....	39
1.2.2. Optimization Methods.....	39
1.2.3. Crystal Structure Determination.....	40
1.2.3.1. Crystallographic Data Collection.....	40
1.2.3.2. Molecular Replacement.....	41
<b>2. EXPERIMENTAL SETUP.....</b>	<b>42</b>
2.1. Expression and Purification of the WrbA.....	42
2.2. Kinetic Assays.....	43
2.3. Crystallization of the WrbA.....	44
2.3.1. Diffraction Data Collection and Processing. Structure Solution and Refinement.....	44
2.4. Proteolysis of the WrbA.....	45
2.5. MS Sequencing of the WrbA.....	46
2.6. Ligand Docking and QM/MM Binding Energies.....	47
2.7. NMR.....	48
2.8. AUC.....	48
<b>3. REFERENCES.....</b>	<b>49</b>
<b>PART III RESULTS AND DISCUSSION.....</b>	<b>53</b>
<b>1. TRANSFORMATION, EXPRESSION AND PURIFICATION OF THE WRBA.....</b>	<b>53</b>
<b>2. CRYSTALLIZATION OF WRBA PROTEIN.....</b>	<b>57</b>
2.1. Co-crystallization of HoloWrbA Protein with FMN as Cofactor with Different Substrates.....	57
2.2. Co-crystallization of HoloWrbA Protein with FAD as Cofactor with and without Presence of Different Substrates.....	59
2.3. Preliminary X- ray Diffraction Analysis of the WrbA.....	63
2.3.1. Structure Determination.....	65
2.3.2. FMN Binding.....	68
<b>3. LIMITED PROTEOLYSIS OF WRBA PROTEIN.....</b>	<b>72</b>

<b>4. KINETIC STUDY OF THE WRBA PROTEIN .....</b>	<b>77</b>
<b>4.1. Michaelis-Menten kinetics. ....</b>	<b>77</b>
<b>4.2. Dependence Activity of WrbA on the Concentration of One of the         Substrate. ....</b>	<b>79</b>
<b>4.3. Effect of Temperature on the Steady-State Kinetics. ....</b>	<b>81</b>
<b>4.4. Effect of Different Physical-Chemical Factors on the Activity Rate of         WrbA.....</b>	<b>82</b>
4.4.1. Influence of pH and Salt on the Steady-State Kinetics of WrbA.....	82
4.4.2. Effect of Different Modulators on the WrbA Protein. ....	83
<b>4.5. Kinetic Mechanism. ....</b>	<b>85</b>
<b>4.6. Stability of WrbA Protein.....</b>	<b>89</b>
4.6.1. Reactivation Temperature Inactivated Protein.....	89
4.6.2. CD-Experiments. ....	90
<b>4.7. Substrate Affinity. ....</b>	<b>90</b>
<b>4.8. FMN vs. FAD. Activity of the HoloWrbA Reconstituted with Two         Different Co-Factors. ....</b>	<b>91</b>
<b>4.9. Explanation of Two Plateau Kinetics. Allosteric Regulation of WrbA. ...</b>	<b>92</b>
<b>5. CONCLUSIONS. ....</b>	<b>95</b>
<b>6. REFERENCES. ....</b>	<b>97</b>

## PART I. INTRODUCTION.

### 1. ELECTRON-TRANSFER PROTEINS.

There are many processes in living cells catalyzed with various enzymes. Many of them catalyze oxidation-reduction processes by transferring electrons or hydrogen atoms from donor to acceptor.

A nomenclature of electron-transferring proteins by G. Palmer (NC-IUB, 1991) presents a classification of enzymes, which catalyze redox reactions in biological systems. According to this nomenclature, electron-transferring protein can be divided into:

- Flavodoxins

Proteins contain FAD and/or FMN as prosthetic groups. Flavoproteins are involved in metabolic processes; also catalyze redox reactions, one- and two-electron transport (Yatsyshyn *et al.*, 2009).

- Proteins with reducible disulfide group

Proteins contain disulfide group as a prosthetic group.

- Cytochromes

Hemoproteins contain heme as a prosthetic group. There are four main groups of cytochrome: cytochrome *a*, cytochrome *b*, cytochrome *c*, cytochrome *d*.

- Non-heme iron proteins

Iron-sulfur proteins: rubredoxins, ferredoxins and other simple iron-sulfur proteins.

- Copper proteins

Proteins contain Copper. There are Type-1, Type-2, Type-3 copper proteins, multi-copper oxidases (contain contain 1,2 and 3 types in different stoichiometry)

- Molybdenum, Nickel, Vanadium proteins

- Quinoproteins

Proteins have a pyrroloquinoline quinone or amino-acid-derived quinone as a cofactor.

- Metal-substituted metalloproteins.

All these proteins belong to one big group of enzyme called “oxidoreductases”.

### 1.1. OXIDOREDUCTASES.

Oxidoreductases are a group of enzymes, which catalyze oxidation and reduction reactions in cell by transfer of protons and electrons from an electron donor to an electron acceptor (Webb, 1992). Class “oxidoreductases” is divided into oxidases and dehydrogenases.

Oxidases use a molecule of oxygen as an acceptor of electrons or atoms of hydrogen. This type of oxidoreductases participates in aerobic metabolism. (Mosby’s Medical Dictionary, 2009)

Dehydrogenases take part in an anaerobic metabolism. Enzyme oxidizes a substrate and transfers an atom of hydrogen to  $\text{NAD}^+/\text{NADP}^+$  acceptor or a flavin coenzyme. (Mosby’s Medical Dictionary, 2009; NC-IUB, 1991)

There are several classifications of oxidoreductases based on different factors. The most common classification is based on catalytic activity of the enzyme and is called a numerical classification the Enzyme Commission number (EC number; Table I-1). A transfer of electrons and protons by electron-transfer enzymes generally is performed by coenzymes and cofactors. Oxidoreductases can be divided into few subclasses on the basis of coenzymes and cofactors they contain: Pyridine Nucleotide–Dependent Dehydrogenases, Oxidases and Oxygenases, and Flavoproteins (NC-IUB, 1991).

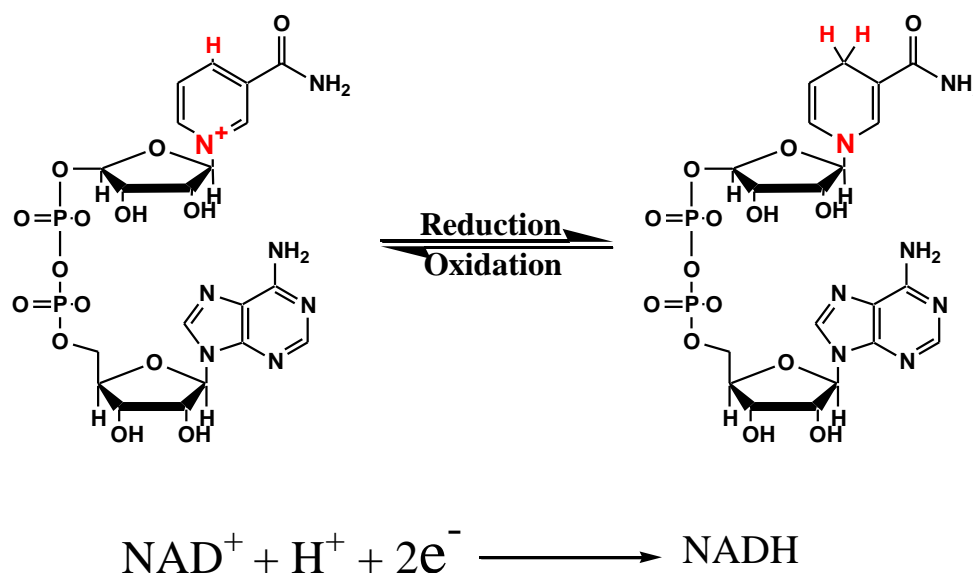
Oxidoreductases. Subclasses.	Examples
EC 1.1 Acting on the CH-OH group of donors	alcohol dehydrogenase
EC 1.2 Acting on the aldehyde or oxo group of donors	formate dehydrogenase, aldehyde dehydrogenase
EC 1.3 Acting on the CH-CH group of donors	dihydrouracil dehydrogenase dihydropyrimidine dehydrogenase
EC 1.4 Acting on the CH-NH <sub>2</sub> group of donors	alanine dehydrogenase glutamate dehydrogenase
EC 1.5 Acting on the CH-NH group of donors	dihydrofolate reductase saccharopine dehydrogenase
EC 1.6 Acting on NADH or NADPH	NAD(P)H dehydrogenase (quinone) (DT-diaphorase) NADPH—hemoprotein reductase
EC 1.7 Acting on other nitrogenous compounds as donors	nitrate reductase (NADH) acetylxindoxyl oxidase
EC 1.8 Acting on a sulfur group of donors	sulfite reductase (NADPH) dihydropolyl dehydrogenase
EC 1.9 Acting on a heme group of donors	cytochrome-c oxidase nitrate reductase (cytochrome)
EC 1.10 Acting on diphenols and related substances as donors	ubiquinol—cytochrome-c reductase catechol oxidase
EC 1.11 Acting on a peroxide as acceptor	NADH peroxidase fatty-acid peroxidase
EC 1.12 Acting on hydrogen as donor	hydrogen dehydrogenase hydrogen:quinone oxidoreductase
EC 1.13 Acting on single donors with O <sub>2</sub> as oxidant and incorporation of oxygen into the substrate (oxygenases). The oxygen incorporated need not be derived from O <sub>2</sub>	Lipoxygenase sulfur dioxygenase
EC 1.14 Acting on paired donors, with O <sub>2</sub> as oxidant and incorporation or reduction of oxygen. The oxygen incorporated need not be derived from O <sub>2</sub>	$\gamma$ -butyrobetaine dioxygenase procollagen-proline dioxygenase
EC 1.15 Acting on superoxide as acceptor	superoxide reductase superoxide dismutase
EC 1.16 Oxidizing metal ions	aquacobalamin reductase ferroxidase
EC 1.17 Acting on CH or CH <sub>2</sub> groups	leucoanthocyanidin reductase xanthine dehydrogenase
EC 1.18 Acting on iron-sulfur proteins as donors	rubredoxin—NAD <sup>+</sup> reductase ferredoxin—NADP <sup>+</sup> reductase
EC 1.19 Acting on reduced flavodoxin as donor	nitrogenase (flavodoxin)
EC 1.20 Acting on phosphorus or arsenic in donors	phosphonate dehydrogenase mycoredoxin
EC 1.21 Acting on X-H and Y-H to form an X-Y bond	columbamine oxidase aureusidin synthase
EC 1.22 Acting on halogen in donors	iodotyrosine deiodinase
EC 1.97 Other oxidoreductases	chlorate reductase sulfur reductase

**Table I-1.** Table presents the numerical classification the Enzyme Commission number (EC number) based on cofactors and coenzymes enzyme contains. (According to Webb, 1992)

### 1.1.1. Pyridine Nucleotide-Dependent Dehydrogenases.

Pyridine nucleotide-dependent dehydrogenases are a class of redox active proteins with nicotinamid adenine dinucleotide (NAD) or nicotinamid adeninedinucleotid phosphate (NADP) as a coenzyme (Frey & Hegeman, 2007).

In metabolism, enzyme oxidizes the substrate and reduces NAD by transfer of the hydrogen to a nicotinamid ring (Scheme I-1).



**Scheme I-1.** Scheme of a redox reaction of nicotinamide adenine dinucleotide.

Structurally, NADP differs from NAD by the presence of additional phosphate group in the structure, but functionally, these coenzymes play different roles in metabolism.

NAD-dependent dehydrogenases are involved in oxidation processes in mitochondria: beta-oxidation, glycolysis and the citric acid cycle (Frey & Hegeman, 2007; Pollak *et al.*, 2007; Bakker *et al.*, 2001; Heineke *et al.*, 1991).

NADP-dependent dehydrogenases participates in lipid and nucleic acid synthesis. A reduced form of NADP-dependent dehydrogenase is a source of energy and hydrogen. It transfers hydrogen to flavin enzymes (Foster & Moat, 1980).

Most of the pyridine nucleotide dehydrogenases catalyze reactions with two substrates and two products (Hanukoglu & Rapoport, 1995).

### 1.1.2. Oxidases and Oxygenases.

Oxidases and oxygenases are enzymes that catalyze redox reactions involving molecular oxygen. Oxidases use molecular oxygen as an electron acceptor and reduce it to either water or hydrogen peroxide. Most of oxidases have FMN or FAD as cofactor. Flavoprotein oxidases catalyze redox reactions with two substrates where one is an electron donor and the second one – oxygen – as an electron acceptor (Scheme I-2.).



**Scheme I-2.** Scheme of a redox reaction catalyzed by flavoprotein oxidase (E-FAD); S is a substrate, P is a product.

In catalytic reactions oxidases majorly work by a ping-pong or a ternary complex mechanisms (Schulz, 1994).

Oxidases are involved in mitochondrial electron transfer chain and in dehydrogenation of fatty acyl-CoA in peroxisomes.

Oxygenases are redox active proteins that oxidize a substrate by transferring one or two atoms of oxygen to it. Oxygenases can be divided into two subclasses: monooxygenases and dioxygenases (van Berkel, 1999).

Monooxygenases catalyze oxidation reaction using only one atom of oxygen transferred to substrate. One atom of oxygen oxidizes substrate and the other atom of oxygen reduces to water. Usually NAD(P)H is a donor of electrons (Scheme I-3.). The monooxygenases play important role in drug metabolism in liver. These enzymes participate in oxidative stress defence. (van Berkel, 1991; van Berkel, 1999; Ziegler, 1993).



**Scheme I-3.** Scheme of a redox reaction is catalyzed by flavin-containing monooxygenase (E-FAD); S is a substrate.

Dioxygenases catalyze oxidation reactions with the insertion of two oxygen atoms in product by oxidative cleavage of double bonds. Dioxygenases are involved in the oxidation of fatty acids, tryptophan and cysteine, etc. One of the main functions of dioxygenases is degradation of aromatic compounds by means of aromatic rings cleavage (Frey & Hegeman, 2007; Schulz, 1994).

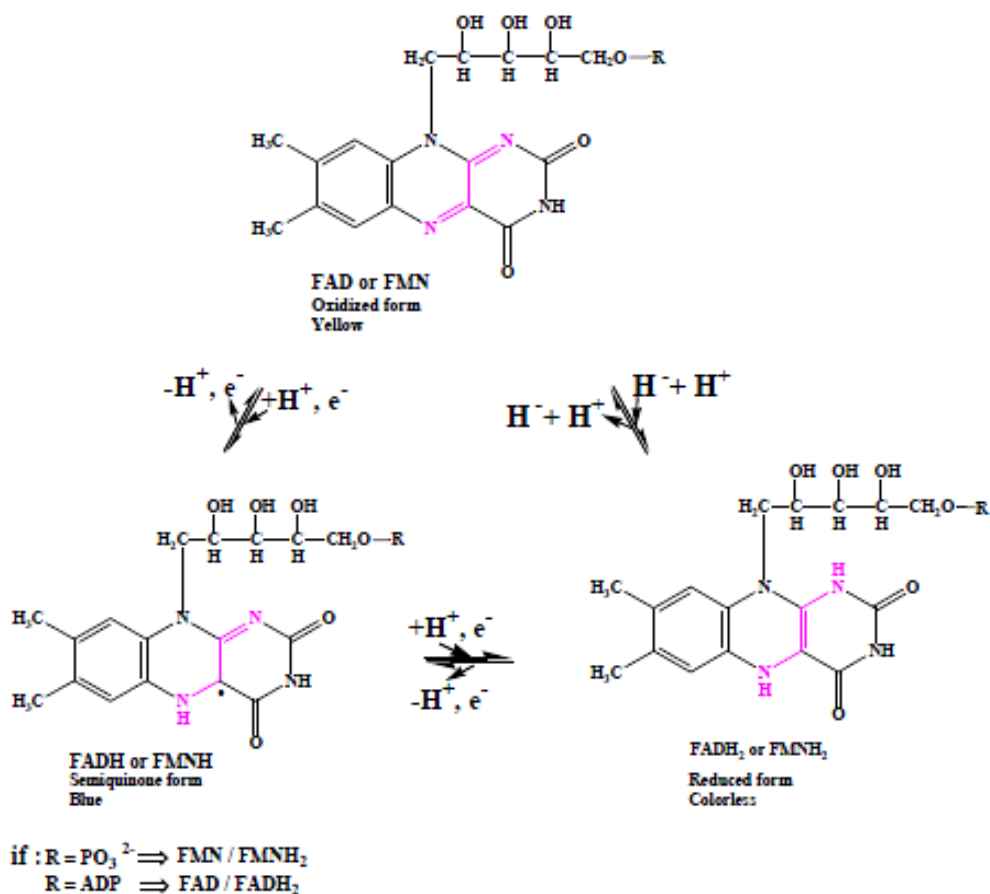
### 1.1.3. Flavoproteins.

Flavoproteins is a group of enzymes containing flavin nucleotide (flavin adenine dinucleotide (FAD) or flavin mononucleotide (FMN) as redox cofactors. Flavoenzymes participate in a number of biological processes such as bioluminescence, cell defense against oxidative stress, photosynthesis, DNA repair,



apoptosis, oxidative degradation of pyruvate, fatty acids and amino acids, and electron transport processes (Broderick, 1999; Massey, 1995; Karplus *et al.*, 1995).

Flavin molecules can exist in different redox states: oxidized, one-electron reduced (semiquinone) and two-electron reduced states (Fig. I-1.). This property of flavins allows flavoenzymes to participate in many biological redox reactions by either one-electron or two-electron transfer mechanism (Frey & Hegeman, 2007).



**Figure I-1.** Structure of a flavin coenzymes. Different redox states of flavins.

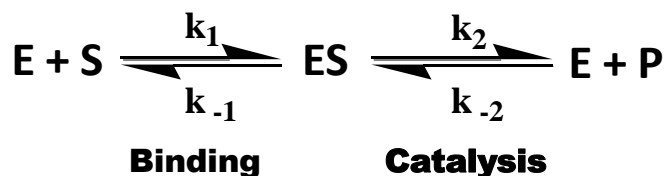
Flavoproteins present in both prokaryotic and eukaryotic organisms (e.g. bacterial FMN-dependent flavodoxins, mammalian FAD-dependent oxidoreductases; Boyer, 1976).

## 1.2. ENZYME KINETIC REACTION MECHANISM.

Enzyme kinetics studies the reaction rates of enzyme-catalyzed reactions and how the rates are affected by changes in experimental conditions. Michaelis-Menten kinetic parameters  $K_m$  and  $V_{max}$  can be used for characterization an enzymatic reaction. These parameters describe specificity and affinity of substrates for the enzyme, velocity of the reaction (Frey & Hegeman, 2007). In other words, enzyme kinetics helps to understand kinetic properties of particular enzyme, reaction mechanism and enzyme specificities.

### 1.2.1. One-Substrate Enzyme-Catalyzed Reactions.

The simplest model of enzymatic reaction is a one-substrate reaction (Scheme I-3.). The mechanism of one-substrate reaction includes the binding of the substrate (S) to the enzyme (E) and formation of enzyme-substrate complex (ES) which then reacts to give a product (P) and free enzyme (E).



**Scheme I-3.** Single-substrate reaction. E- enzyme, S-substrate, ES- enzyme-substrate complex, P- product,  $k_1$ ,  $k_2$  and  $k_{-1}$ ,  $k_{-2}$  are the rate constants. The Michaelis-Menten model for enzyme kinetics includes two reactions: the substrate binds to enzyme (Binding) and the substrate is converted to a product (Catalysis)

The result of the enzyme-catalyzed reaction is a forming of a product. An amount of a product formed per unit of time is called a velocity of the reaction or a reaction rate. Velocity of the reaction changes with the substrate concentration within time. Initial velocity or initial rate is the rate of the reaction at the very beginning of reaction, when time changes and the amount of utilized substrate is negligible yet. The Michaelis-Menten model describes a single-substrate enzyme reaction by equation that shows how the initial rate of this reaction,  $V_0$ , depends on the substrate concentration, [S]:

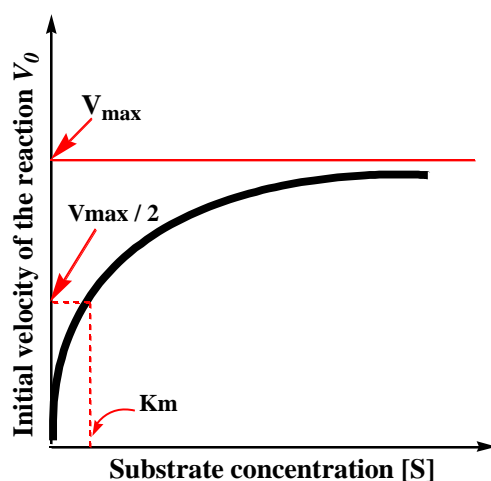
$$V_0 = \frac{V_{max} [S]}{K_m + [S]}$$

Where  $V_0$  is an initial rate of this reaction,  $V_{\max}$  is a maximal velocity of the reaction and  $K_m$  is a Michaelis constant, which corresponds to the affinity of enzyme for the substrate (Frey & Hegeman, 2007).

The Michaelis-Menten equation was derived by making several assumptions:

- The binding is fast, that allows reaction to reach equilibrium ratios of  $[E]$ ,  $[S]$ , and  $[ES]$  quickly. And the catalytic step is slower, and thus rate-limiting.
- At early time points, where initial velocity ( $V_0$ ) is measured,  $[P] = 0$ .
- $ES$  immediately comes to steady state, so  $[ES]$  is constant.
- $[S] \gg [E_{\text{total}}]$ , so the amount of Substrate molecules that binds to Enzyme and forms  $ES$ -complex is negligible, thus  $[S]$  is constant at early time points.
- The enzyme exists only in two forms: free ( $E$ ), and substrate-bounded ( $ES$ ). Thus, the total enzyme concentration ( $E_{\text{total}}$ ) is the sum of the free and substrate-bounded concentrations:  $[E_{\text{total}}] = [E] + [ES]$

Figure I-2. presents the Michaelis-Menten plot that demonstrates how the initial velocity is increasing hyperbolically with the substrate concentration and approaches  $V_{\max}$  (Dixon & Webb, 1958).



**Figure I-2.** Michaelis-Menten saturation curve.  $K_m$  is a Michaelis constant.  $V_{\max}$  is a maximum velocity of the reaction.

$V_{\max}$  or maximum velocity of the reaction reaches when all enzyme molecules are bound to the substrate.  $K_m$  (Michaelis constant) is a substrate concentration is

needed to attain the half of the maximum velocity of the reaction or, in other words, it is the substrate concentration necessary for efficient catalysis to occur.

### **1.2.2. Multi-Substrates Enzyme-Catalyzed Reactions.**

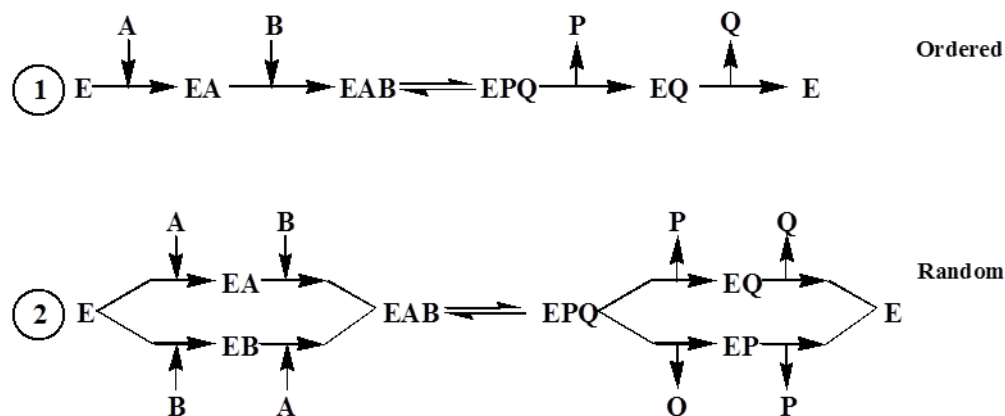
Many enzymes use two or more substrates in the reactions (e.g. oxidoreductases, transferases etc.). The kinetic analysis for this type of reactions is more complicated than the Michaelis-Menten kinetics and demands study of initial velocity for each substrate. Cleland classified the multi-substrate reactions to simplify kinetic mechanism analysis (Frey & Hegeman, 2007; Cleland, 1963).

#### **1.2.2.1. Classification.**

According to Cleland, 1963 bi-substrate reaction is a reaction between an enzyme (E) and two substrates A and B with forming of two products P and Q respectively. Characterization of the kinetic mechanism could be achieved by measuring the initial rate of the two-substrate enzymatic reaction for each substrate at several concentrations with fixed concentration of the second substrate. Thus, the two-substrate reaction can be described as a simple half-reaction.

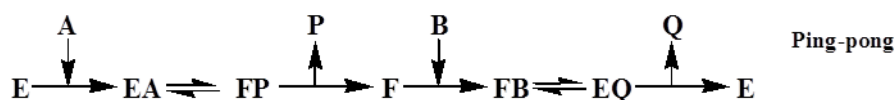
The kinetic mechanism of two-substrate reactions can be divided into two different types either a sequential or ping-pong.

The enzyme kinetic mechanism calls a sequential when the enzyme forms a complex with both of the substrates in the reaction. Sequential mechanism can be either ordered or random. Ordered binding mechanism means that substrates bind to enzyme in an obligatory order. A reaction is working by random binding mechanism if the substrates are bound to enzyme in a random order (Scheme I-4.).

**Sequential kinetic mechanism:**

**Scheme I-4.** Schemes of sequential ordered and sequential random kinetic mechanisms. E is an enzyme, A, B are substrates, P, Q are products.

In case of a ping-pong kinetic mechanism (Scheme I-5.), enzyme forms complex with one of the substrates (A), reacts with the substrate (changing of the redox status and/ or conformation) and produces the first product (P). Then the enzyme is able to react with the second substrate (B) producing of the second product (Q).



**Scheme I-5.** Scheme of ping-pong kinetic mechanism. E, F are the two forms of the enzyme, A, B are substrates, P, Q are products.

### 1.2.3. Inhibition Patterns.

Usually the study of inhibition patterns is using for characterization of a kinetic mechanism of the enzyme-catalyzed reactions. There are several compounds which can play role of an inhibitor in reaction. First of all, one of the products of the reaction can be an inhibitor, if it binds an enzyme as a substrate for reverse reaction. Also compounds, which are similar to substrate or product but are not able to react with this enzyme, can inhibit the reaction by occupying the active site of the enzyme (Frey & Hegeman, 2007; Schulz, 1994).

Inhibition analysis can be studied by measuring of the initial rate of reaction at different concentrations of the substrate at fixed concentration of the inhibitor. Usually it is enough to study several concentrations of inhibitor to get complete

information about inhibition mechanism. A type of inhibition mechanism depends on a concentration of inhibitor, which affects the reaction rate (Schulz, 1994).

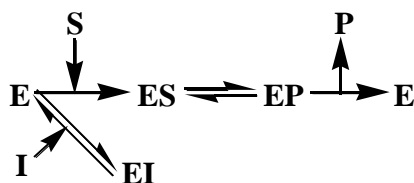
There are two types of inhibition kinetics: reversible (competitive, uncompetitive mixed, noncompetitive) and irreversible (suicide inactivators).

Irreversible inhibition mechanism:

- Suicide inactivator binds to the enzyme irreversibly, forms irreversible inhibitor-enzyme complex and destroys functional group need for the enzyme reaction (Cleland, 1963c; Schulz, 1994).

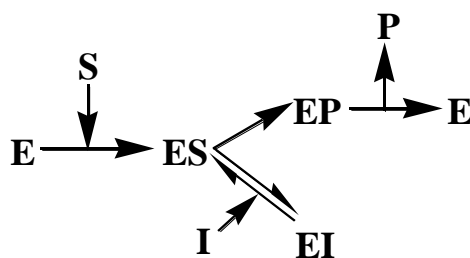
Reversible inhibition mechanism:

- Competitive inhibition (Scheme I-6.). A competitive inhibitor (substrate analog) reversibly binds to the same place as the substrate. It means that the substrate and inhibitor compete for an active site. In this type of inhibition, an inhibitor binds to free enzyme form same as a substrate and as a result, increases enzyme-dissociation constant  $K_m$  while the maximum velocity of the reaction  $V_{max}$  stays the same (Cleland, 1963c, Schulz, 1994).



**Scheme I-6.** Scheme of competitive inhibition mechanism. **E** is an enzyme, **S** is a substrate, **P** is a product, **I** is an inhibitor

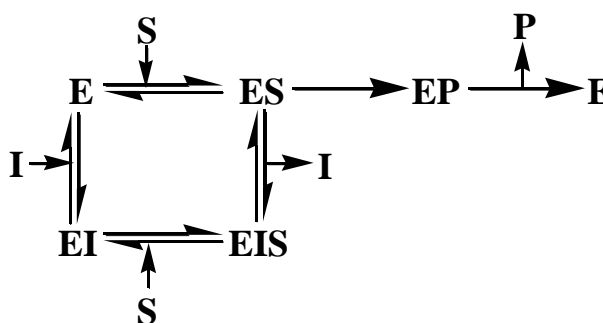
- Uncompetitive inhibition (Scheme I-7.). An uncompetitive inhibitor binds to enzyme-substrate complex, but not to a free enzyme form. This type of inhibitor does not need to be structurally similar to the substrates or the products and in this case both kinetic parameters  $K_m$  and  $V_{max}$  decrease.



**Scheme I-7.** Scheme of uncompetitive inhibition mechanism. **E** is an enzyme, **S** is a substrate, **P** is a product, **I** is an inhibitor.

- Linear mixed inhibition. An inhibitor interacts with the free enzyme form or with enzyme-substrate complex at place different to active site. This type of inhibition induces increase of  $K_m$  parameter with decrease of  $V_{max}$  parameter. The special case of mixed inhibition mechanism is a noncompetitive inhibition (Cleland, 1963c; Frey & Hegeman, 2007).

- Noncompetitive inhibition (Scheme I-8.). A noncompetitive inhibitor binds to a different place from active site and it can bind both free enzyme and enzyme-substrate complex with the same affinity. Result of this type of inhibition is a decreasing of  $V_{max}$  without any effect on a  $K_m$ .



**Scheme I-8.** Scheme of noncompetitive inhibition mechanism. **E** is an enzyme, **S** is a substrate, **P** is a product, **I** is an inhibitor.

To specify an inhibition mechanism for two-substrate reactions, it is necessary to study kinetic assays at several different concentrations of products with respect to each substrate as a variable substrate.

Kinetic mechanism	Inhibitor	Varied Substrate			
		S1		S2	
		Not saturated	Saturated with S2	Not saturated	Saturated with S1
Ordered bi-bi	P	NonC	UnC	NonC	NonC
	Q	C	C	NonC	No effect
Iso ordered bi-bi	P	NonC	UnC	NonC	NonC
	Q	NonC	NonC	NonC	UnC
Theorell chance	P	NonC	No effect	C	C
	Q	C	C	NonC	No effect
Equilibrium random bi-bi	P	C	No effect	C	No effect
	Q				
Ping-pong bi-bi	P	NonC	No effect	C	C
	Q	C	C	NonC	No effect
Iso ping-pong bi-bi	P	NonC	No effect	C	C
	Q	NonC	NonC	NonC	NonC

Bisubstrate Reaction:  $E + S1 + S2 = E + P + Q$ ;

S1, S2 – substrates of the bisubstrate reaction; P, Q – products of the bisubstrate reaction reaction;

Iso- isomerisation of the enzyme;

C – Competitive inhibition; NonC – Noncompetitive inhibition; UnC – Uncompetitive inhibition.

**Table I-2.** Product inhibition patterns in two-substrate enzymatic reaction (according to Cleland, 1963c).

Table I-2 presents the inhibition patterns for the most common reaction mechanisms of two substrate reactions.

There are several enzymes that react in two-substrate reactions and their kinetic mechanism is similar to one of common kinetic mechanism, but they have an inhibition pattern different from one is presented in table below. For example, two-site ping-pong mechanism is generally similar to classic ping-pong kinetics, but inhibition study gives an opposite result to one is shown in table. The two-site ping pong mechanism is a special case of the classic ping-pong mechanism, where donor and acceptor substrates bind to different sites and bind it independently (Cleland, 1963b).

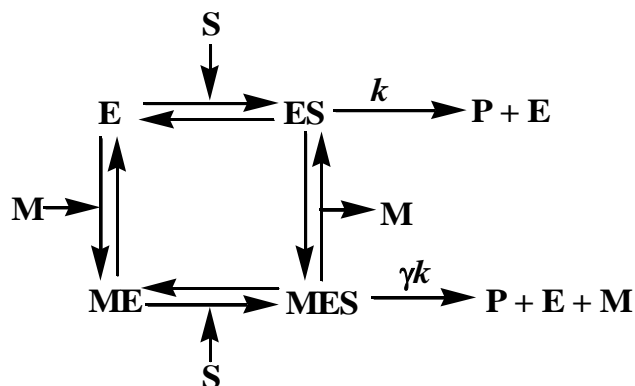
#### 1.2.4. Principles of Allostery.

Allostery is a particular ability of enzymes to change conformation between active and inactive shape under binding of allosteric effectors at place different from



active site, and, thereby, may influence the affinity of enzyme to substrates, the maximum velocity of the reaction etc (Fersht, 1999; Bisswanger, 2002).

Allosteric enzymes consist of multiple subunits and have a quaternary structure. These enzymes have an active site for substrate binding and modulatory (allosteric) site, which fits an inhibitor or an activator (Scheme I-9.; Bisswanger, 2002).



**Scheme I-9.** Schematic representation of a general mechanism for allosteric modulation of enzyme activity. E is an enzyme, M – allosteric modulator, S – substrate, P – product,  $k$  – activity rate of the reaction,  $\gamma k$  – activity rate changed by allosteric modulator.

Allosteric enzymes are inhibited by final product activated by substrate and other positive modulators and do not follow the Michaelis-Menten kinetics (Purich, 2010).

Allosteric enzymes can be regulated between very low and very high reaction rates with small changes in substrate concentration. The main role of allosteric enzymes in cell is the regulation of metabolic pathways where the concentration of cellular substrates changes in narrow concentration ranges (Marangoni, 2003; Purich, 2010).

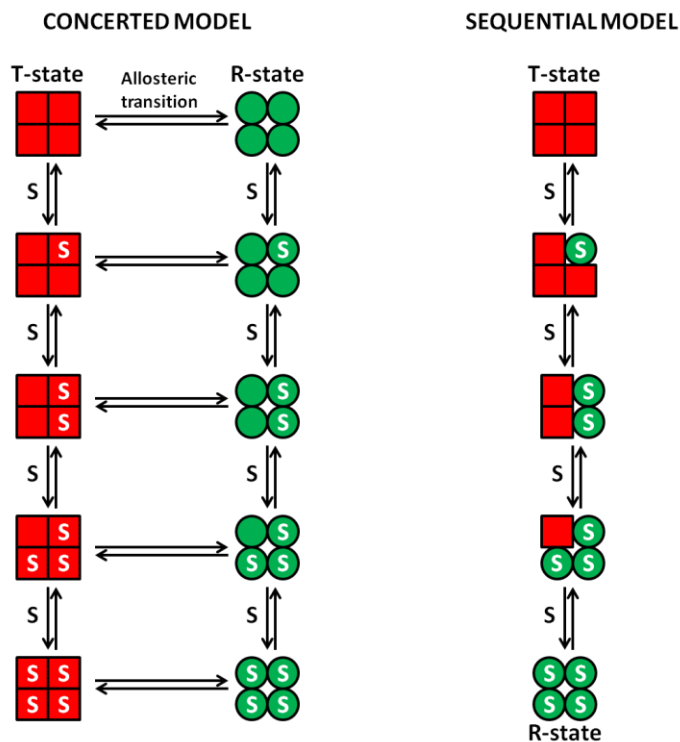
Allosteric enzymes have two conformations:

- 1. T-state (tense): less active, lower affinity to substrate, stabilized by inhibitors;
- 2. R-state (relaxed): more active, higher affinity to substrate, stabilized by substrate and activators.

Cooperativity results in a transition process from the R-state to T-state of subunits and the interaction of these subunits (quaternary structure).

To describe the allosteric transition from T-state to R-state two models can be used (Concerted, Sequential) based on different principles. Concerted model suggests that all enzyme subunits must be in same conformation: either T or R. Sequential model presupposes that the binding of substrate induces a conformational change

from the T-form to the R-form increasing the sites available to substrate (Fig. I-3.; Fersht, 1999).



**Figure I-3.** Schematic representation of concerted and sequential models of allosteric transition. S is a substrate, red squares is an inactive enzyme form, green rings is an active form of the enzyme.

### 1.2.5. The Monod-Wyman-Changeux (MWC) Concerted Model.

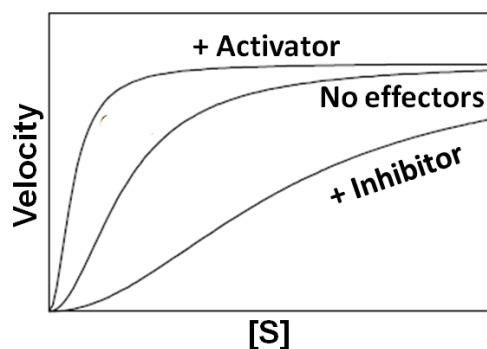
The Monod-Wyman-Changeux (MWC) is a concerted mechanism got its name from its founders: J. Monod, J. Wyman and J.-P. Changeux. This model is based on several assumptions (Bisswanger, 2002; Schulz, 1994):

1. The protein is an oligomer containing identical subunits – protomers. A protomer is a structural unit with unique binding site for each specific ligand (substrate, activator).
2. Protein assumed to exist only in two conformational states: either T (tense) or R (relaxed), which differ in their energy potential. Both of these states are in equilibrium and transition from one into the other happens spontaneously.
3. R and T enzyme forms differ in their affinity to the ligands. T-form has a lower affinity (less active state).

4. The binding affinity to ligands varies in different conformational states (R or T), but it is identical for each of the binding sites in each conformation (either R or T).

The demonstration of cooperativity (sigmoid curve) on the concentration-dependent plot is the result of MWC transition model. The cooperativity effect in the presence of allosteric effectors can be explained in the way that the first ligand (activator) binds to molecules in R-state, stabilizes the R-state and removes it from equilibrium. System directs to restoring the equilibrium, so molecules from T-state transform to R-state molecules. (Fig. I-3.) So as a result, the concentration of R-state molecules is increasing, thus the number of available binding sites is increasing faster than the ligand concentration. At the end, all molecules transform to R-state, what results in kinetic behavior the same as Michaelis-Menten. (Fig. I-4.; Schulz, 1994)

In case inhibitors came into the system, they bind to the T-state molecule and, as a result, the transition of T molecules to R becomes more difficult. (Fig. I-4.)



**Figure I-4.** Graphical demonstration of the enzyme kinetics on the concentration dependent plot for allosteric enzyme under the influence of activators and inhibitors.

A big disadvantage of this model is a limited number of intermediate states (either R or T, no mixed states) which does not correspond to a real system (Bisswanger, 2002; Marangoni, 2003; Purich, 2010).

### 1.2.6. The Koshland-Némethy-Filmer (KNF) Sequential Model.

The Koshland-Némethy-Filmer (KNF) sequential model is based on the assumption that the transition process from T-state to R-state is a sequential process thus conformational changes of the subunits start with the ligand binding (Fersht, 1999). In contrast to MWC model, the KNF uses not a quaternary conformational

change but a series of the tertiary structural changes. (Fig I-3.; Bisswanger, 2002; Schulz, 1994)

The KNF model is based on following assumptions:

1. All molecules exist in one conformational state in the system at the initial state (in the absence of ligand);
2. Ligand binds to the molecule, induces a conformational change of this subunit. This change may be diffused to neighboring free subunits due to (with aid of) subunit interfaces.

In the KNF model, subunits convert from T to R individually under positive or negative cooperativity. Ligand binds to T-subunit, converts this subunit and the one next to it to relaxed form. So the transition of molecule from T form to R form is sequential without the immediate switch from one state to another. On the concentration dependent plot this model also exhibits the sigmoid curve as one presented for MWC model. The effect of activators and inhibitors is similar to one presented for MWC. (Fig. I-4.; Schulz, 1994)

## 2. E.COLI FLAVOPROTEIN WRBA.

The 21kDa flavoprotein WrbA from *Escherichia coli* was discovered as a founding member of a new family of multimeric flavodoxin-like proteins with FMN as a physiological cofactor. WrbA is a redox active protein, which transfers a pair of electrons. *In vitro* WrbA catalyzes oxidation of NADH with benzoquinone or other quinones as an electron acceptor.

Structurally, WrbA is related to bacterial FMN-dependent flavodoxins and eukaryotic FAD dependent oxidoreductases (Nqo1) (Carey *et al.*, 2007). Structural analysis of apo- and holo- WrbA crystal structures (Wolfova *et al.*, 2007; Wolfova *et al.*, 2009) suggests a new hypothesis about evolutionary relationship within and between these two classes. The exact physiological role of the WrbA is still unclear, but available evidence is consistent with its role in cells protection against the oxidative stress (Lacour & Landini, 2004) and / or cell signaling (Bianco *et al.*, 2006).

### 2.1. THE STRUCTURE OF THE E.COLI PROTEIN WRBA AND ITS CONJECTURED FUNCTIONS.

*E. coli* WrbA got its name from its investigation as tryptophan (W)-repressor - binding protein A (Grandori & Carey, 1994). However, close studies demonstrate that the WrbA has no relationship neither with TrpR-DNA complex nor with DNA itself (Yang *et al.*, 1993). Thus, the suggestion, that the function of WrbA is related with the blocking of TrpR-specific transcriptional events, was rejected. Further investigations of WrbA conclude that the WrbA function is related to indols. Indol is a signaling molecule in cell stationary phase (Lacour & Landini, 2004). Indole acetic acid improves cell defense against the oxidative stress in *E. coli* (Bianco *et al.*, 2006). Also it has been proposed that the function of WrbA homolog from *Arabidopsis thaliana* and *Schizosaccharomyces pombe* could be related to cell signaling (Laskowski *et al.*, 2002; Daher *et al.*, 2005). However, the real physiological role is still unknown.

A closer structural analysis of WrbA demonstrates significant similarities and differences in structure and function with flavodoxins (Grandori & Carey, 1994). WrbAs are multimeric, as some flavodoxins, but with significant distinction, like the absence of known recognizable domains to function in subunit assembly. FMN is a physiological cofactor for WrbA. WrbA binds it specifically, but the affinity is lower

than demonstrated in flavodoxins (Kd in the range  $10^{-5}$  -  $10^{-6}$  M vs.  $10^{-7}$  -  $10^{-10}$  M for flavodoxins; Lacour & Landini, 2004; Lopez-Liano *et al.*, 2004).

It has been reported that the *E. coli* WrbA and its homologue from *Archeoglobus fulgidus* demonstrate FMN-dependent NAD(P)H: quinone oxidoreductase activity (Patridge & Ferry, 2006). This fact confirms the hypothesis, that WrbA could be involved in quinone detoxication (Lopez-Llano *et al.*, 2004; Patridge & Ferry, 2006; Jensen *et al.*, 2002). WrbA transfers a pair of electrons without forming flavin semiquinone similar to quinone oxidoreductases, which also transfers a pair of electrons, and in contrast to flavodoxins, which transfer a single electron (Noll *et al.*, 2006). Expression of *E.coli* WrbA is going under transcriptional control of the central regulator of the general stress response RpoS (Yang *et al.*, 1993). Upon closer investigation of the influence of stress conditions on expression of WrbA the intensification of WrbA protein expression has been demonstrated (Martinez & Kolter, 1997; Bianco *et al.*, 2006). These facts are consistent with the role of the WrbA in oxidative stress and/or cell signaling.

The mammalian NAD(P)H: quinone oxidoreductase (Nqo1) is a structural homologue of *E.coli* WrbA (Li *et al.*, 1995; PDB ID 1QRD). It is a FAD-dependent oxidoreductase (DT-diaphorase) with function related to oxidative stress defense by two-electron reduction of quinones and other electrophiles (Ernster, 1987). Two-electron reduction, which DT-diaphorase provides, wins vs. the one-electron reduction to semiquinones, because the semiquinones can be involved in oxygen-dependent redox cycles with forming of reactive oxygen forms participating in oxidative damage of macromolecules. WrbA function could be related to cell protection from reactive oxygen forms due to two-electron transfer WrbA demonstrates. Similar to Nqo1s, WrbAs can reduce a wide range of electrophilic substrates and their catalytic rates with NADH or NADPH are similar (Patridge & Ferry, 2006). Laskowski and co-workers investigated the functional and structural differences between WrbA and Nqo1s and they have proposed (Laskowski *et al.*, 2002) that the WrbA family should be renamed the FQR (FMN-dependent quinone reductase) family.

## 2.2. STRUCTURE OF THE WRBA PROTEIN.

The results of primary sequence analysis and homology-based structural modeling of the *E.coli* WrbA suggest that the *E.coli* WrbA is a founding member of a

new family of multimeric flavodoxin-like proteins. This suggestion is confirmed by similarities between *E. coli* WrbA crystal structure and crystal structures of WrbA homologues from *Deinococcus radiodurans* (shows 37% identity with *E.coli* WrbA sequence) and *Pseudomonas aeruginosa* (demonstrate 40% identity with *E. coli* WrbA sequence). Crystal structure of WrbA is tetrameric with dimers in the asymmetric units, it possess the  $\alpha/\beta$  twisted open-sheet fold, which is typical for flavodoxins (Natalello *et al.*, 2007).

A more detailed study of *E. coli* WrbA folding, oligomerization, and stability using following techniques: CD, FT-IR, and ESI-MS (Natalello *et al.*, 2007) suggested that the FMN can play important role in thermostability of WrbA monomers, which is similar to its effect on the monomeric flavodoxin from *D. desulfuricans* (Muralidhara & Wittung-Stafshede, 2004). It has been reported that the tetramers show higher thermoresistance than the monomers or dimers. Thermophilic organisms often demonstrate thermoresistance features achieved by oligomerization due to higher-order quaternary structures they have in contrast to the mesophilic organisms (Das & Gerstein, 2000). The denaturation of WrbA by heat or GuHCl results in formation of metastable partially folded intermediates with native-like secondary structure. Similar trait feature has been reported for some homologous flavodoxins (van Mierlo *et al.*, 1998; Campos *et al.*, 2004; Irun *et al.*, 2001), thus, this could be a property of twisted, open  $\alpha/\beta$  fold. It has been demonstrated for some low-affinity flavodoxins that under some conditions cofactor remains bound in the partially folded state (Higgins *et al.*, 2005; Muralidhara & Wittung-Stafshede, 2005).

Structure analysis of apo- and holoprotein WrbA from *D. radiodurans* displays no difference associated with FMN binding (Gorman & Shapiro, 2005), in contrast to results reported for *E. coli* WrbA (Natalello *et al.*, 2007). From other hand, *D. radiodurans* is a eubacterial extremophile (Hensel *et al.*, 1986) and its protein sequences demonstrate some of the adaptational characteristics typical for thermophiles (Makarova *et al.*, 2001). The crystal structure of WrbA reported for mesophilic *P. aeruginosa* (Gorman & Shapiro, 2005) presents many disordered residues on both inner and outer surfaces of monomers in the tetramer.

Structurally, *E. coli* WrbA is related to liver Nqo1 (PDB ID 1QRD; Li *et al.*, 1995). The structure-based multiple alignment for *E. coli* WrbA, Nqo1 sequences together with *D. radiodurans* WrbA, display new insights into domains and

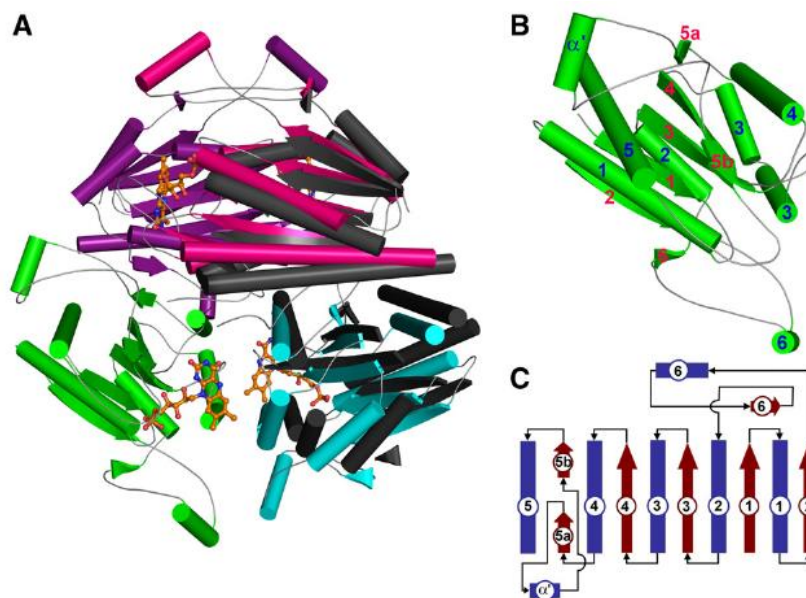
subdomain organization of these proteins. From one side, both Nqo1 and WrbAs have an inserted subdomain after the second strand of the open sheet; from the other side, Nqo1s have an additional small C-terminal domain, which is absent in WrbAs. Also WrbAs have a highly conserved for the family insertion located at the same site as poorly conserved insertion that distinguishes them from the long- and short-chain flavodoxins (Grandori & Carey, 1994; Lopez-Llano *et al.*, 2004). The results of the alignment of all three sequences demonstrates differences in the region of the  $\beta 2$  insertion. This insertion in 1QRD (Nqo1) is twice longer than in WrbA (*E. coli*), and the 1YRH (*D. radiodurans*) is intermediate in length. The insertion forms a small subdomain on a solvent-exposed surface of the dimer or tetramer in all three secondary structures. However, the tertiary structure and quaternary interactions of the insertion are different. The longer length of insertion of the 1QRD allows the subdomain to fold back on it-self. In contrast to Nqo1, WrbA insertion from each monomer is located on the surface of the second monomer. It results in creating a reciprocal connection between domain-swaps, thus reinforcing the smaller dimer-dimer contact. In 1YRH the swap augments by packing between the insertion and the main body of the fold. The swap helps tetramer to form of WrbA, and the functional significance of this swap may be forming on the protein surface a hydrophobic crevice and that leads to the active site. Nqo1 does not possess crevice similar those WrbA has. The second insertion offers the conserved sequence feature that characterizes the WrbA family. 1QRD (Noq1) has the shortest second insertion, the longest one belongs to WrbA and 1YRH presents the intermediate length of the second insertion. This insertion plays a very important functional role in WrbA since it forms an irregularly structured segment that lies above each active site. In contrary to WrbA, this segment is helical in 1YRH and placed into the subunit interface in tetramer.

In one of the resolved structures of WrbA this segment presents well-ordered residues that form one wall of the FMN-binding pocket. It completes the cavity formed by three other subunits. That could be a possible explanation why WrbA is functional as a tetramer. From the other hand, this segment obstructs substrate access to the active site from the protein surface. But in the solution, substrate may access the active site thanks to hydrophobic crevice formed by the domain-swapped helix. Alternatively ordered conformation this segment is located away from the body of the fold and packs against an adjacent dimer. This conformation may permit one or both



substrates access the active site. But both ways of access to the active site may be used in the catalytic cycle.

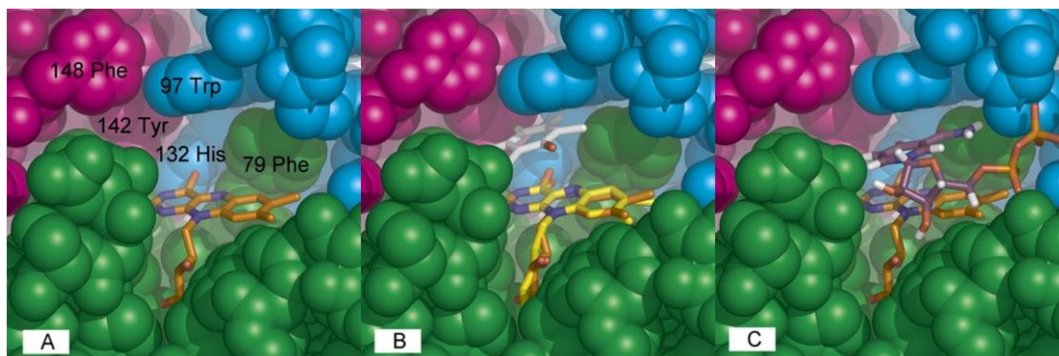
Comparison of the *E.coli* WrbA structures of apo (PDB ID 2RG1; Wolfova *et al.*, 2009) and holoWrbAs (PDB ID 2R97, PDB ID 2R96; Carey *et al.*, 2007; Wolfova *et al.*, 2005; Wolfova *et al.*, 2007; Wolfova *et al.*, 2009) displays that the WrbA tetramer is formed by two dimers in asymmetric units (Figure I-5 A).



**Figure I-5.** Structure of WrbA protein. A. Apo- and HoloWrbA tetramers. HoloWrbA subunits are green, purple, pink, and cyan; apoWrbA subunits are green, purple, light grey, and dark grey; FMN is shown as a skeletal model in atomic colors with orange carbon. B. Monomer. The viewpoint is approximately that of the green subunit of panel A, but with slight rotation to enable unobstructed labeling of secondary structure elements (helix labels, blue; strands, red). C. Topology. The central line of alternating helices (blue rectangles) and strands (red arrows) numbered 1–5 represents the main body of the flavodoxin fold, with the characteristic insertion of the WrbAs containing  $\alpha 6$  and  $\beta 6$  shown above, and the  $\beta 5$  insertion containing  $\alpha'$  below. (Picture is from Wolfova *et al.*, 2009)

The dimer of holoWrbA molecule consists of two monomers, the FMN binding site of each monomer is facing each other (Fig. I-5.). In contrast to holoWrbA, in apoWrbA area across the FMN binding site is larger, because monomers do not face each other in asymmetric unit. The location of active site in WrbA is similar to flavodoxins family with one significant difference. WrbA does not contain crevice, which is presented in flavodoxins.

The existed crystal structures of holoWrbA co-crystallized with substrates (NADH, and quinone; Andrade *et al.*,2007) demonstrate that the benzoquinone is located between izoalloxazine ring of FMN and Trp98 indol side chain in active site, what is ideal for electron transfer (Fig. I-6.; Carey *et al.*, 2007).



**Figure I-6.** Crystal structure of holoWrbA active site. **A.** FMN-binding side; **B** Quinone location in FMN-binding site; **C** NADH bound on the surface, close to FMN binding site. (Picture taken from Carey *et al.*, 2007 Protein Science. Volume 16, Issue 10, pages 2301-2305, 1 JAN 2009 DOI: 0.1110/ps.073018907. <http://onlinelibrary.wiley.com/doi/10.1110/ps.073018907/full#fig2>)

NADH position in crystal structure presented Andrade *et al.* (PDB ID 3B6J) is non-functional. Molecule of NADH is bound the protein via a single hydrogen bond far from the flavin isoalloxazine ring and transfer of electron from this position is not possible (fig. I-6.; Carey *et al.*, 2007). Presence of PEG molecules (crystallization precipitant) in binding site of crystal structure can be a reason of non-functional position of NADH because it could block NADH access to active site.

### 3. AIMS.

The WrbA flavoprotein from *Escherichia coli* is a redox active protein with FMN as a physiological cofactor. Structural analysis of apo and holo WrbA shows significant similarities of this protein to both bacterial FMN dependent flavodoxins and eukaryotic FAD dependent oxidoreductases (Nqo1; Carey *et al.*, 2007). These facts allowed to suggest a new hypothesis concerning the evolutionary position of WrbA as a link between and within these two classes.

*In vitro* WrbA catalyzes oxidation of NADH with benzoquinone or other quinones as an electron acceptor. But the physiological role of the WrbA is still unknown.

The main aim of this thesis is a detailed characterization of the kinetics of WrbA and to give an underlying molecular explanation. For this purpose we have chosen the following tasks and sub-aims:

1. To express and purify the *E. coli* protein WrbA;
2. To find optimal crystallization conditions to obtain good quality crystals for crystallography analysis;
  - Crystallization of holoWrbA with FAD as a cofactor;
  - Crystallization of holoWrbA (with FAD) with the substrates (NADH, BQ).
3. To collect and analyze the diffraction data, determine the atomic structure of the protein;
4. To carry out the limited proteolysis experiments
  - Limited proteolysis by using different proteases;
  - Range-finding experiments for apo and holoWrbA;
  - Time course digestion experiments for apo and holoWrbA;
  - MS analysis of cleaved parts of apo and holoWrbA.
5. To determine the kinetic properties of WrbA:
  - Dependence activity of *E.coli* WrbA protein on concentration of one of the substrates;
  - Influence of physical and chemical parameters (temperature, pH, salt) on WrbA properties;
  - Effect of different modulators on the kinetic properties of WrbA protein;
  - Estimation of substrates affinity (NADH, BQ);

- Evaluation of the kinetic mechanism of WrbA including inhibition patterns analysis;
6. To examine stability of WrbA (temperature inactivation/ reactivation, CD-analysis)
  7. In collaboration with the Carey group to examine the dimer-tetramer equilibrium under various conditions by NMR and analytical ultracentrifugation.
  8. To study and analyze the protein structure using computational methods and the information gained by the above mentioned experiments.

#### 4. REFERENCES.

- Andrade SL, Patridge EV, Ferry JG, Einsle O (2007) Crystal structure of the NADH:quinone oxidoreductase WrbA from *Escherichia coli*. *J Bacteriol* **189**: 9101–9107.
- Bakker B.M., Overkamp, K.M., van Maris, A.J., Kotter, P., Luttik, M.A., van Dijken, J.P., and Pronk, J.T. (2001). Stoichiometry and compartmentation of NADH metabolism in *Saccharomyces cerevisiae*. *FEMS Microbiol. Rev.* **25** (1): 15–37
- Berg JM, Tymoczko JL, Stryer L. (2007) *Biochemistry*. 6th ed. New York: WH Freeman.
- Bianco C, Imperlini E, Calogero R, Senatore B, Amoresano A, Carpentieri A, Pucci P, Defez R. (2006) Indole-3-acetic acid improves *Escherichia coli*'s defences to stress. *Arch Microbiol.* **185**: 373-82.
- Bisswanger H. (2002) *Enzyme Kinetics: Principles and Methods*. Wiley-VCH, Weinheim.
- Boyer P. D. (1976) *The Enzymes*. 3rd Ed., Vol. 13, Part C. Academic, New York.
- Broderick J. B. (1999). Catechol dioxygenases. *Essays Biochem.* **34**: 173-89.
- Campos L. A., Bueno M., Lopez-Llano J., Jimenez M. A., Sancho J. (2004) Structure of stable protein folding intermediates by equilibrium phi-analysis: the apoflavodoxin thermal intermediate. *J Mol Biol.* **344**: 239-255.
- Carey J., Brynda J., Wolfová J., Grandori R., Gustavsson T., Ettrich R., Kuta-Smatanova (2007): WrbA bridges bacterial flavodoxins and eukaryotic NAD(P)H:quinone oxidoreductases. *Protein Science* **16** (10): 2301-2305.
- Cleland, W. W. (1963a) The kinetics of enzyme-catalyzed reactions with two or more substrates or products. I. Nomenclature and rate equations. *Biochim. Biophys. Acta* **67**: 104–137
- Cleland, W. W. (1963b) The kinetics of enzyme-catalyzed reactions with two or more substrates or products. II. Inhibition: nomenclature and theory. *Biochim. Biophys. Acta* **67**: 173–187
- Cleland, W. W. (1963c) The kinetics of enzyme-catalyzed reactions with two or more substrates or products. III. Prediction of initial velocity and inhibition patterns by inspection. *Biochim. Biophys. Acta* **67**: 188–196

- Daher, B. S., E. J. Venancio, S. M. de Freitas, S. N. Bao, P. V. Vianney, R. V. Andrade, A. S. Dantas, C. M. Soares, I. Silva-Pereira, and M. S. Felipe. (2005) The highly expressed yeast gene pby20 from *Paracoccidioides brasiliensis* encodes a flavodoxin-like protein. *Fungal Genet. Biol.* **42**: 434-443.
- Das R, Gerstein M. (2000) The stability of thermophilic proteins: a study based on comprehensive genome comparison. *Funct Integr. Genomics.* **1**: 76-88.
- Dixon M., & Webb E. C. (1958) *Enzymes*. Academic Press, Inc., New York.
- Ernster, L. 1987. DT-Diaphorase: A historical review. *Chem. Scripta* **27A**: 1-13.
- Fersht A. (1999) *Structure and mechanism in protein science. A guide to enzyme catalysis and protein folding*. New York: WH Freeman.
- Foster JW, Moat AG (1980). Nicotinamide adenine dinucleotide biosynthesis and pyridine nucleotide cycle metabolism in microbial systems. *Microbiol. Rev.* **44** (1): 83–105.
- Frey P. A., Hegeman A. D. (2007) *Enzymatic Reaction Mechanisms*, Oxford University Press, Oxford.
- Gorman J, Shapiro L. (2005) Crystal structures of the tryptophan repressor binding protein WrbA and complexes with flavin mononucleotide. *Protein Sci.* **14**: 3004-12.
- Grandori R, Carey J. (1994) Six new candidate members of the alpha/beta twisted opensheet family detected by sequence similarity to flavodoxin. *Protein Sci.* **3**: 2185-93.
- Grandori R, Khalifah P, Boice JA, Fairman R, Giovanielli K, Carey J. (1998) Biochemical characterization of WrbA, founding member of a new family of multimeric flavodoxin-like proteins. *J Biol Chem.* **273**: 20960-6.
- Hanukoglu I., Rapoport R. (1995) Routes and regulation of NADPH production in steroidogenic mitochondria. *Endocrine research.* **21**(1-2):231–241
- Heineke D, Riens B, Grosse H, Hoferichter P, Peter U, Flügge UI, Heldt HW. (1991) Redox Transfer across the Inner Chloroplast Envelope Membrane. *Plant Physiol* **95** (4): 1131–1137
- Hensel R.W., Demharter O., Kandler R., Kroppenstedt M., Stackebrandt E. (1986) Chemotaxonomic and molecular-genetic studies of the genus *Thermus*: evidence for a

- phylogenetic relationship of *Thermus aquaticus* and *Thermus ruber* to the genus *Deinococcus*. *Int. J. Syst. Bacteriol.* **36**: 444–453
- Higgins C. L., Muralidhara B. K., Wittung-Stafshede P. (2005) How do cofactor modulate protein folding? *Protein Pept Lett.* **12**: 165-170.
- Irun M. P., Garsia-Mira M. M., Sanchez-Ruiz J. M., Sancho J. (2001) Native hydrogen bonds in a molten globule: apoflavodoxin thermal intermediate. *J Mol Biol* **306**: 877-888.
- Jensen Jr KA Jr, Ryan ZC, Vanden Wymelenberg A, Cullen D, Hammel KE. (2002) An NADH:quinone oxidoreductase active during biodegradation by the brown-rot basidiomycete *Gloeophyllum trabeum*. *Appl Environ Microbiol.* **68**: 2699-703.
- Karplus P. A., Fox K. M. and Massey V. (1995) Structure-function relations for old yellow enzyme. *FASEB J.* **9**: 1518-1526.
- Lacour S, Landini P. (2004) SigmaS-dependent gene expression at the onset of stationary phase in *Escherichia coli*: function of sigmaS-dependent genes and identification of their promoter sequences. *J Bacteriol.* **186**: 7186-95.
- Laskowski MJ, Dreher KA, Gehring MA, Abel S, Gensler AL, Sussex IM. (2002) FQR1, a novel primary auxin-response gene, encodes a flavin mononucleotide-binding quinone reductase. *Plant Physiol.* **128**: 578-90.
- Li R, Bianchet MA, Talalay P, Amzel LM. (1995) The three-dimensional structure of NAD(P)H:quinone reductase, a flavoprotein involved in cancer chemoprotection and chemotherapy: mechanism of the two-electron reduction. *Proc Natl Acad Sci U S A.* **92**: 8846-50.
- Lopez-Llano J, Maldonado S, Bueno M, Lostao A, Angeles-Jimenez M, Lillo MP, Sancho J. (2004) The long and short flavodoxins: I. The role of the differentiating loop in apoflavodoxin structure and FMN binding. *J Biol Chem.* **279**: 47177-83.
- Makarova KS, Aravind L, Wolf YI, Tatusov RL, Minton KW, Koonin EV, Daly MJ. (2001) Genome of the extremely radiation-resistant bacterium *Deinococcus radiodurans* viewed from the perspective of comparative genomics. *Microbiol Mol Biol Rev.* **65**: 44-79.
- Marangoni AG. (2003) *Enzyme Kinetics: a Modern Approach*. John Wiley & Sons, Ltd, Chichester

- Martinez A, Kolter R. (1997) Protection of DNA during oxidative stress by nonspecific DNA-binding protein Dps. *J. Bacteriol.* **179**: 5188- 5194
- Massey V. (1995) Introduction: flavoprotein structure and mechanism. *FASEB J* **9**:473.
- Mosby (2009) Mosby's Medical Dictionary. 8th edition. Elsevier
- Muralidhara B. K., Wittung-Stafshede P. (2004) Thermal unfolding of Apo and Holo Desulfovibrio desulfuricans flavodoxin: cofactor stabilizes folded and intermediate states. *Biochemistry.* **43**: 12855- 12864.
- Muralidhara B. K., Wittung-Stafshede P. (2005) FMN binding and unfolding of Desulfovibrio desulfuricans flavodoxin: “hidden” intermediates at low denaturant concentrations. *Biochim Biophys Acta.* **1747**: 239-250.
- Natalello A., Doglia S.M., Carey J. and Grandori R. (2007). Role of flavin mononucleotide in thermostability and oligomerization of Escherichia coli stress-defense protein WrbA. *Biochemistry.* **46**: 543-553.
- NC-IUB (Nomenclature Committee of the International Union of Biochemistry). Nomenclature of electron-transfer proteins. Recommendations 1989. (1991) *Eur J Biochem.* **200**(3):599-611
- Noll G, Kozma E, Grandori R, Carey J, Schodl T, Hauska G, Daub J. (2006) Spectroelectrochemical investigation of a flavoprotein with a flavin-modified gold electrode. *Langmuir.* **22**: 2378-83.
- Patridge EV, Ferry JG. (2006) WrbA from Escherichia coli and Archaeoglobus fulgidus is an NAD(P)H:quinone oxidoreductase. *J Bacteriol.* **188**: 3498-506.
- Pollak N., Dölle C., Ziegler M. (2007). The power to reduce: pyridine nucleotides – small molecules with a multitude of functions. *Biochem. J.* **402** (2): 205–18.
- Purich D. L. (2010). Enzyme kinetics: Catalysis & control: a reference of theory and best-practice methods. San Diego, Calif: Elsevier Academic.
- Schulz, A. R. 1994. Enzyme kinetics. From diastase to multi-enzyme systems. Cambridge: Cambridge University Press.



- van Berkel W. J. H. and Muller F. (1991) Flavin-dependent monooxygenases with special reference to p-hydroxybenzoate hydroxylase. *In Chemistry and biochemistry of flavoenzymes*, vol. 2 (Muller F., ed.), CRC Press, Boca Raton, FL, pp. 1–29.
- van Berkel W. J. H., Benen J. A. E., Eppink M. H. M., and Fraaije M. W. (1999) Flavoprotein Kinetics. p. 61-85. *In* S. K. Chapman and G. A. Reid (ed.), *Flavoprotein protocols*, vol. 131. Humana Press, Totowa, N.J.
- van Berkel W. J. H., Eppink M. H. M., van der Bolt F. J. T., Vervoort J., Rietjens I. M. C. M., and Schreuder H. A. (1997) p-Hydroxybenzoate hydroxylase: mutants and mechanism, in *Flavins and Flavoproteins XII* (Stevenson K., Massey V. and Williams C. H. Jr., eds.), University of Calgary Press, Calgary, Alberta, Canada, pp. 305–314.
- van Mierlo CP, van Dongen WM, Vergeldt F, van Berkel WJ, Steensma E. (1998) The equilibrium unfolding of *Azotobacter vinelandii* apoflavodoxin II occurs via a relatively stable folding intermediate. *Protein Sci.* 7: 2331-2344.
- Webb E. C. (1992). *Enzyme nomenclature 1992: recommendations of the Nomenclature Committee of the International Union of Biochemistry and Molecular Biology on the nomenclature and classification of enzymes*. San Diego: Published for the International Union of Biochemistry and Molecular Biology by Academic Press.
- Wolfova J, I. Kuta Smatanova, J. Brynda, J. R. Mesters, M. Lapkouski, M. Kutý, A. Natalello, N. Chatterjee, S. Chern, E. Ebbel, A. Ricci, R. Grandori, R. Ettrich & J. Carey, (2009) Structural organization of WrbA in apo- and holoprotein crystals. *Biochim. Biophys. Acta*, **1794**: 1288-1298.
- Wolfova J., Grandori R., Kozma E., Chatterjee N., Carey J., Kuta Smatanova I. (2005) Crystallization of the flavoprotein WrbA optimized by using additives and gels. *Journal of Crystal Growth* 284 (3-4), 502-505.
- Wolfova, J., Mesters, J.R., Brynda, J., Grandori, R., Natalello, A., Carey, J., Kuta Smatanova, I. (2007) Crystallization and preliminary diffraction analysis of *Escherichia coli* WrbA in complex with its cofactor flavin mononucleotide, *Acta Crystallogr., Sect. F*, F63, 571-575.
- Yang W, Ni L, Somerville RL. (1993) A stationary-phase protein of *Escherichia coli* that affects the mode of association between the trp repressor protein and operator-bearing DNA. *Proc Natl Acad Sci U S A.* 90, 5796-800.

Yatsyshyn V. Yu., Fedorovych D. V., Sibirny A. A. (2009). The microbial synthesis of flavin nucleotides: a review. *Applied Biochem. and Microbiol.*, **45** (2): 115–124.

Ziegler D. M. (1993) Recent studies on the structure and function of multisubstrate flavin-containing monooxygenases. *Annu. Rev. Pharmacol. Toxicol.* **33**, 179–199.

## **PART II. METHODS.**

### **1. THEORETICAL ASPECTS.**

#### **1.1. MOLECULAR BIOLOGY METHODS.**

To start the specific experiments with the protein we need to go through few basic steps. The first step is an expression and purification of a protein. Number of basic biochemical methods for protein expression and purification are well described in the literature (McPherson, 1999; Lorber *et al.*, 1999; Muller & Buttner, 1994; Bollag *et al.*, 1996).

During the purification process we need to control purity, homogeneity and quantity of a protein. Methods commonly used for this matter are SDS-PAGE (SDS Polyacrylamide gel electrophoresis)- to control homogeneity of the protein sample, UV-spectroscopy- to calculate the concentration of the protein, Dynamic light scattering (DLS) – characterization of a particle size, monodispersity/ aggregation.

##### **1.1.1. Electrophoresis.**

Protein Electrophoresis is a separation of protein molecules in electric field. The most widely used method is called sodium dodecyl sulfate polyacrylamide gel electrophoresis (SDS-PAGE). Important components in this method of protein separation are polyacrylamide gel as a support medium and sodium dodecyl sulfate (SDS) to denature the proteins (Shapiro *et al.*, 1967; Weber & Osborn, 1969).

SDS is an anionic detergent, which molecules have a negative charge within a wide pH range. The negative charges on SDS destroy the complex structure of proteins. Also it gives strong attraction of anode (positively-charged electrode) in electric field (Shapiro *et al.*, 1967; Weber & Osborn, 1969).

Polyacrylamide gels impede bigger molecules migrate as fast as smaller ones and the final separation of proteins is dependent on the differences in the molecular mass of polypeptides (Weber & Osborn, 1969).

Molecular mass of the protein is expressed in Daltons (Da). One Dalton is defined as 1/12 of the mass of carbon 12. Often we can meet the term Molecular weight in literature. The terms “Molecular weight” “Molecular mass” are different.

Molecular weight is defined as the ratio of the mass of a macromolecule to 1/12 the mass of a carbon 12 atom. It is a dimensionless quantity (Shapiro *et al.*, 1967).

### 1.1.2. Liquid Chromatography.

A method of a molecular separation based on a specific binding interactions between solid stationary phase, liquid mobile phase and chemical compounds is called Liquid chromatography. These specific binding interactions determine the difference between several classes of chromatography (Deutcher, 1990; Cooper, 1977)

The most common types of chromatography are:

1. Ion exchange chromatography (IEC) .Separation of the molecules based on differences in their surface charges.
2. Hydrophobic chromatography (HIC). Separation of the molecules based on the hydrophobic group on their surfaces.
3. Reversed-phase chromatography. Separation of the molecules based on differences in hydrophobicity.
4. Affinity chromatography is based on bio-specific binding interactions between a ligand bound to the chromatographic packing and a target molecule in the sample.
5. Gel filtration chromatography separates molecule on the basis of their size (Cooper, 1977; Chicz & Regnier, 1990; Colowick, 1955).

### 1.1.3. UV-visible Absorption Spectroscopy.

Different molecules absorb radiation of different wavelengths. The Beer-Lambert law is showing the linear relationship between absorbance and concentration of an absorbing solution (Cooper, 1977):

$$A = \log_{10} \frac{I_0}{I} = \epsilon cl$$

where  $I_0$  is the intensity of the incident radiation;  $I$  is the intensity of the transmitted radiation;  $\epsilon$  is the molar wavelength dependent absorption coefficient or extinction coefficient ( $M^{-1}cm^{-1}$ );  $l$  is the path length of the absorbing solution (cm);  $c$  is the concentration of the absorbing species in  $mol\ dm^{-3}$ .

In other words,  $\log_{10} (I_0/I)$  - is an absorbance at the chosen wavelength ( $A$ ). If absorbance ( $A$ ), extinction coefficient ( $\epsilon$ ) and the path length of the absorbing solution ( $l$ ) are known for a protein, the concentration can be easily calculated.

This is the most common application of UV/visible spectroscopy. The Lambert-Beer Law however is valid only for diluted solutions. The limits for its validity differ for different materials. As a general rule, one can understand that every material showing absorption of up to 0.5 - 0.6 still obeys the Lambert-Beer Law.

#### **1.1.4. Enzyme Kinetics.**

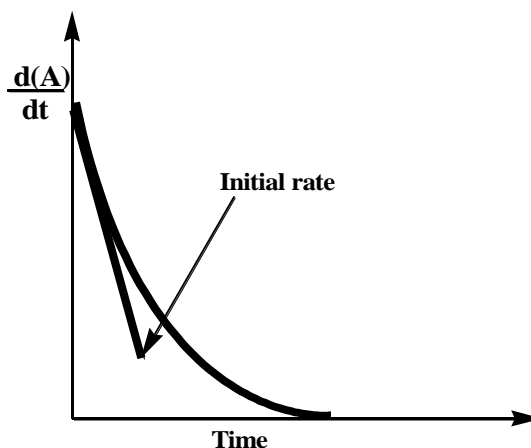
Enzyme kinetics is a study of a reaction rate of time dependent enzyme-catalyzed reaction, which helps to understand and to explain mechanism of enzyme catalysis (Frey & Hegeman, 2007).

The study of enzyme kinetics is very important. It helps to define chemical properties and functions of enzyme, best conditions for the action of catalyst, mechanism of enzyme action in chemical and molecular terms. Also could be described enzyme functions in the cell, various factors influence on enzyme activity and help understand various biological phenomena (Frey & Hegeman, 2007).

An activity rate can be determined by measuring the amount of product formed or substrate that depletes during the reaction.

The enzyme kinetics of an enzymatic reaction can be studied when the concentration of the substrate is much higher than the total enzyme concentration. In this case, the rate does not depend on the substrate concentration, and the reaction will be zero order with respect to substrate (Frey & Hegeman, 2007). Thus, the Michaelis-Menten model can be used for reaction analysis with a steady-state assumption, meaning that the concentration of the enzyme-substrate complex is constant during the reaction. The Michaelis-Menten equation and its hyperbolic graph describe dependence of the initial reaction rate on substrate concentration for one-substrate reaction. For two-substrate reaction in which initial rate is determined as a function of two variables (concentrations of two substrates) can be done analysis of the dependence of reaction rate when one is variable while the second one is constant (Stein, 2011).

Kinetic experiments describe how the rate of an enzyme-catalyzed reaction changes with the substrate concentration. The initial rate is an amount of the substrate transformed to the product over the time of reaction (Fig. II-1.). It is the slope of early linear phase of the reaction. To measure the initial velocity of a reaction, it is necessary to detect product formation or substrate depletion over time, for example, spectrophotometrically (Copeland, 2000).



**Figure II-1.** Schematic representation of disappearance of the substrate A as a function of time.

Data obtained from the measurement can be plotted and fitted to the Michaelis-Menten equation and then presented in double-reciprocal plot. A plot of dependence initial velocity on the substrate concentration is a hyperbolic curve, which is consistent with the Michaelis-Menten model. The important kinetics parameters ( $V_{\max}$  and  $K_M$ ) can be obtained from these graphs. Exact values for  $V_{\max}$  and  $K_M$  can be calculated by using a curve-fitting program (Frey & Hegeman, 2007; Schulz, 1994; Marangoni, 2003).

$K_m$  is the "kinetic activator constant" derived from rate constants which is an estimate of the dissociation constant of enzyme from substrate. So, small  $K_m$  means that the binding is tight and high  $K_m$  value means the binding is weak.  $V_{\max}$  is the theoretical maximal velocity. To reach  $V_{\max}$  all enzyme molecules have to be tightly bound with the substrate (Frey & Hegeman, 2007).

Many factors, such as enzyme concentration, temperature, pH, ionic strength, activators, inhibitors etc., have an influence enzyme activity. To have a total information about enzyme kinetics is important to study the influence of these factors. The inhibition effect on the enzyme kinetic helps to determine kinetic mechanism for two-substrate reaction (Bisswanger, 2002). Inhibition analysis is performed by measurement of a reaction rate at different concentrations of one single substrate and constant concentration of the second substrate at several inhibitor concentrations. To determine kinetic mechanism of two-substrate enzyme-catalyzed reaction, the products is used as the inhibitors for this reaction (Frey & Hegeman, 2007).

### 1.1.5. Circular Dichroism Spectroscopy.

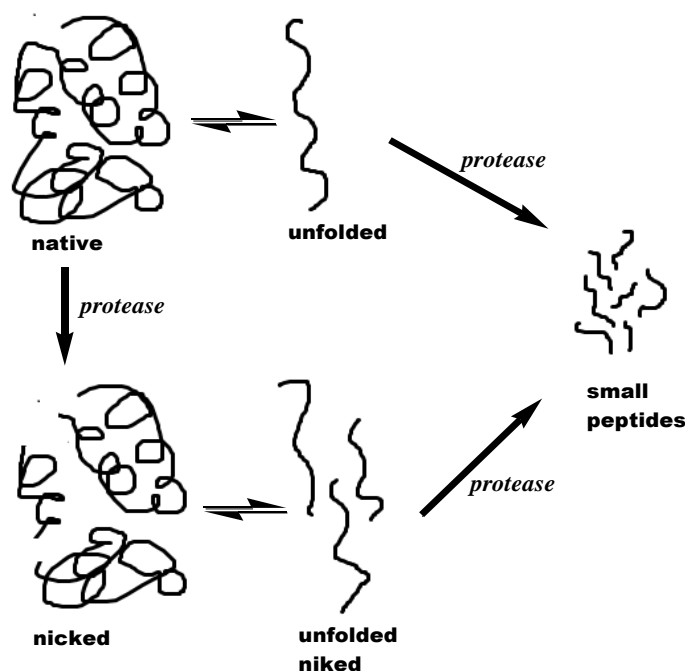
Circular dichroism spectroscopy (CD) is one of the types of light absorption spectroscopy. This method is based on measuring the difference in absorbance of right and left circularly polarized light as a function of wavelength. CD spectrum shows the dependence of CD on the wavelength  $\lambda$  and also can be presented as a difference of right and left absorbance at  $\lambda$ .

The CD spectra in the range 180-260 nm can describe different types of secondary structures, thus CD technique is often applied to proteins in solutions. Another application of the CD spectroscopy is the monitoring of conformational changes in protein structure, what can progress in many experiments (Johnson, 1990).

### 1.1.6. Limited Proteolysis.

Proteolysis is a reaction of a breaking down the protein by proteolytic enzymes partially to peptides or completely to amino acids. Limited proteolysis is a very useful tool due to protein mass spectrometry, which helps to identify stable partial proteolytic products corresponding to individual domains (Carey, 2000).

Limited proteolysis is most useful for protein fragments isolation that can fold autonomously and behave as protein domains. Moreover, the technique can be used to identify and prepare protein fragments that are able to associate into a native-like and often functional protein complex (Koth *et al.*, 2003).



**Figure II-2.** Schematic view of the mechanism of proteolysis of a globular protein.

As shown in the Scheme of Fig. II-2., native globular proteins can be cut by a protease and, in a number of cases, it has been shown that the peptide bond fission occurs only at one or a few peptide bonds.

Analysis of the proteolytic digestion of a protein usually is done with the SDS-PAGE, where we can identify cleaved parts of the protein molecule.

Proteolytic experiment includes two main basic steps:

1. Range-finding experiment is used to optimize the protease activity.
2. Time-course experiment is used to select the best digestion of the protein (Carey, 2000).

The main goal of a partial proteolysis experiment is to find one or more proteolytic sensitive regions in a protein by cutting it with proteases. These regions are sensitive to protease because they are more accessible than those folded within a domain (Gao *et al.*, 2005). For the proteolytic sensitivity studies we should compare the partial proteolytic pattern using several proteases, control the cleavage by SDS-PAGE electrophoresis, what will help to indicate and characterize the proteolytic products and to find the approximate domain borders (Hubbard, 1998; Fontana *et al.*, 1999).

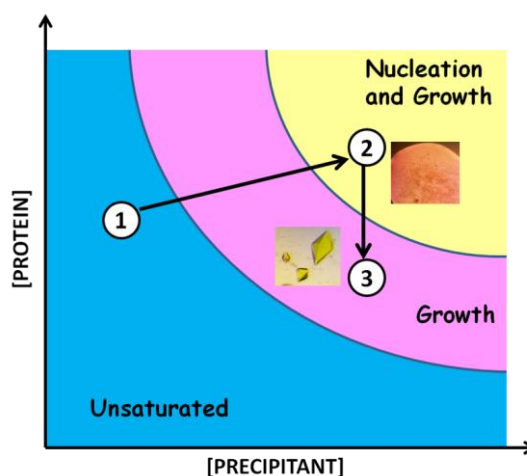
The cleavage sites for proteases in a globular protein usually are located in loops, which are flexible, whereas the domains stay strongly folded, thus, inaccessible to proteolysis (Hubbard, 1998). Often the limited proteolysis is used for a partially folded protein, because the number of flexible regions in this case is higher. But on the other hand, this method helps to identify chain regions (unfolded or mobile), which correlate to those detected by other biophysics methods (NMR, CD). This method is the most informative for multifunctional proteins. Where domains responsible for different functions could be found and can help to understand the biological mechanism (Fontana *et al.*, 1999).

Limited proteolysis is a very informative method for the study of folding intermediates even for proteins with known structure. Proteolytic digestions usually happen at flexible regions, which are available for solvent interaction (e.g. disordered N- and C-terminus, loops and chains between domains). Proteolytic intermediates can be analyzed with the mass spectrometry (MS) (matrix-assisted laser desorption ionization or electrospray ionization (ESI) techniques). The MS data results in definition of the locations of the cleavage places, thus domain boundaries. The MS technique is the most effective for domain interpretation.



## 1.2. CRYSTALLIZATION.

Protein crystals growth is an important step for determining crystal structure of a protein by X-ray diffraction. Usually, to grow a protein crystal, pure protein is mixed with a precipitant such as ammonium sulfate or polyethylene glycol, at non-saturated concentration of precipitant. Then the crystal growing is going under slow evaporation, and the concentration of a protein increases while solution becomes supersaturated. Protein starts to aggregate: this is the beginning of a crystal formation. This process goes through two steps: nucleation and growth. The phase diagram demonstrates what occurs during the protein crystallization. It represents the protein concentration as a function of the precipitant concentration (McPherson, 1999; Asherie, 2004) **Fig. II-3**. Aggregation starts in a supersaturated solution (yellow area on the phase diagram), at this step nuclei occur, then in ideal case they continue to grow, but additional nucleation does not take place (pink area on the phase diagram) **Fig. II-3**. (Rhodes, 2006)



**Figure II-3.** Phase diagram for protein crystallization description presents protein concentration as a function of concentration of a precipitant. Scheme represents a pathway of growing proper quality crystal for diffraction analysis. The first step starts when protein reaches the state of nucleation (moving from the blue area (protein solution is unsaturated, thus aggregates do not appear) to the yellow area (a nucleation and growth region of supersaturated solution) and then slowly moves to the pink area (supersaturated solution, where crystal grows)

There are many methods for biomacromolecules crystallization. Such techniques as hanging drop, sitting drop and sandwich drop vapor diffusion, batch, microbatch under oil, microdialysis can be used for setting up crystallization experiments.

### 1.2.1. Vapor Diffusion Methods.

The most frequently used crystallization technique is the vapor diffusion technique. In this method a small droplet, which contains mixture of protein with crystallization solution (buffer, salt, precipitation agent), is placed on a platform in a closed container, which contains also a reservoir with a crystallization solution. The difference in concentration between drop and reservoir moves system to equilibrium due to evaporation. When the protein solution becomes supersaturated, the crystal starts to grow.

Different parameters have influence on the crystallization of a protein. Varying these parameters helps to search for optimal crystallization conditions. The most common parameters are protein concentration, the nature and the concentration of the precipitant, pH, and temperature. Specific additives that affect the crystallization can also be added in low concentrations (McPherson, 1990).

The crystals of good quality suitable for diffraction analysis are usually transparent, without cracks and defects, and have a definite form. There are several methods, such as crush test, dehydration test, gel electrophoresis etc., help to define whether a crystal has a protein origin. In case when microcrystal is obtained, the seeding methods can be used, where the microcrystal is moved with a crystal transfer syringe to a new protein-precipitant drop (Ducruix & Giege, 1999).

### 1.2.2. Optimization Methods.

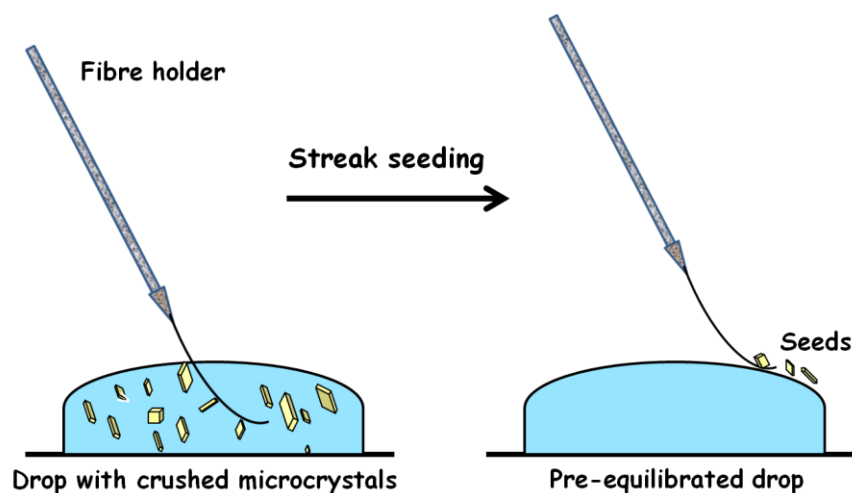
Often we have to optimize physical-chemical parameters to find suitable conditions not only for nucleation but to grow large single 3D crystal. To optimize the crystallization conditions following techniques can be used:

- mixing inorganic and organic precipitating agents,
- crystal seeding method,
- addition of stabilizing agents, additives, glycerol or other small molecules.

#### **Seeding methods**

The advantage of the seeding techniques is in their easier possibility to add already existing nucleus into crystallization drop than create one *de novo*. Seeding techniques is used usually for increasing the size and quality of crystal. During seeding, processes leading to the spontaneous nucleation are separated from those allow a crystal nucleus to grow. In practice the seeding is performed by adding of

crystal seeds to a pre-equilibrated protein solution that was prepared according to previous crystallization experiments or in slightly changed conditions (Fig. II-4.;Bergfors, 1999; Bergfors, 2003).



**Figure II-4.:** Schematic representation of the streak seeding procedure. An animal whisker is lifted from the solution and streaked through a second drop in which it deposits seed along its path. New crystals can grow from these seeds if the conditions are suitable for enlargement.

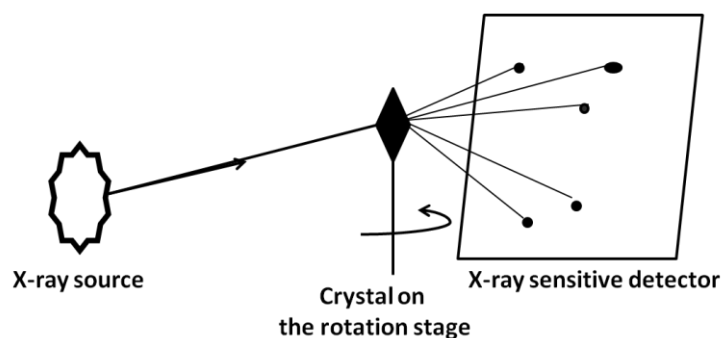
One of the most common optimization technique is macroseeding, when single, pre-grown, washed crystal is transferred to a new pre-equilibrated drop. The next one is microseeding, when microscopic crystals, crushed up into fragments are transferred into a new drop (Ducruix & Giege, 1999; Stura & Wilson, 1990).

### 1.2.3. Crystal Structure Determination.

#### 1.2.3.1. Crystallographic Data Collection.

The X-ray diffraction experiment includes also the preparation of a crystal for the experiment, the actual diffraction data collection and the processing and validation of these data.

Diffraction experiments start from placing of a crystal at the cryo-stream between the X-ray source and X-ray detector. The diffracted rays pass through the crystal and the intensity of X-rays coming from a crystal are detected and accurately measured. The actual X-ray scattering occurs from electrons of molecules (McPherson, 1982). (Fig. II-5.)



**Figure II-5.** Schematic representation of diffraction experiment.

The crystal is rotating around its axis during the data-collection. The collection of data is achieved by recording of all possible reflections up to resolution limit. List of images is a result of recording data during the rotation. Then the collected reflections are transformed to electron density map using the mathematical Fourier transform technique. Determination of atoms position is possible from density map.

There are following methods using for retrieving the phase from the diffraction data (Rhodes, 2006; Wilmanns & Weiss, 2005):

- 1) Molecular replacement
- 2). Isomorphous replacement
- 3). Anomalous dispersion
- 4). Exploitation of radiation damage

### **1.2.3.2. Molecular Replacement.**

Molecular replacement technique is based on correction of orientation and position of atoms on density map by using coordinates from a known structure (or from a fragment of a known structure). The initial step in the determination of the molecular replacement structure is the determination of three rotation and three translation parameters, which define the correct orientation and the correct translation of the search model (the known structure) in the unit cell of the target structure. (Wilmanns & Weiss, 2005).

Currently about two thirds of all newly characterized structures are determined by molecular replacement.

## 2. EXPERIMENTAL SETUP.

### 2.1. EXPRESSION AND PURIFICATION OF THE WRBA

Protein WrbA was overexpressed in BL21(DE3) *Escherichia coli* (Novagen) from the plasmid pET3a (Grandori *et al.*, 1998). The overnight culture of cells was grown in 5ml LB (Luria-Bertani) medium containing ampicillin in concentration 100  $\mu\text{g ml}^{-1}$ . Culture was incubated at 310 K with shaking at 180  $\text{rev. min}^{-1}$ . Then overnight culture was diluted 1:100 in fresh 1liter LB medium with ampicillin to a final concentration of 100  $\mu\text{g ml}^{-1}$  and grown with shaking at 310 K, 180  $\text{rev. min}^{-1}$  for 8-12 hours. Cells were harvested by centrifugation (4500 rpm 15 min) and resuspended in buffer A (20 mM sodium phosphate pH 6.5, containing 1mM ethylenediaminetetraacetic acid (EDTA) and 1mM phenylmethanesulfonyl fluoride (PMSF)). Cells were broken down with the French press (THERMO electron corporation, 40K cell, USA) at 100MPa. Unbroken cells and cell debris were removed by ultracentrifugation (15000 rpm for 30min at 277 K). The supernatant was passed through DEAE-cellulose column (DEAE Highprep, Sigma) preequilibrated with buffer A. The WrbA protein was eluted form the DEAE column with a salt linear gradient up to 0.5M NaCl at a flow rate of 2ml  $\text{min}^{-1}$ . Yellow fractions containing WrbA were collected and dialyzed against buffer A and then applied to the Affi-Gel Blue (BioRad) affinity column. The WrbA protein was eluted with a linear gradient of NaCl from 0 to 1M, with a flow rate of 1 ml  $\text{min}^{-1}$ . The purity of fractions was monitored with the SDS polyacrylamide gel electrophoresis (SDS-PAGE) using 12% acrylamide gel. The sample was concentrated using centrifuge filter devices (Amicon Ultra 10.000 MWCO, 15 ml capacity; Millipore (Billerica, MA)). The final concentration of the purified protein was determined by UV absorption spectroscopy (Eppendorf BioPhotometer Plus) using extinction coefficient  $\epsilon_{\text{wrbA}} = 22\,831\text{ M}^{-1}\text{cm}^{-1}$  at 280 nm. Pure WrbA protein loses FMN during affinity chromatography. The WrbA holoprotein for kinetic experiments was prepared by incubation of pure apoprotein with FNM cofactor ( $K_d = 2\mu\text{M}$ ) and with FMN or FAD cofactor for crystallization experiments. Protein was stored at 250 K.

## 2.2. KINETIC ASSAYS.

The WrbA activity was determined spectrophotometrically by following the decrease in absorbance of NADH at 340 nm or in absorbance of DCPIP (2,6-dichlorophenol-indophenol) at 600 nm. The assay solution contained 20 mM NaP buffer, pH6.5 with 1mM EDTA, 5-500 $\mu$ M of NADH or 5-55 $\mu$ M DCPIP or 5-500  $\mu$ M BQ (benzoquinone) and 20nM of the enzyme in a total volume of 1 ml. The assays were carried out with Beckman Spectrophotometer using cuvettes of 1 cm light path. The reaction was started by the addition of the WrbA holoprotein.

Different conditions for the assay measurements were used to determine the kinetic properties of the WrbA. To study the Michaelis-Menten behavior of the WrbA and temperature influence on it assays were done at 278K for 60 seconds with the enzyme pre-incubated at 278K, room temperature and at 310K for two hours. The absorbance was monitored continuously and the initial rate was obtained from the slope of absorbance changes. The concentration of one substrate was varied in the range from 0 to 500  $\mu$ M for NADH and BQ and in the range from 0 to 55 for DCPIP with the fixed concentration of the second substrate (50 or 100 $\mu$ M for NADH and BQ and 35 $\mu$ M for DCPIP). To study reversibility of the temperature effect on the kinetic behavior of the WrbA, protein was kept at room temperature for two hours, after pre-incubation, the kinetic assays were done, then the WrbA was cooled at 278K for two hours and the kinetic measurements were done again.

To determine the mechanism of WrbA, assays were held for enzyme pre-incubated at room temperature. The Michaelis-Menten curves were performed for one substrate (NADH or BQ) in the range 0-500 $\mu$ M at four fixed concentrations (10, 20, 50, 100 $\mu$ M) of the second substrate. The values  $K_M$  and  $V_{max}$  were obtained by non-linear fit with the help of Microsoft Excel tool. The ratios of  $V_{max}$  to  $K_M$  were used to establish kinetic mechanism (Walsh, 1979).

The patterns of products inhibition were analyzed (Walsh, 1979). NAD and HQ at concentrations 10, 20, 50, 100 $\mu$ M were used as the product inhibitors. Assays were done for one of the substrates (NADH or BQ) in the range 0-500 $\mu$ M at non-saturated and saturated concentrations of the second fixed substrate, 20 $\mu$ M and 2mM respectively.

The effect of change in conditions and influence of modulators on the kinetic behavior of the WrbA was also studied. It was done by adding to the test system

different concentrations of modulators or by changing the initial conditions (effect of salt concentration, pH). Assays were done for several modulators such as indole, 8-hydroquinoline etc. Also effect of different salt concentrations (0.25M and 0.5M NaCl) on the kinetic behavior of the WrbA was studied.

### 2.3. CRYSTALLIZATION OF THE WRBA.

Reconstituted WrbA holoprotein (WrbA with FAD cofactor) at the concentration of 0.25mM (5 mg ml<sup>-1</sup>) in 20 mM Tris pH 6.5 has been used for crystallization experiments. Initial crystallization trials were performed in Cryschem 24-well plates (Hampton Research, Aliso Viejo, USA) using the sitting drop vapour diffusion technique (Ducruix & Giege, 1999). Commercial crystal screen low ionic kit for proteins #86684 from Sigma was used for initial screening of crystallization conditions. Drops consisting of 1-2 µl protein solution and 1µl reservoir solution were equilibrated with 700 µl reservoir solution containing 28% PEG 3350 and 0.05 M Bis-Tris-HCl, pH 6.5. All experiments were carried out at 288 K. Yellow tetragonal crystals were obtained within 7 days in the drops consisting of protein solution plus precipitant solution in ratio 1:1.

#### 2.3.1. Diffraction Data Collection and Processing. Structure Solution and Refinement.

Four-weeks old crystal was used for diffraction experiment. Diffraction data for WrbA holoprotein crystal were collected at the beamline MX-14-2 at the BESSY in Berlin using a MAR CCD 225 mm detector. Crystal was flash-cooled in nitrogen stream at 100 K without additional cryoprotection. The crystals diffracted to a maximum resolution of 1.20 Å. A total of 200 diffraction images were collected, at 0.5° oscillation angle. The measured data were integrated using *MOSFLM* (Leslie, 2006) and scaled using *SCALA* (Evans, 2006).

The structure of WrbA was solved by molecular replacement using the program *Molrep* (Vagin & Teplyakov, 2010) and the coordinates of *E.coli*. WrbA in complex with FMN (PDB code 2R97, Wolfova *et al.*, 2009) as a search model. The Matthews coefficient of 1.85 Å<sup>3</sup> Da<sup>-1</sup> and a solvent content of 34% (Matthews, 1968) indicated the presence of two monomers in the asymmetric unit. Refinement was carried out in *PHENIX* (Adams *et al.*, 2010) and included restrained individual coordinate refinement, restrained individual anisotropic refinement of atomic displacement

parameters (except for the poorly defined loop portions and water molecules) and individual occupancy refinement. Bulk solvent correction and anisotropic scaling was applied. Density for FMN was clearly defined. Manual building and model correction was performed in *COOT* (Emsley & Cowtan, 2004). Comprehensive validation of the model with diffraction data was performed with the validation tool in *PHENIX*, which includes *Molprobit* analysis (Chen *et al.*, 2010) of the protein geometry. The final model has an *R* factor of 15.45 % and an *R*<sub>free</sub> of 18.60 % 99.2 % of residues are in Ramachandran favoured regions with no outliers. Refinement statistics are given in Table 2. Diagram of the FMN binding site interactions was produced with *LIGPLOT+* (Laskowski & Swindells, 2011). Analysis of surface areas and interactions were made using the PISA server (Krissinel & Henrick, 2007). All figures were made with *PyMOL* (DeLano, 2002). Structure and experimental data were deposited to PDB with the entry ID 3ZC2.

#### 2.4. PROTEOLYSIS OF THE WRBA.

For limited proteolysis experiments for the WrbA were used apo and holo forms of the protein WrbA APO at concentrations 50µM (~0.80 mg/ml) in 20mM Na-phosphate, pH 6.5 and WrbA HOLO 50µM (~0.80 mg/ml) in 20mM Na-phosphate, pH 6.5 with 200µM FMN.

Experiments were done for four different proteases. These were Subtilisin, Papain, Trypsin, Chymotrypsin (Table II-1.). Stock solutions were prepared by dissolving the powder in 1 ml of the dilution buffer, then aliquoted and stored in -80°C.

Subtilisin <b>S</b>	2 mg/ml in 50 mM Tris pH 8
Chymotrypsin <b>CH</b>	2.3 mg/ml in 1 mM HCl
Trypsin <b>T</b>	1.5 mg/ml in 1 mM HCl
Papain <b>P</b>	1.1 mg/ml in 50 mM Tris pH 8

**Table II-1.** Initial Stock solutions

Preliminary time course analysis for apo and holo WrbA were done by member of our group J Wolfova. Further experiments were done for all four proteases during 60



minutes with 10 minutes time-point intervals. Different dilutions of proteases were used in the experimental trials.

Proteolysis reactions were carried out in eppendorf tubes with volume ratio of protein to protease is 2:1.

At different time points reaction were stopped by adding of 4x SDS-loading buffer, immediate boiling for the SDS-PAGE electrophoresis control and by adding of ice cold TFA to the final concentration equal to 1%, sample was frozen in the liquid nitrogen and stored at -80°C for the further MS analysis.

## 2.5. MS SEQUENCING OF THE WRBA.

Following limited proteolysis the samples were desalted on a peptide microtrap (Michrom Bioresources, Auburn, CA) and dried down in a speedvac concentrator. Dried samples were reconstituted in 30 µl of 10% acetonitrile / 0.2% formic acid in water and loaded into vials which were placed into an autosampler of Agilent 1200 high performance liquid chromatography (HPLC) system (Agilent Technologies, Waldbronn, Germany). Samples were separated on a reversed phase capillary column (0.2 × 150 mm , MAGIC C18 AQ, 3µm, 200 Å, Michrom Bioresources, Auburn, CA) using gradient elution from 0% B to 55% B in 27 min where solvent A was 0.2% formic acid / 2.5% acetonitrile / 2.5% isopropanol in water and B was 0.16% formic acid / 5% water / 5% isopropanol in acetonitrile. The outlet of the column was directly interfaced to a hybrid quadrupole – Fourier Transform - Ion Cyclotron Resonance (FT-ICR) mass spectrometer (Apex Qe ultra, Bruker Daltonics, Bremen, Germany) via the electrospray ion source (ESI). The instrument was operated in positive MS mode.

Data were processed in Data Analysis 4.0 (Bruker Daltonics, Bremen, Germany) using SNAP algorithm. List of unique masses was exported and sorted in MS Excel. Masses were searched against the sequence of WrbA using program GPMW v 7.1 (Lighthouse data, Denmark) with no enzyme specificity and mass tolerance set to 3 ppm. Uniquely identified fragments were then visualized using Draw Map script, a part of MS Tools available at <http://ms.biomed.cas.cz/MSTools/>.

## 2.6. LIGAND DOCKING AND QM/MM BINDING ENERGIES.

Ligand docking and QM/MM binding energies were calculated and analyzed by members of our group. Crystal structure 3B6J (Andrade *et al.*, 2007) was used for docking of NAD and NADH. PEG fragments, AMP (adenosine monophosphate), NADH, and crystal waters were removed and hydrogen atoms were added using the Maestro program from the Schrödinger software package (Schrödinger, 2011a). Two systems were prepared in this way, one with FMN and NADH and another one with FMNH<sub>2</sub> and NAD. The positions of the hydrogen atoms as well as the heavy atoms of the FMNH<sub>2</sub> were optimized by a short steepest-descent minimization using Impact from Schrödinger (Schrödinger, 2011b). Initial molecular docking of NADH or NAD to the binding pocket with the largest part formed by chain A was performed using the program Glide from the Schrödinger software package (Schrödinger, 2011c). The QM/MM calculations, where NADH (NAD) was selected as the QM region and the rest of the system as MM region including implicit solvation using the Poisson-Boltzmann approach (PBS), were performed for the highest-ranked pose with a position suitable for reaction by the program Qsite from the Schrödinger package (Schrödinger, 2011d). The resulting QM polarized charges of NADH (NAD) were then used for re-docking of the ligand using Glide.

Subsequent calculations of binding energies were performed for the most suitable docking poses from polarized docking as well as for the crystal structures. Calculations were also performed for the dimeric form of the protein, which was prepared by removing chains C and D in crystal structure 3B6J from the tetrameric structure. The selected structures were calculated using the QM/MM method, where NADH and FMN (NAD and FMNH<sub>2</sub>) were selected as QM region and the rest of the protein as MM region. Implicit solvent was included using PBS implemented in Qsite (Schrödinger, 2011d). The QM energies as well as the electrostatic contribution to QM/MM coupling energy were calculated using Gaussian 03 (Frisch *et al.*, 2003) by the density functional theory method (DFT) with a B3LYP functional including additive dispersion (treated by DFTD3 (Grimme *et al.*, 2010) with 6-31G\* basis set. The basis set superposition error was treated by the counterpoise correction method (Boys & Bernardi, 1970). Van der Waals contribution to the QM/MM coupling energy was calculated by the MM program Impact (Schrödinger, 2011c) using the OPLS2005

forcefield (Jorgensen & Tirado-Rives, 2005). The same calculations were also performed using the crystal structure 3B6K (Andrade *et al.*, 2007) containing benzoquinone (hydroquinone) as ligand.

### **2.7. NMR.**

NMR spectra were taken by our collaborators in Princeton. Phosphorous-31 NMR spectra were collected at room temperature on a 500MHz Bruker spectrometer. At each titration point, 512 scans were collected; the spectra were centered at -10 ppm with a sweep width of 50 ppm. The spectra were analyzed on MestRenova NMR software MNova with identical phasing parameters at each titration point to enable comparison of the spectra.

### **2.8. AUC.**

Analytical ultracentrifugation experiments were performed by our collaborators from Princeton with a Beckman-Coulter XL-I instrument at the national facility at University of Connecticut. Samples were prepared at pH 7.2 in buffer containing 20mM phosphate and 100mM NaCl. Data analysis was done with software SEDANAL (Stafford, 1992). Sedimentation coefficients were calculated from the crystal structure of apoWrbA (PDB ID: 2RG1), using the program HYDROPRO (Garcia de la Torre, 2000).

### 3. REFERENCES

- Adams PD, Afonine PV, Bunkóczi G, Chen VB, Davis. I. W., et al. (2010) PHENIX: a comprehensive Python-based system for macromolecular structure solution. *Acta Crystallogr. D66*: 213-221.
- Andrade SL, Patridge EV, Ferry JG, Einsle O (2007) Crystal structure of the NADH:quinone oxidoreductase WrbA from *Escherichia coli*. *J Bacteriol* 189: 9101-9107.
- Bisswanger H. (2002) *Enzyme Kinetics: Principles and Methods*. Wiley-VCH, Weinheim.
- Bollag DM, Rozycki MD and Edelstein SJ (1996) *Protein methods*. Wiley, New York
- Boys SF, Bernardi F (1970) Calculation of small molecular interactions by differences of separate total energies – some procedures with reduced errors. *Molecular Physics* 19: 553-&.
- Carey J: A systematic and general proteolytic method for defining structural and functional domains of proteins. *Methods Enzymol.* 382, 499-514 (2000).
- Chen VB, Arendall WB 3rd, Headd JJ, Keedy DA, Immormino RM, Kapral GJ, Murray LW, Richardson JS, Richardson DC. (2010) MolProbity: all-atom structure validation for macromolecular crystallography. *Acta Crystallographica D66*:12-21.
- Chicz RM and Regnier FE (1990) High performance liquid chromatography: Effective protein purification by various chromatographic modes. *Methods Enzymol.* 182, 392.
- Colowick SP (1955) Separation of proteins by use of absorbents. *Methods Enzymol.* 1, 90.
- Cooper TG (1977) *The tools of biochemistry*. Wiley, New York.
- Copeland RA (2000) *Enzymes: A Practical Introduction to Structure, Mechanism, and Data Analysis*. Wiley, New York.
- DeLano, W.L. *The PyMOL Molecular Graphics System* (2002) DeLano Scientific, San Carlos, CA, USA. <http://www.pymol.org>
- Deutcher M (1990) *Guide to protein purification*. *Methods Enzymol.* 182, Academic Press, San Diego, California.
- Ducruix, A. & Giege', R. (1999). *Crystallization of Nucleic Acids and Proteins: A Practical Approach*, 2nd ed. Oxford University Press.

- E. Krissinel and K. Henrick (2007). Inference of macromolecular assemblies from crystalline state. *J. Mol. Biol.* 372, 774--797.
- Emsley, P., Cowtan, K. (2004). Coot: model-building tools for molecular graphics, *Acta Crystallogr. D60*: 2126–2132.
- Evans, P. (2006). Scaling and assessment of data quality. *Acta Cryst. D62*, 72–82.
- Fontana A., Polverino de Laureto P., De Filippis V., Scaramella E., Zambonin M. (1999) Limited proteolysis in the study of protein conformation. In E.E. Sterchi, W. Stocker (eds.) *Proteolytic Enzymes: Tools and Targets*, Springer Verlag, Heidelberg. 257-284.
- Frey PA and Hegeman AD (2007) *Enzymatic reaction mechanisms*. Oxford University Press, Oxford
- Frisch MJ, Trucks GW, Schlegel HB, Scuseria GE, Robb MA, et al. (2003) *Gaussian 03*, Revision C.02.
- Garcia de la Torre J., Huertas M.L. and Carrasco B. (2000) Calculation of hydrodynamic properties of globular proteins from their atomic-level structure. *Biophys. J.* 78, 719-730.
- Grandori R, Khalifah P, Boice JA, Fairman R, Giovanielli K, Carey J. (1998) Biochemical characterization of WrbA, founding member of a new family of multimeric flavodoxin-like proteins. *J Biol Chem.* 273, 20960-6.
- Grimme S, Antony J, Ehrlich S, Krieg H (2010) A consistent and accurate ab initio parametrization of density functional dispersion correction (DFT-D) for the 94 elements H–Pu. *J Chem Phys* 132:154104
- Hubbard S. J. (1998) The structural aspects of limited proteolysis of native proteins. *Biochim Biophys Acta* 1382: 191-206
- Johnson, W. C. 1990. Protein secondary structure and circular dichroism: a practical guide: *Proteins* 7: 205-214
- Jorgensen WL, Tirado-Rives J (2005) Potential energy functions for atomic-level simulations of water and organic and biomolecular systems. *Proceedings of the National Academy of Sciences of the United States of America* 102: 6665-6670.
- Koth CM, Orlicky SM, Larson SM, Edwards AM. (2003) Use of limited proteolysis to identify protein domains suitable for structural analysis. *Methods Enzymol.*;368:77-84.
- Laskowski RA, Swindells MB. (2011) LigPlot+: multiple ligand-protein interaction diagrams for drug discovery. *J Chem Inf Model.* 51(10):2778-86.

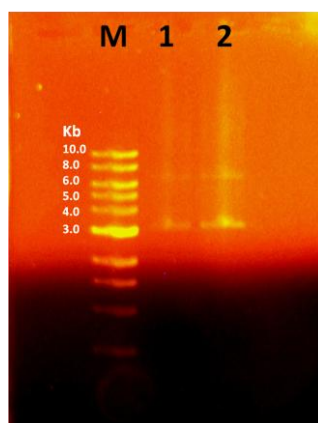
- Leslie, A. G. W. (2006). The integration of macromolecular diffraction data. *Acta Cryst. D62*, 48–57.
- Lorber B, Sauter C, Robert MC, Capelle B, Giege R (1999) Crystallization within agarose gel in microgravity improves the quality of thaumatin crystals. *Acta Crystallogr D55*, 1491-1494.
- Marangoni AG. (2003) *Enzyme Kinetics: a Modern Approach..* John Wiley & Sons, Ltd, Chichester
- Matthews, B.W. 1968. Solvent content of protein crystals. *J. Mol. Biol.* 33 491–497
- McPherson A., (1999) *Crystallization of biological macromolecules.* Cold Spring Harbor Laboratory Press, New York.
- Muller R, Buttner P (1994) A critical discussion of intraclass correlation coefficients. *Stat. Med.* 3, 2465-76
- Rhodes, G. (2006) *Crystallography Made Crystal Clear* Academic Press, 1250 Sixth Ave., San Diego, CA 92101-4311.
- Schrödinger (2011a), *Maestro 9.2*, Schrödinger, LLC, New York.
- Schrödinger (2011b), *Impact 5.7*, Schrödinger, LLC, New York.
- Schrödinger (2011c), *Glide 5.7*, Schrödinger, LLC, New York.
- Schrödinger (2011d), *Qsite 5.7*, Schrödinger, LLC, New York.
- Schulz AR (1994) Cambridge University Press, New York.
- Shapiro AL, Viñuela E, Maizel JV Jr. (1967). "Molecular weight estimation of polypeptide chains by electrophoresis in SDS-polyacrylamide gels.". *Biochem Biophys Res Commun.* 28 (5): 815–820
- Stafford, W.F. (1992) Boundary analysis in sedimentation transport experiments- a procedure for obtaining sedimentation coefficient distributions using the time derivative of the concentration profile. *Analytical Biochem.* 203, 295-301.
- Stein RL (2011) *Kinetics of Enzyme Action: Essential Principles for Drug Hunters.* Wiley, Hoboken, NJ
- Stura EA and Wilson IA: Analytical and production seeding techniques. *Methods.* 1, 38 (1990)
- Vagin A, Teplyakov A (2010) Molecular replacement with MOLREP. *Acta Crystallogr D66*:22–25
- Walsh C (1979) *Enzymatic Reaction Mechanisms.* San Francisco: W.H. Freeman and Company

- 
- Weber K, Osborn M (1969). "The reliability of molecular weight determinations by dodecyl sulfate-polyacrylamide gel electrophoresis.". *J Biol Chem.* 244 (16): 4406–4412.
- Wilmanns, M. & Weiss, M.S. (2005). Molecular crystallography In "Encyclopedia of Condensed Matter Physics", Bassani, G, Liedl, G. & Wyder, P. (eds.), pp.453-458, Academic Press
- Wolfova J, Kuta Smatanova I, Brynda J, Mesters JR, Lapkouski M et al. (2009) Structural organization of WrbA in apo- and holoprotein crystals. *Biochim Biophys Acta* 1794: 1288-1298.
- X Gao, K Bain, J B. Bonanno, M Buchanan, D Henderson, D Lorimer, C Marsh, J A. Reynes, J. M Sauder, K Schwinn, C Thai, S K. Burley High-throughput limited proteolysis/mass spectrometry for protein domain elucidation *Journal of Structural and Functional Genomics* 6: 129–134, 2005.

## PART III RESULTS AND DISCUSSION

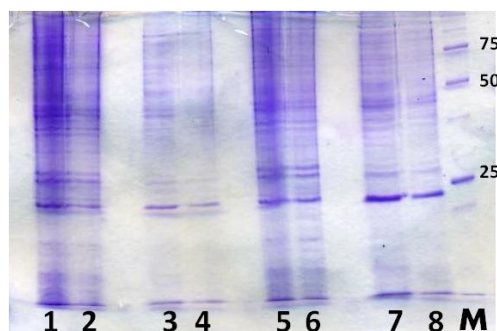
### 1. TRANSFORMATION, EXPRESSION AND PURIFICATION OF THE WRBA.

The plasmid pET3a cloned with the WrbA gene (Grandori *et al.*, 1998) was monitored on Agarose-gel electrophoresis before the start of transformation experiments with *Escherichia coli* competent (BL21(DE3)) cells. (fig. III-1.)



**Figure III-1.** First lane **M** is a Quick-load 1kb DNA Ladder (New England Biolabs, Ipswich, MA), loaded 10  $\mu$ l (0.5  $\mu$ g) per lane marker, lane **1** is 1 $\mu$ l of plasmid sample, and lane **2** is 2 $\mu$ l of plasmid sample.

1 $\mu$ l of DNA plasmid was mixed with 50  $\mu$ l of competent cells BL21(DE3) *Escherichia coli* in eppendorf tube. After standard procedure of transformation (Bergmans *et al.*, 1981), the sample was stirred on ampicillin containing agar plates and incubated at 290K for 12 hours. All single colonies were harvested and tested for expression (fig. III-2.). Sample with the best expression of WrbA protein has been chosen for further manipulations.

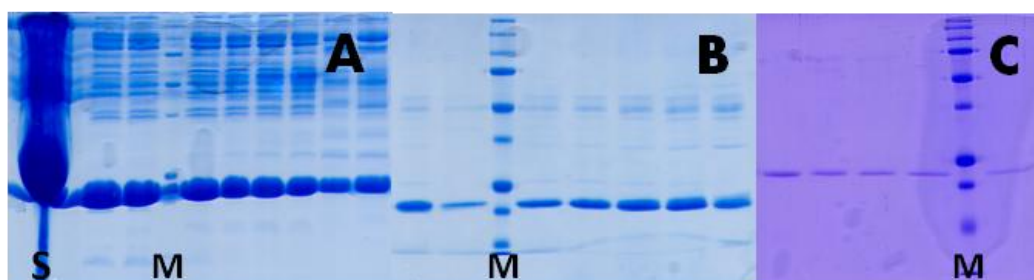


**Figure III-2.** Monitoring of protein expression. Lane **M** is a precision plus protein standard (Bio-Rad); lanes **1 – 8** are samples prepared from *E.coli* colonies for protein expression test.



Previously, protein WrbA was overexpressed in BL21(DE3) *Escherichia coli*. Three samples with 200ml LB medium with ampicillin to a final concentration of 100  $\mu\text{g ml}^{-1}$  were prepared. Expression of WrbA was induced by adding 1mM, 5mM isopropyl  $\beta$ -D-thiogalactopyranoside (IPTG). One culture was prepared without adding IPTG. After the cell cultures were incubated additional four hours at 290 K, cells were harvested by centrifugation (4500 rpm 15 min) and resuspended in buffer P (20 mM sodium phosphate pH 7.2, containing 1mM ethylenediaminetetraacetic acid (EDTA) and 1mM phenylmethanesulfonyl fluoride (PMSF)). Cells were broken down with the French press (THERMO electron corporation, 40K cell, USA) at 100MPa. Unbroken cells and cell debris were removed by ultracentrifugation (15000 rpm for 30min at 277 K). The same volume of supernatant (10 $\mu$ l) from each of three samples was monitored on SDS-PAGE. Further expressions of WrbA were done without adding IPTG, as the amount of expressed WrbA was the same in all other three samples, thus expression of WrbA is not dependent on the IPTG concentration.

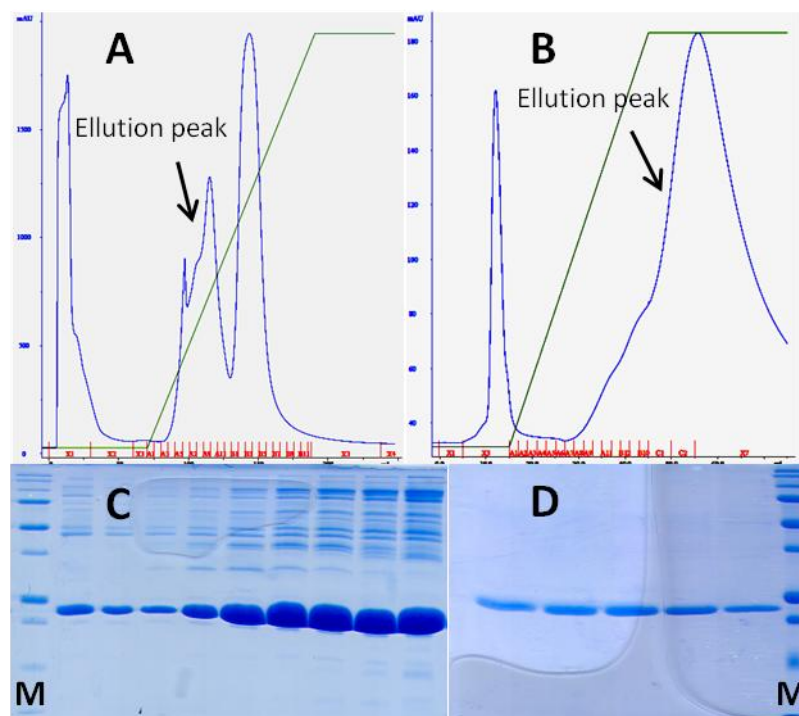
The WrbA protein was purified by method described R. Grandori (Grandori et al, 1998). Figure III-3. shows the results of all purification steps: DEAE column-chromatography, Affi-DEAE-Gel Blue column chromatography and saturation with ammonium sulfate.



**Figure III-3.** SDS-PAGE (12% acrylamide in separating gel). **A. Monitoring of fractions after DEAE column-chromatography:** Lane **S** – sample, which was injected into DEAE column; lane **M** – molecular weight marker. Other lanes are fractions collected from DEAE. **B. Affi-DEAE Gel Blue column chromatography:** lane **M** – molecular weight marker; other lanes present fractions collected from Affi-DEAE Gel Blue. **C. Ammonium sulfate saturation:** lane **M** – molecular weight marker; other lanes are samples after ammonium sulfate precipitation step.

Then the purification protocol was optimized to exclude the last purification step. Sample for purification was prepared the same way as was described above and then was passed through DEAE-cellulose column (DEAE Highprep, Sigma) preequilibrated with buffer A (20 mM sodium phosphate pH 6.5, containing 1mM

ethylenediaminetetraacetic acid (EDTA) and 1mM phenylmethanesulfonyl fluoride (PMSF)). Whereas the isoelectric point (pI) of WrbA protein is 5.5, thus the pH of purification buffer for ion-exchange chromatography DEAE has to be in the range 6.0 – 9.0. Isoelectric point is a pH of the solution of protein at which the negatively and positively charged molecular species are present in equal concentration. Most of the proteins in biological systems have the pI in the range 6.0-6.5, due to this a lot of proteins do not bind the DEAE matrix at the same pH range, whereas the WrbA is binding to matrix at this pH. The WrbA protein was eluted from the DEAE column with a salt linear gradient up to 0.5M NaCl at a flow rate of  $2\text{ml min}^{-1}$ . Yellow fractions containing WrbA were collected at NaCl concentration equal 0.4M. (Fig III-4A). The sample was dialyzed against buffer A and then applied to the Affi DEAE-Gel Blue (BioRad) affinity column. The WrbA protein was eluted with a linear gradient of NaCl from 0 to 1M, with a flow rate of  $1\text{ ml min}^{-1}$  (Fig. III-4B). The purity of fractions was monitored with the SDS polyacrylamide gel electrophoresis (SDS-PAGE) using 12% acrylamide gel (Fig. III-4C, D).



**Figure III-4.** Purification of WrbA protein analyzed by SDS-PAGE. **A. DEAE cellulose column, elution peak was detected at 280nm.** Green line is a gradient in range 0-1M NaCl. First elution peak correspond to yellow fractions of WrbA. **B. Elution peak of Affi-DEAE Gel Blue chromatography.** Green line is a gradient from 0 to 1M NaCl. **C. Fractions of WrbA eluted from DEAE column analyzed by SDS-PAGE. Lane M, molecular weight marker.** **D. Fractions eluted from Affi-DEAE Gel Blue column. Line M – molecular weight marker.**

However, the saturation of WrbA by ammonium sulfate was used in case when the purity of the protein fractions was not good. Fractions which contained WrbA, were saturated by 50% of ammonium sulfate (final 314 g/liter) and incubated for 1 hour. Then the sample was centrifuged at 30,000 g for 30 min and the supernatant was dialyzed against buffer A and was concentrated using centrifuge filter devices (Amicon Ultra 10.000 MWCO, 15 ml capacity; Millipore (Billerica, MA)). In addition, Gel-filtration chromatography (Superdex 75) was used for the same reason.

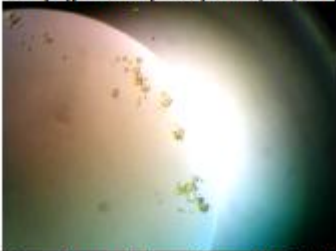
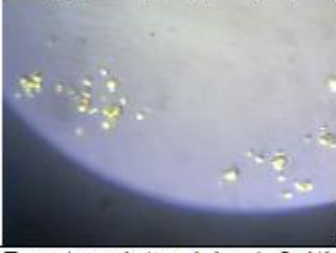
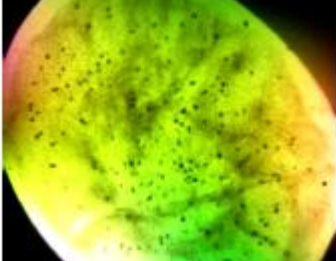
The final concentration of the purified protein was determined by UV absorption spectroscopy (Eppendorf BioPhotometer Plus) using extinction coefficient  $\epsilon_{\text{wrbA}} = 22\,831\text{ M}^{-1}\text{cm}^{-1}$  at 280 nm. Pure WrbA protein loses FMN during affinity chromatography. The WrbA holoprotein for kinetic experiments was prepared by incubation of pure apoprotein with FNM cofactor ( $K_d = 2\mu\text{M}$ ) and with FMN or FAD cofactor for crystallization experiments. Protein was stored at 250 K.

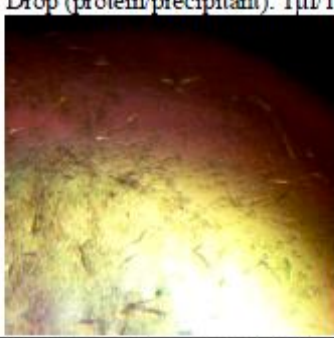
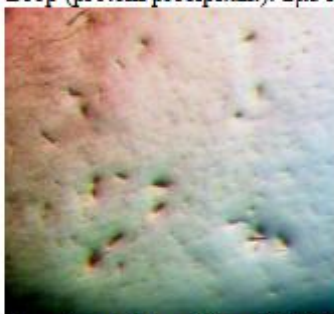

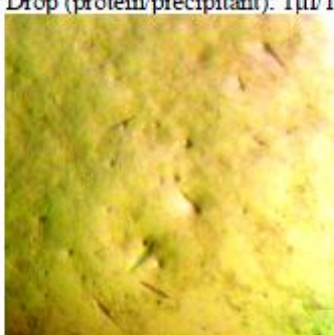
## 2. CRYSTALLIZATION OF WRBA PROTEIN.

### 2.1. CO-CRYSTALLIZATION OF HOLOWRBA PROTEIN WITH FMN AS COFACTOR WITH DIFFERENT SUBSTRATES.

Standard equipment was used for the co-crystallization experiments. The conditions established by member of our group J. Wolfova for the holo protein crystals were used for preliminary crystallization experiments. The main goal of crystallization experiments is the obtaining of good quality crystals of WrbA holo-form with FMN and FAD cofactor in the presence and absence of the substrates.

Unfortunately, efforts to grow the good quality crystals of WrbA-FMN holoprotein in the presence of one of the substrates were not successful. The best result obtained was a big amount of microcrystals. The seeding technique (*Stura et al. 1992*) did not show any progress. The conditions used for optimization of the WrbA crystallization and results of these manipulations are presented in table III-1.

Sample	Conditions	Result
<b>WrbA + FMN + NAD<sup>+</sup></b>  0.25mM apoWrbA + 0.25mM FMN + 5mM NAD <sup>+</sup>  20mM Na <sub>2</sub> HPO <sub>4</sub> , pH 6.5  <b>the sitting drop vapour diffusion technique</b>	20% PEG 8000, 0.1M TRIS, pH 7.5	Drop (protein/precipitant): 1μl/1μl 
	20% PEG 8000, 0.1M TRIS, pH 8.0	Drop (protein/precipitant): 2μl/1μl 
	30% PEG 4000, 0.1M TRIS, pH 7.5, 0.2M MgCl <sub>2</sub>	Drop (protein/precipitant): 2μl/1μl 

Sample	Conditions	Result
<b>WrbA + FMN + Benzoquinone (BQ)</b>  0.25mM apoWrbA + 0.25mM FMN + 2mM BQ  20mM Na <sub>2</sub> HPO <sub>4</sub> , pH 6.5  the sitting drop vapour diffusion technique	30% PEG 4000, 0.1M TRIS, pH 7.5, 0.2M MgCl <sub>2</sub>	Drop (protein/precipitant): 1μl/1μl 
	20% PEG 8000, 0.1M TRIS, pH 7.5	Drop (protein/precipitant): 2μl/1μl 
<b>WrbA + FMN + NAD<sup>+</sup> + Benzoquinone (BQ)</b>  0.25mM apoWrbA + 0.25mM FMN + 2mM NAD <sup>+</sup> + 2mM BQ  20mM Na <sub>2</sub> HPO <sub>4</sub> , pH 6.5  the sitting drop vapour diffusion technique	20% PEG 8000, 0.1M TRIS, pH 8.0	Drop (protein/precipitant): 1μl/1μl 
	30% PEG 4000, 0.1M TRIS, pH 7.5, 0.2M MgCl <sub>2</sub>	Drop (protein/precipitant): 1μl/1μl 

**Table III-1.** The representation of successful conditions and results of holoWrbA crystallization with FMN as cofactor and with presence of the substrates.



## 2.2. CO-CRYSTALLIZATION OF HOLOWRBA PROTEIN WITH FAD AS COFACTOR WITH AND WITHOUT PRESENCE OF DIFFERENT SUBSTRATES.

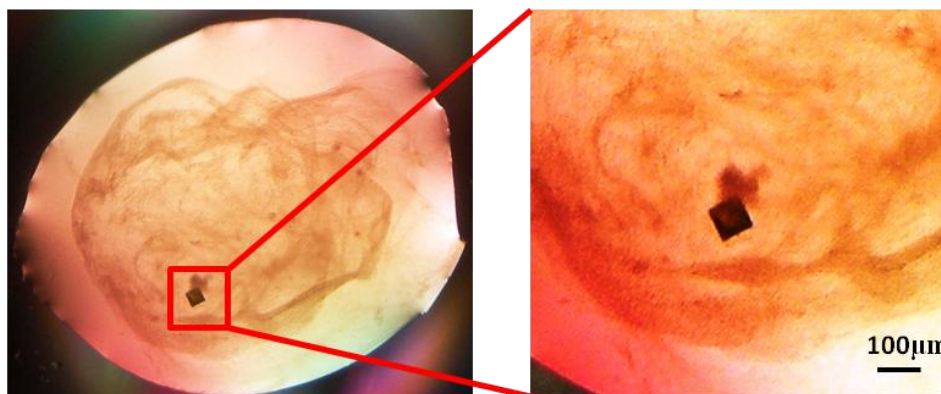
Previous crystallization of reconstituted holoWrbA (with FAD as a cofactor) was performed using sitting drop vapor diffusion method at a room temperature Ducruix & Giege, 1999. Initial crystallization trials were done in Cryschem 24-well plates (Hampton Research, Aliso Viejo, USA). Commercial crystal screen kit from Sigma and conditions similar to those used to crystallize the holoWrbA with FMN cofactor (Wolfova *et al.*, 2009) were used for initial screening of crystallization conditions. A droplet was prepared by mixing equal volumes of protein solution and reservoir solution. Each droplet was placed over 700  $\mu$ l reservoir solution. Results of the initial screening are presented in table III-2.

<b>N<sup>o</sup></b>	<b>Fluka N<sup>o</sup></b>	<b>Name</b>	<b>Result</b>
1	89781	MES-Na (pH 6.0) 0.05M, PEG 3350 20%	Microcrystals
2	92179	MES-Na (pH 6.0) 0.05M, PEG 3350 28%	3D Crystals, needles
3	89776	Bis-TRIS-HCl (pH 6.5) 0.05M, PEG 3350 20%	Microcrystals
4	87316	Bis-TRIS-HCl (pH 6.5) 0.05M, PEG 3350 28%	3D Crystal, tetragonal
5	92538	HEPES Na-salt (pH 7.5) 0.05M, PEG 3350 4%	Microcrystals
6	92021	HEPES Na-salt (pH 7.5) 0.05M, PEG 3350 20%	Microcrystals
7	92146	HEPES Na-salt (pH 7.5) 0.05M, PEG 3350 28%	Microcrystals
8	92154	TRIS-HCl (pH 8.0) 0.05M, PEG 3350 4%	Microcrystals
9	80866	TRIS-HCl (pH 8.0) 0.05M, PEG 3350 12%	Microcrystals
10	89785	TRIS-HCl (pH 8.0) 0.05M, PEG 3350 20%	Microcrystals
11	95129	TRIS-HCl (pH 8.0) 0.05M, PEG 3350 28%	2D crystals
12	94845	TRIS-HCl (pH 8.5) 0.05M, PEG 3350 28%	Microcrystals

**Table III-2.** Overview of successful crystallization conditions for holoWrbA (0.25mM apoWrbA + 0.35mM FAD) enzyme. 86684 Crystallization low ionic kit for proteins. One drop contains crystallization reagent 1  $\mu$ l, protein sample 1  $\mu$ l. Incubation temperature was 24°C.

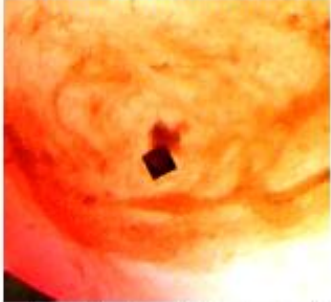


After the optimization of successful conditions the crystal for X-ray diffraction analysis was obtained. (fig. III-5.) The crystal appeared in 14 days after the start of

crystallization and it was growing during four weeks before it was taken for X-ray diffraction analysis.




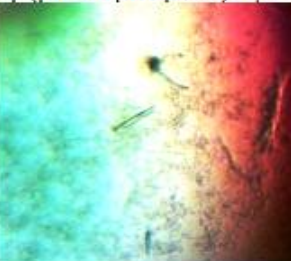




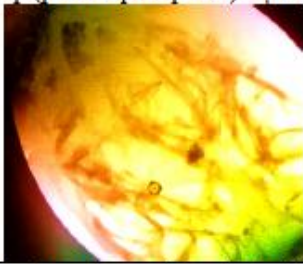
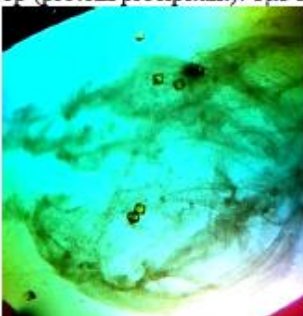
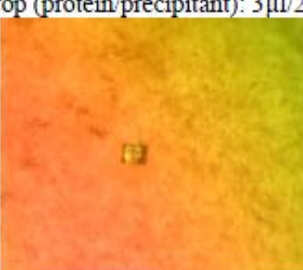
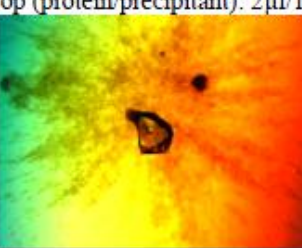
**Figure III-5.** WrbA holoprotein crystals (0.25mM apoWrbA + 0.35mM FAD) grown by the sitting drop vapour-diffusion method from reservoir containing 28% PEG 3350 and 0.05 M Bis-Tris-HCl, pH 6.5.

The crystallization trials of WrbA holoprotein in complex with the substrates also gave successful results. The crystallization experiments were done by using both sitting and hanging drop vapour diffusion methods. First crystals were obtained in 14 days after the start of the crystallization. The best crystals were obtained by using the hanging drop vapor diffusion technique. Several crystals will be used for X-ray diffraction analysis. Successful results are presented in TABLE III-3.

<b>Sample</b>	<b>Conditions</b>	<b>Result</b>
<b>WrbA + FAD</b> 0.25mM apoWrbA + 0.35mM FAD  20mM Na <sub>2</sub> HPO <sub>4</sub> , pH 6.5  <b>the sitting drop vapour diffusion technique</b>	0.05M Bis-TRIS, 28% PEG 3350, pH 6.5	Drop (protein/precipitant): 2µl/1µl 
<b>WrbA + FAD</b> 0.25mM apoWrbA + 0.35mM FAD  20mM Na <sub>2</sub> HPO <sub>4</sub> , pH 6.5  <b>the hanging drop vapour diffusion technique</b>	0.05M Bis-TRIS, 28% PEG 3350, pH 6.5	Drop (protein/precipitant): 1µl/1µl 
	0.1M Bis-TRIS, 28% PEG 3350, pH 6.5	Drop (protein/precipitant): 1µl/1µl 



Sample	Conditions	Result
<b>WrbA + FAD + Benzoquinone (BQ)</b>  0.25mM apoWrbA + 0.35mM FAD + 2mM BQ  20mM Na <sub>2</sub> HPO <sub>4</sub> , pH 6.5  <b>the sitting drop vapour diffusion technique</b>	0.05M MES, 28% PEG 3350, pH 6.0	Drop (protein/precipitant): 2µl/1µl 
		Drop (protein/precipitant): 3µl/2µl 
<b>WrbA + FAD + Benzoquinone (BQ)</b>  0.25mM apoWrbA + 0.35mM FAD + 2mM BQ  20mM Na <sub>2</sub> HPO <sub>4</sub> , pH 6.5  <b>the hanging drop vapour diffusion technique</b>	0.05M MES, 28% PEG 3350, pH 6.0	Drop (protein/precipitant): 1µl/1µl 
		Drop (protein/precipitant): 3µl/2µl 
<b>WrbA + FAD + NAD<sup>+</sup></b>  0.25mM apoWrbA + 0.35mM FAD + 2mM NAD <sup>+</sup>  20mM Na <sub>2</sub> HPO <sub>4</sub> , pH 6.5  <b>the sitting drop vapour diffusion technique</b>	0.05M Bis-TRIS, 28% PEG 3350, pH 6.5	Drop (protein/precipitant): 2µl/1µl 
		Drop (protein/precipitant): 3µl/2µl 

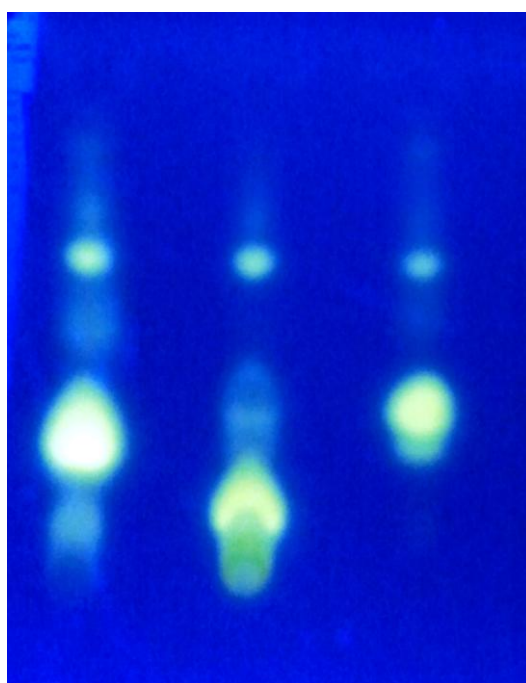
Sample	Conditions	Result
<b>WrbA + FAD + NAD<sup>+</sup></b>  0.25mM apoWrbA + 0.35mM FAD + 2mM NAD <sup>+</sup>  20mM Na <sub>2</sub> HPO <sub>4</sub> , pH 6.5  <b>the hanging drop vapour diffusion technique</b>	0.05M Bis-TRIS, 28% PEG 3350, pH 6.5	Drop (protein/precipitant): 1μl/1μl 
	0.1M Bis-TRIS, 30% PEG 3350, pH 6.5	Drop (protein/precipitant): 1μl/1μl 
		Drop (protein/precipitant): 3μl/2μl 
	0.1M Bis-TRIS, 28% PEG 3350, pH 6.5	Drop (protein/precipitant): 2μl/1μl 

**Table III-3.** Representation of successful results of crystallization WrbA holoprotein with FAD as a cofactor. Experiments were carried out with and without presence of substrates (NADH and BQ).

### 2.3. PRELIMINARY X- RAY DIFFRACTION ANALYSIS OF THE WRBA.

Crystal of holoWrbA (apoWrbA + FAD) was used for diffraction experiment. It diffracted to a maximum resolution of 1.20 Å. The crystal belongs to the space group P4<sub>1</sub>2<sub>1</sub>2, with unit-cell parameters a = b = 61.15, c = 169.6 Å with two monomers in the asymmetric unit. Surprisingly, in structure of holoWrbA due to hydrolysis was found the FMN cofactor instead of FAD, which was used for crystallization.

It is well known that the FAD is a stable flavin (Chappelle & Picciolo, 1971) which was also checked by TLC (Thin layer chromatography). Samples were prepared by dissolving FAD (Sigma) in distilled water to concentration 1mM. The sample was incubated at 24°C for one month. Freshly prepared FAD and one-month old sample were monitored in the dark by TLC on Silica Gel SIL-G-25 (20 cm × 20 cm, thickness 0.25 mm) plates. The moving phase was a solution of butanol: acetic acid: water (12:3:5). Flavin TLC spots were visually examined and scanned by determining their fluorescence under an ultraviolet light. The results of this experiment demonstrated that the FAD did not hydrolyze to FMN after one month incubation at room temperature. In a next step the experiment was repeated using additionally a protein-flavin mixture. Figure III-6. Demonstrates that FAD is hydrolyzed after one-month incubation at room temperature in the presence of WrbA, with the solvent containing about 99% of FMN. This fact allows us to suggest that the reason of hydrolysis might be WrbA itself, that would participate in the reaction, or one could imagine also a contamination by pyrophosphatases, which could be present in protein solution after the purification, or, probably could provoke the FAD hydrolysis.



**Figure III-6.** Resolution by thin layer chromatography of the FMN, FAD and holoWrbA. From left to right: 1mM FMN, 1mM FAD, 0.25mM WrbA+0.35mM FAD after one-month incubation.

However, EDTA is an inhibitor of pyrophosphatases (Akiyama *et al.*, 1982) and to eliminate the possibility of pyrophosphatase contamination, new crystallization

trials were set up with holoprotein (WrbA-FAD) in phosphate buffer in the presence of 1mM EDTA. The crystal was obtained after one month incubation at 22°C. However, in the resolved crystal structure only FMN was observed and thus the role of pyrophosphatases in the FAD hydrolysis can be excluded. These results strongly hint to the ability of WrbA to hydrolyze FAD, a property that has not been reported so far and needs to be further investigated.

The statistics of the crystallographic data are summarized in **Table III-4**.

	WrbA holoprotein
Radiation source	MX-14.2/BESSY II
Detector	MAR Mosaic CCD 225 mm
Wavelength (Å)	0.9171
Number of images	200
Rotation range per image (°)	0.5
Resolution range (Å)	22.71- 1.2 (1.23-1.20)
Space group	<i>P</i> 4 <sub>1</sub> 2 <sub>1</sub> 2
Unit-cell parameters (Å, °)	<i>a</i> = <i>b</i> = 61.15, <i>c</i> = 169.6; $\alpha = \beta = \gamma = 90$
Measured reflections	732496 (27490)
Unique reflections	97715 (5478)
Multiplicity	7.6 (5.0)
Wilson B (Å <sup>2</sup> )	10.2
Mosaicity (°)	0.2
Completeness (%)	96.6 (75.1)
<i>R</i> <sub>merge</sub> <sup>a</sup> (%)	6.4 (68.0)
$\langle I/\sigma(I) \rangle$	14.3 (2.2)

<sup>a</sup> $R_{\text{merge}} = \frac{\sum hkl \sum i |I_i(hkl) - \langle I(hkl) \rangle|}{\sum hkl \sum i I_i(hkl)}$ , where  $I_i(hkl)$  is the intensity of the *i*th measurement of reflection *hkl* and  $\langle I(hkl) \rangle$  is the average intensity of the reflection.

**Table III-4.** Data collection statistic for the holoWrbA crystal. Values in parentheses correspond to the highest resolution shell.

### 2.3.1. Structure Determination.

Structure of WrbA protein in complex with FMN was solved and refined to 1.2 Å. The structure consists of two compact monomers in asymmetric unit in chains A and B. Chain A contains 195 residues with residues 154-155 are not resolved. Chain B contains 180 residues built with two loops of 144-155 and 167-171 are being disordered.

Pairwise 3D alignment using PDBeFold service (Krissinel & Henrick, 2004) identified ten close PDB entries based on the combination of alignment length and rmsd (at least 70% of the secondary structure matching). The highest structural alignment match is with *E.coli* WrbA/FMN complex PDB ID 2R97 (Wolfova *et al.*, 2009) solved to 2.0 Å in the same space group with similar unit cell parameters and rmsd of 0.32 Å. The structure reported here contains FMN and has the highest resolution amongst available WrbA structures – 1.20 Å. All refinement statistics data is presented in table III-5.

	WrbA holoprotein
Resolution range (Å)	21.45- 1.20 (1.21-1.20)
No. of reflections	
working/test set	97637/4864
$R_{\text{work}}/R_{\text{free}}$ (%) <sup>a</sup>	15.31/18.60
No. of atoms	
protein/FMN/solvent	2829/62/306
<B> (Å <sup>2</sup> )	
protein/FMN/solvent	15.33/13.54/25.98
R.m.s. deviations	
Bond lengths (Å)	0.010
Bond angles (°)	1.40
Residues in Ramachandran plot (%)	
Most favoured regions	99.21
Allowed regions	0.79
Outliers	0.00
PDB code	3ZC2

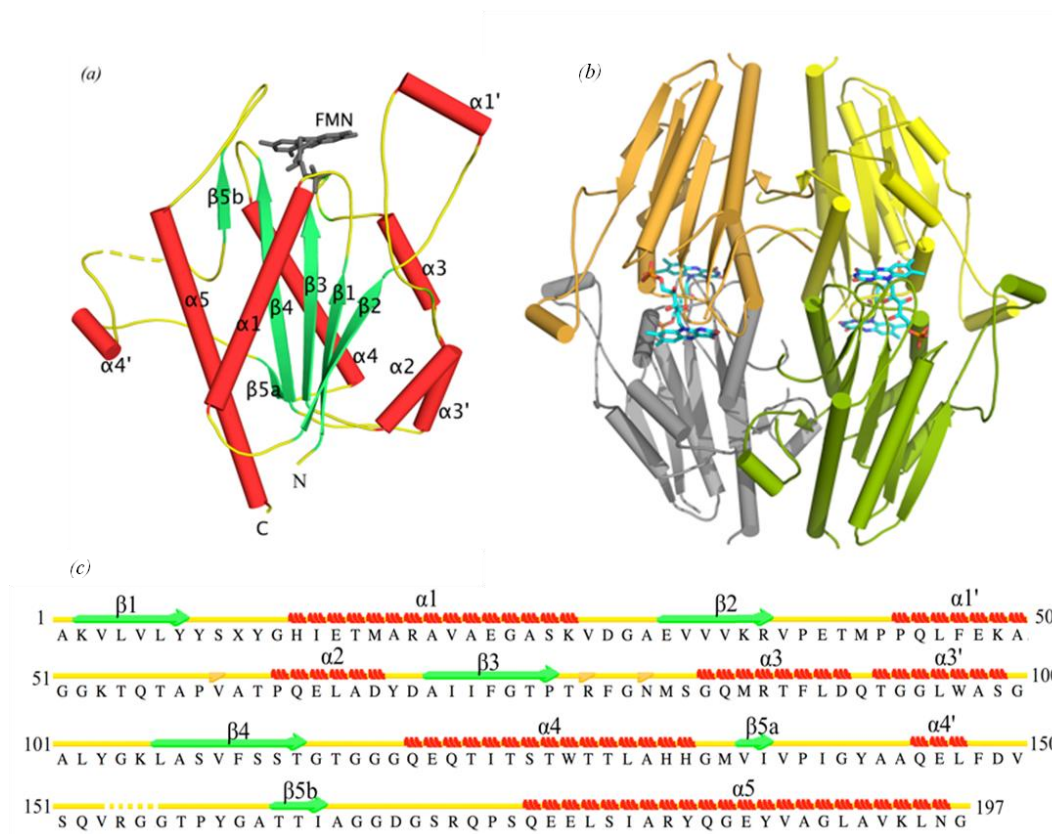
<sup>a</sup> $R = \frac{\sum |F_o| - |F_c|}{\sum |F_o|}$ , where  $F_o$  represents the observed structure factors and  $F_c$  the calculated structure factors based on the model,  $R_{\text{work}}$  was calculated based on the working set of reflections used in the refinement,  $R_{\text{free}}$  was calculated based on the test set of reflections excluded from the refinement.

**Table III-5.** Structure refinement statistics. The values in parentheses correspond to the highest resolution shell.



It was used the residue numbering in the structure follows as defined in Wolfova *et al.*, 2009 with the first residue an alanine. Wrba has a characteristic Flavodoxin-like fold of twisted five-stranded parallel  $\beta$ - sheets ( $\beta$ 1-  $\beta$ 5) with each strand followed by an  $\alpha$ -helix ( $\alpha$ 1-  $\alpha$ 5).

Secondary structure assignment by several algorithms in DSSP (Kabsch & Sander, 1983), STRIDE (Frishman & Argos 1995), PROMOTIF (Hutchinson & Thornton, 1996), HELANAL (Kumar & Bansal, 1996) based on our model showed that Wrba helix previously referred as  $\alpha$ 3 is split into two helices:  $\alpha$ 3 and  $\alpha$ 3' (Fig. III-7.).  $\alpha$ 3 of *E.coli* Flavodoxin forms a single helix corresponding to  $\alpha$ 3 of Wrba which is kinked with an average bending angle is  $28^\circ$ .



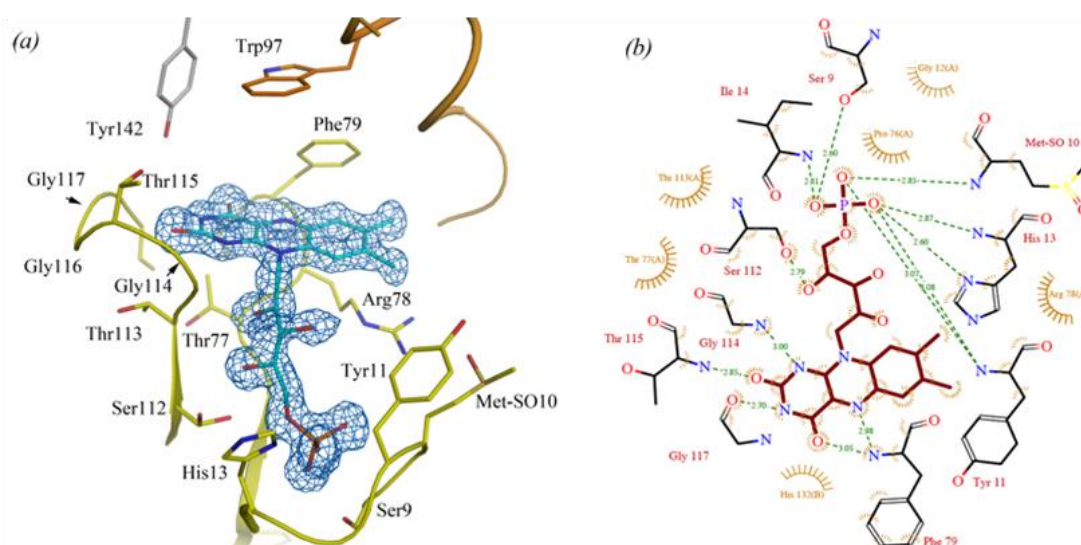
**Figure III-7.** (a) Representation of the monomer, chain A, of *E.coli* Wrba in complex with FMN. Secondary structure elements are coloured green ( $\beta$ -sheets) and red ( $\alpha$ -helices) and labelled accordingly. FMN is shown as a stick model. (b) Cartoon representation of the tetrameric arrangement of Wrba with different color of each monomer and FMN shown as a stick model. (c) Sequence of the *E.coli* Wrba protein chain A with the corresponding secondary structure assignment derived from the crystal structure was calculated with STRIDE. The numbering of secondary structure elements follows *E.coli* nomenclature (Wolfova *et al.*, 2009). Residues highlighted in yellow make contact with FMN.

Additionally to Flavodoxin fold there are three insertions in WrbA. Insertion 1 is between  $\beta 2$  and  $\alpha 2$  and contains an  $\alpha$ -helix ( $\alpha 1'$ ) and an isolated  $\beta$ -bridge ( $\beta 2'$ ). Insertion 2 forms a loop containing 3-10 helix ( $\alpha 4'$ ) and splits  $\beta 5$  into  $\beta 5a$  and  $\beta 5b$ . Insertion 2 is also specific for long-chain flavodoxins (Sancho, 2006). Lastly, there is a short loop insertion between  $\beta 5b$ - $\alpha 5$ . Residues 154-155 and 144-155 are disordered in Loop 2 in molecule A and B respectively. Above loops have different molecular environment and participate in lattice contacts. They also lie close to the FMN binding sites of the symmetry related molecules. Therefore disorder can be lattice and cofactor induced. The dimer interface in both protomers in an asymmetric unit is realized through the whole length of  $\alpha 4$  (119-133), residues following  $\beta 2$  (77- 83) and the  $\alpha 3$  (84-91) via hydrogen bonds and non-bonded interactions.

Analysis of the structure by PISA service indicates that the quaternary structure of WrbA is tetrameric with buried area of 12517.0 Å<sup>2</sup> and each monomer binding one FMN molecule, which is in agreement with the biochemical data (Grandori *et al.*, 1998).

### 2.3.2. FMN Binding.

FMN is located at the periphery of each monomer and forms a network of hydrogen bond contacts with the protein (fig. III-8.). Isoalloxazine ring of FMN is coordinated by the backbone atoms of the 114-118 loop between  $\beta 4$ - $\alpha 4$  by Gly114, Thr115 and Gly117 and from the second monomer by the sidechain of His132. Corresponding 114-118 loop position is altered in the second monomer resulting in additional bond with amide hydrogen of Gly116 while the bond with amide of Thr115 is lost. Phe79 and Arg78 are stacking on the *re* and *si* side of the ring respectively in both molecules with amide of Phe79 forming hydrogen bond with the N5 of the FMN ring. Trp97 is located ~7 Å away from the *re* face of the isoalloxazine ring and forms a roof of the hydrophobic substrate binding pocket.



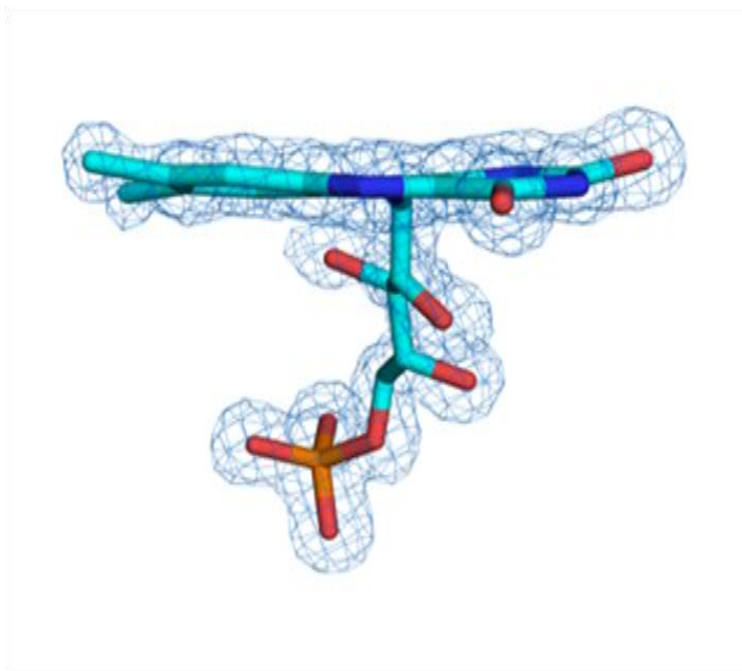
**Figure III-8.** Schematic diagram showing contacts of the FMN cofactor to protein residues, chain A. Hydrogen bonds are shown as dotted green lines (red residue numbers) and van der Waals interactions by red shading (black residue numbers); atoms are in standard colours. Figure was generated using LigPlot+ (Laskowski & Swindells, 2011).

Structure of WrbA with its natural substrate showed that nicotinamide ring of NADH is specifically positioned between highly conserved Trp97 and the ring of FMN for the electron transfer, although PEG molecule was modeled in this position in PDB (Andrade *et al.*, 2007). In the corresponding region of our structure we observed an unexplained density in the *Fo*-*Fc* map, which resembles a flat ring structure and a tail, stacking against Tyr11 which is conserved amongst WrbA proteins. We cannot explain the density by the PEG molecule and hypothesis WrbA could have been co-purified with the natural substrate bound in the substrate binding pocket with low occupancy. The FMN ribityl tail is surrounded by water molecules and forms hydrogen bonds with carbonyl of Thr77 and sidechain of highly conserved Ser112 found in two conformations. Phosphate oxygens are coordinated by peptidyl atoms of His13, Met10, Tyr11, Ser9 and Ile14. FMN was modeled in a single conformation in both monomers. Conformation of both FMN molecules is similar except for the position of the O3 and O4 of the ribityl tail. In one molecule both are pointing towards the *re* face of the ring, whereas in the second molecule O4 is oriented towards the *si* face. Different conformations share the same protein contacts varying only in water environment. Met10 contacting O3 of the phosphate via the hydrogen bond through the amide nitrogen, in our structure was modeled in a form of methionine sulfoxide (Met-SO) (fig III-8.). In other structures of WrbA (3B6I, 1.66 Å and 2R97 2.0 Å) Met10 was modeled in an alternative conformation. In our case refinement of



Met10 in two alternative conformations rather than in the form of Met-SO does not agree with the positive peak in the Fourier difference map and does not lead to proper hydrogen bonding network with neighboring water molecules and ionic interaction with the Arg78 sidechain. Met10 sidechain is located  $\sim 6.5$  Å away from the benzene ring of the isoalloxazine moiety and may serve to prevent oxidation of residues in the FMN binding pocket thus acting as an antioxidant as was found in other systems (Luo & Levine, 2009). Met10 is not conserved across flavodoxins and WrbA proteins of different species. Further experiments are needed to explore if Met10 oxidation plays any role in protein function or stability. Interestingly, Met42 located 4 Å away is not oxidized. Therefore we doubt the oxidation happened due to the action of oxygen reactive species generated by the X-ray exposure.

High resolution of the data allowed us accurately analyze FMN cofactor geometry. FMN undergoes conformational changes depending on its redox state, which results in the variety of dihedral angle values ( $0^\circ$  to  $34^\circ$ ) between the pyrimidine and benzene planes of the isoalloxazine moiety (Senda *et al.*, 2009). Based on crystallographic and *ab initio* calculation data oxidized flavin and one-electron-reduced semiquinone appears to be planar whereas the two-electron-reduced hydroquinone adapts a bent conformation (Senda *et al.*, 2009). FMN isoalloxazine ring in our model is not bent but has a propeller twist along the length of the ring (fig. III-9.), which agrees with the oxidized and neutral semiquinone models FMN and FMNH derived by molecular simulation methods (Røhr *et al.*, 2010). Yellow colour of crystals before data collection suggested the oxidized form of FMN, although caution should be taken assigning FMN state in the structure as oxidized as it is susceptible to react with photoelectrons generated in the crystal by X-rays during data collection leading to its reduction (Røhr *et al.*, 2010).



**Figure III-9.** FMN is shown as a stick model with the corresponding simulated annealing  $F_o - F_c$  map contoured at 3.5 sigma. Propeller twist along the length of the FMN isoalloxazine ring.

**3. LIMITED PROTEOLYSIS OF WRBA PROTEIN.**

Limited proteolysis of WrbA protein was performed according to Carey (Carey, 2000). Apo and holoWrbA in concentrations of about 50uM apoWrbA and 50uM holoWrbA (50uM WrbA+200uM FMN) in 20 mM Sodium Phosphate buffer, pH 6.5 were used for proteolytic experiments. Proteases, obtained commercially from Sigma Aldrich Company, were diluted from freshly prepared stocks.

<b>Protease</b>	<b>pH optimum</b>	<b>Cleavage</b>
Subtilisin <b>S</b>	6 – 11	aromatics, leucine, glutamic acid
Trypsin <b>T</b>	7 – 9	lysine, arginine
Chymotrypsin <b>Ch</b>	6 – 9	most amino acids
Papain <b>P</b>	6 – 7	basic amino acids, leucine, glycine

The proteolytic reaction was started by mixing the protein solution with the protease in a ratio of 2:1 and the reaction was performed at 25 °C. The reaction was stopped by addition of SDS-PAGE loading buffer and immediate boiling after each 10 minutes for the range-finding experiment and after 15 and 30 minutes in time-course experiment. The proteolytic digestion was analyzed by SDS-PAGE.

The range-finding experiment was performed with four different proteolytic enzymes to identify the best concentrations of protease for a time-course digestion experiments of apo and holoWrbA.

Subtilisin: 1:10, 1:20, 1:50, 1:100, 1:200, 1:400;

Papain: no dilution, 1:5, 1:10, 1:20; 1:30

Trypsin: 1:10, 1:20, 1:30, 1:50;

Chymotrypsin: 1:10, 1:20, 1:30, 1:50.

Following concentrations of the proteases were chosen for further proteolytic experiments after the range finding optimization:

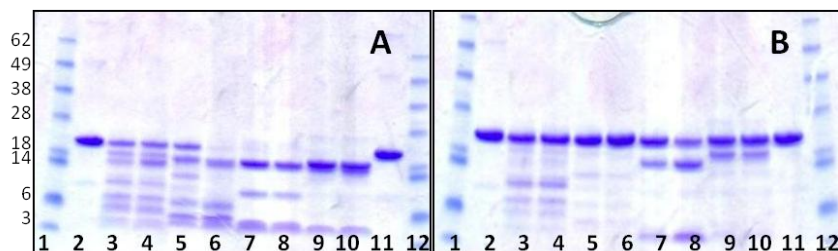
Subtilisin at the dilution 1:400;

Papain at the dilution 1:30;

Trypsin at the dilution 1:30;

Chymotrypsin at the dilution 1:30.

Reactions were stopped after 15 and 30 minutes by adding SDS-loading buffer and immediate boiling for SDS-PAGE monitoring and by adding of 1%TFA and freezing at  $-80^{\circ}\text{C}$  for further MS analysis. (Fig. III-10.)

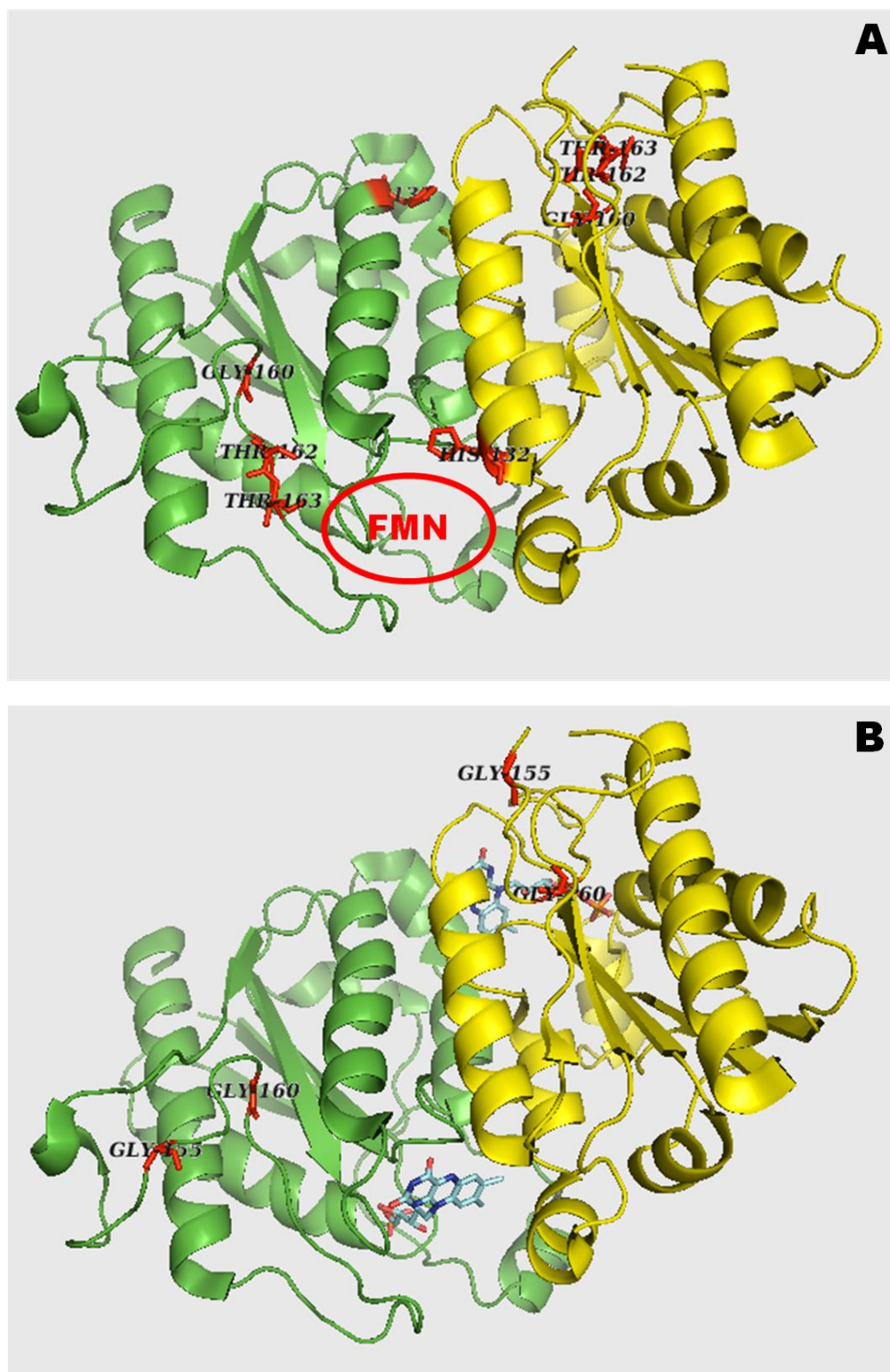


**Figure III-10.** Time-course digestion of apo and holoWrba by four different proteases (subtilisin, trypsin, chymotrypsin, papain). A. Digestion of apo protein. B. Proteolysis experiments for holoWrba. Lane 1 and 12, molecular weight marker; lane 2 and 11, apoWrba (A)/ holoWrba (B) control; lane 3 – 4, digestion of Wrba with Subtilisin at 1:400 dilution, reaction was stopped after 15 (lane 3) and 30 (lane 4) minutes; in lane 5 – 6 protein has been cleaved by Papain (1:30). Time points were 15 (lane 5) and 30 (lane 6) minutes; lane 7 – 8, Wrba was incubated with Trypsin (1:30) for 15 (lane 7) and 30 (lane 8) minutes; lane 9 – 10, effect of limited proteolysis by Chymotrypsin on Wrba. 15 (lane 9) and 30 (lane 10) minutes are the time points, which were monitored on the 12% gel SDS-PAGE.

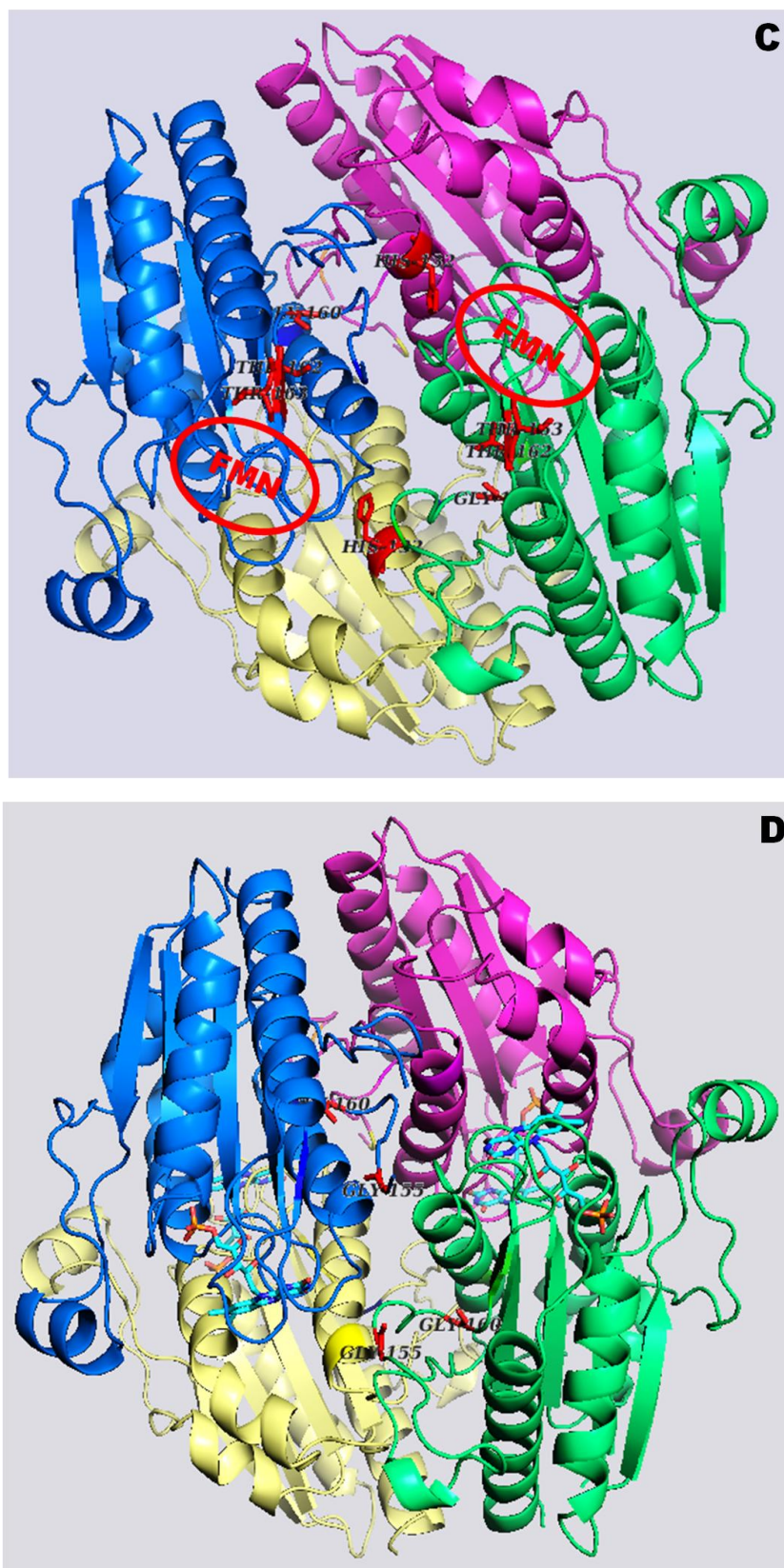
The MS sequencing experiments were carried out by our collaborators in Prague. Proteolytic cleavage usually occurs at solvent-accessible, flexible region. In case of apoWrba initial cuts were detected at 160Gly for Trypsin, 162Thr for Subtilisin, 163Thr for Papain and only Chymotrypsin cut the apo protein at 132His. The location of proteolytic cleavages in holoWrba is very similar to apo protein. Chymotrypsin, subtilisin and papain cleaved the holoWrba at 160Gly, trypsin initial cut was at 155Thr. Picture (fig. III-11.) demonstrates location of those cuts in the dimer and tetramer of apo and holoWrba.

Most of cuts placed at the beginning of flexible loop in position, which is accessible to proteases only in case of dimer. Calculation of dimer-tetramer ratio for apoWrba ( $50\mu\text{M}$ ) shows that dimer is a dominant form of the apo protein in the solution at conditions used for proteolytic experiment. Thus, the proteolytic intermediates appeared mostly from dimers. The monitoring of proteolytic digestion on the SDS-PAGE (fig. III-10.) demonstrates that about 80 % of the apoWrba was cleaved. This also confirms that dimers are dominant form of apoWrba at concentration  $50\mu\text{M}$  at conditions used for proteolytic experiments. Contrariwise, it was calculated that the holoWrba consists of dimers and tetramers in the solution at conditions used

for the proteolytic experiments. Tetramers are not protease-accessible due to the spherical geometry of protease molecule (figure III-11.), thus the proteolytic intermediates were formed from dimers. Comparison of apo and holo protein digestion on the SDS-PAGE also confirms this suggestion. Only about 40% of the HoloWrbA were cleaved by proteases.







**Figure III-11.** Cartoon representation of proteolytic cuts location for dimer and tetramer apo/holo Wrba.

In summary, the proteolytic experiments determined that the WrbA protein exists in the solution in two forms: dimer and tetramer. Analysis of the location of initial cuts in dimer and tetramer results in the conclusion that the tetramer is more resistant to proteolysis in consequence of its highly ordered structure.

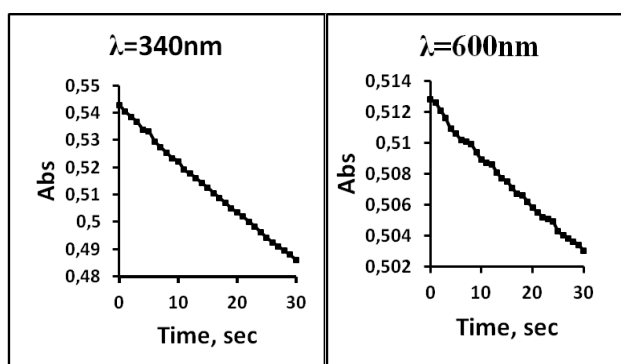
## 4. KINETIC STUDY OF THE WRBA PROTEIN

### 4.1. MICHAELIS-MENTEN KINETICS.

WrbA can transfer two electrons at a time from NADH to quinone acceptors. The electron transfer kinetics can be observed spectrophotometrically (Perkin Elmer Lambda 20 UV VIS Spectrophotometer) under steady-state conditions. These reactions follow the decrease in NADH absorbance at 340 nm upon oxidation during reduction of benzoquinone. The reactions were carried out by manual mixing.

This assay is used to measure the rates of WrbA electron transfer and to evaluate different compounds that might function as the true physiological electron donors or acceptors.

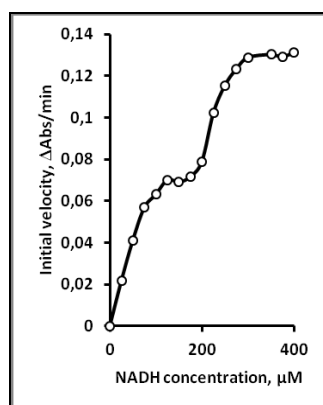
The main goal of preliminary experiments was to determine the optimal conditions for assay kinetic experiments. The single adsorption slopes were monitored with this purpose at different concentrations of the protein in the reaction mixture. The best slope was found for 20nM WrbA for reaction mixture contained NADH (50 $\mu$ M) with BQ (50 $\mu$ M) and for mixture composed of NADH (50 $\mu$ M) and DCPIP (32 $\mu$ M). Measurements were done at 340nm for NADH and at 600nm for DCPIP (Fig. III-12.).



**Figure III-12.** Plots represent the kinetic slopes at 340nm and 600nm. Linear decreasing of absorbance indicates high quality of the kinetic assay.

The next step of kinetics study of WrbA protein was a titration of NADH in the range 0 to 400 $\mu$ M at constant concentration of BQ. All measurements were done at 5 $^{\circ}$ C. Surprisingly, it was found the intermediary plateau region on the concentration-dependence plot for NADH at about 100-200  $\mu$ M NADH (Figure III-13.).

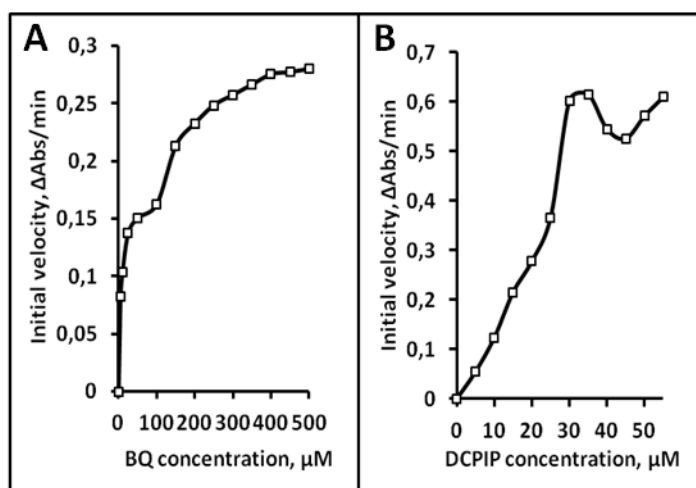




**Figure III-13.** The substrate concentration-dependence plot for NADH demonstrates the presence of an intermediary plateau region on the substrate concentration-dependence plot for NADH at about 100-200  $\mu\text{M}$  NADH.

Preliminary experiments ascertained that the initial rates were directly proportional to the enzyme concentration at 0.23 – 2.3  $\mu\text{g}$  protein per ml. The concentration of WrbA 0.46  $\mu\text{g}/\text{ml}$  was used for further experiments.

An intermediary plateau was discovered also on concentration-dependence plot for BQ (Fig. III-14A). Interestingly, there was a deep on the concentration dependence plot in case of titration of DCPIP (Fig. III-14B).



**Figure III-14.** Titration of BQ and DCPIP at fixed concentration of NADH (50 $\mu\text{M}$ ). **A.** Concentration dependent plot for BQ. Intermediate plateau is present at 75 – 150  $\mu\text{M}$  of BQ. **B.** DCPIP titration at constant NADH (50 $\mu\text{M}$ ) concentration. Deep is present at 30 – 50  $\mu\text{M}$  of DCPIP.

WrbA is a multimeric protein and in solution in equilibrium it exists in two forms- dimer and tetramer. (Grandori *et al.*, 1998) The intermediate plateau could be a consequence of shift from dimer to tetramer population.

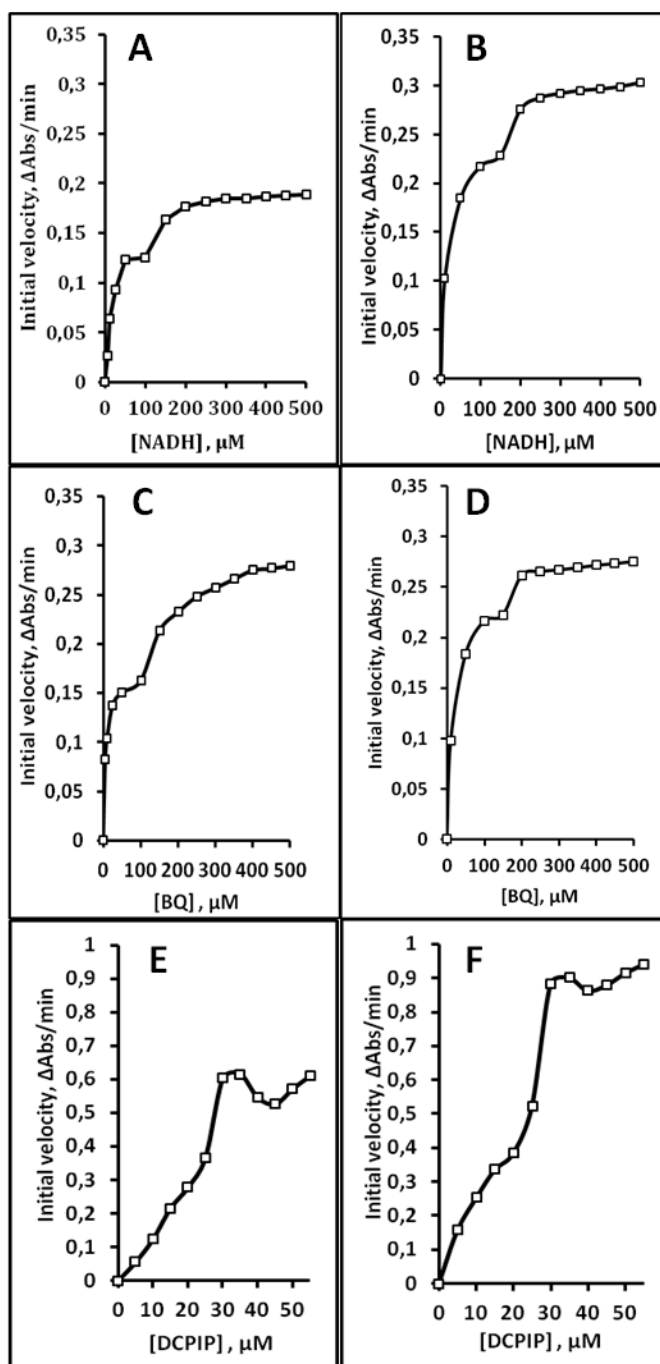
The main aim of further experiments was to investigate kinetic properties of WrbA protein. To study the kinetic properties we can address kinetics from several different perspectives:

- Dependence activity of WrbA on the concentration of one of the substrate;
- Influence of the temperature on WrbA kinetics properties;
- Effect of physical-chemical parameters change on the WrbA kinetics;
- Influence of different modulators on the steady-state kinetics;
- Inactivation and reactivation of WrbA protein by the temperature shift;

The main goal of kinetics study was an evaluation of kinetic mechanism of WrbA protein, which was determined by inhibition experiments. The results are presented below.

#### **4.2. DEPENDENCE ACTIVITY OF WRBA ON THE CONCENTRATION OF ONE OF THE SUBSTRATE.**

Enzymatic assays for different concentrations of one of the substrates were carried out at 5°C. Titration of the first substrate were done in range 0-500  $\mu\text{M}$ , whereas the fixed concentrations of the second substrate were chosen 50, 100, 200, 500  $\mu\text{M}$ . Each curve for NADH and for BQ presented the two plateau behavior (fig. III-15.). This kinetic behavior is a very similar to kinetics published for mammalian DT-diaphorase, but no molecular explanation of this effect has been proposed. The enzymatic assays with DCPIP instead of BQ were examined similar as has been demonstrated for DT-diaphorase. Titrations were done in range 1-55  $\mu\text{M}$  of DCPIP, because it was limited by high absorbance of this substrate. Similar to mammalian DT-diaphorase, deepes were found on the concentration dependent plot for DCPIP.

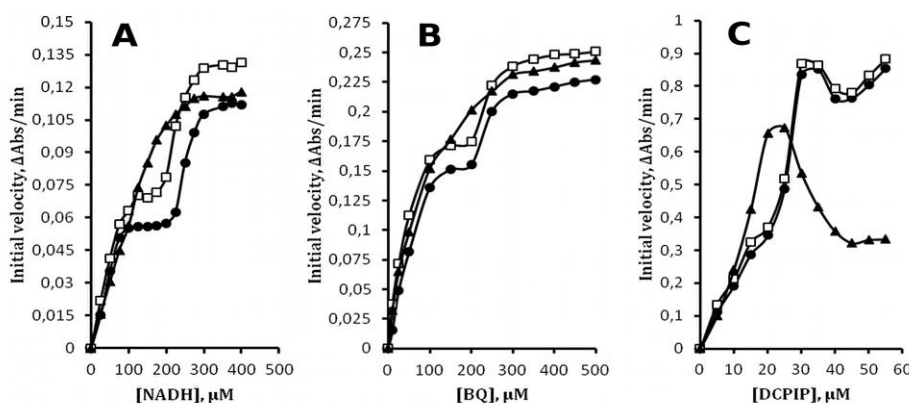


**Figure III-15.** Concentration dependent plots for NADH (A, B), BQ (C, D), DCPIP (E, F). **A, B** – biphasic kinetic behavior of WrbA on the concentration dependent plot for NADH at 50 μM BQ (A) and 500 μM BQ (B); **C, D** – intermediary plateau on the titration plots for BQ at 50 μM NADH (C) and 500 μM NADH (D); **E, F** – presence of deeps on the concentration dependent plot for DCPIP at 50 μM NADH (E) and 500 μM NADH (F).

Existing of the dimer-tetramer equilibrium for apo WrbA with  $K_d=1.4$  has been published by Grandori *et al.*, 1998. Most probably, similar equilibrium exists for holo form WrbA, what could be an explanation of two plateau behavior.

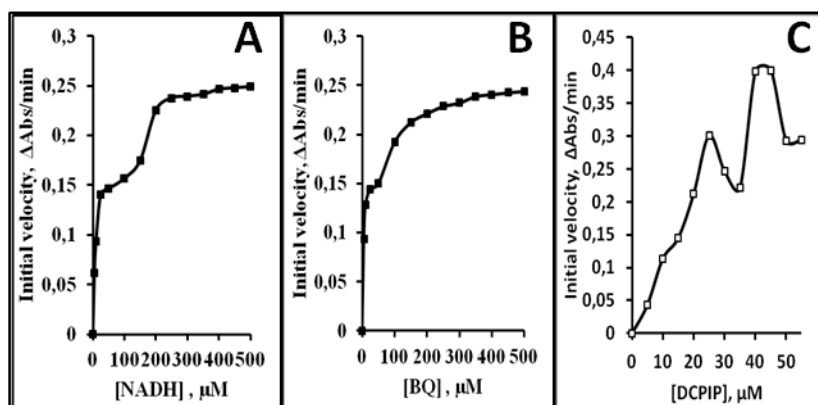
### 4.3. EFFECT OF TEMPERATURE ON THE STEADY-STATE KINETICS.

The next series of experiment was done to investigate the influence of temperature on the kinetic properties of WrbA protein. The WrbA was incubated either at 23°C or kept at 5°C. Figure 4.5.A shows that the intermediary plateau disappears on the substrate concentration-dependence plot for NADH when the enzyme was incubated at 23°C for 120 min before adding it to the test system. But this effect was reversible and after recooling of the previously warmed protein during 120 min at 5°C the intermediary plateau appears again. Similar results were demonstrated for BQ and DCPIP titrations (Fig. III-16.B, C). But these features are not unique only for WrbA. The same kinetics properties of the enzyme have been reported for mammalian DT-diaphorase (Hollander *et al.*, 1975), but no molecular explanation has been proposed.



**Figure III-16.** Effect of warming of the enzyme on the substrate concentration-dependence plot for NADH (A), BQ (B), DCPIP (C). **Squares-** The enzyme was incubated at 5°C prior to addition to the assay mixture. **Triangles-** The enzyme was incubated at 23°C for 120 min prior to addition to the assay mixture. **Rings-** Enzyme first maintained at 23°C for 120 min and then at 5°C for 120 min prior to addition to the assay mixture.

The kinetic assays for WrbA protein incubated at 37°C for 120 minutes were performed. Figure III-17. demonstrates the results of those experiments.



**Figure III-17.** Temperature effect on the concentration-dependence plot for NADH (A), BQ (B), DCPIP (C). Protein was incubated at 37°C for 120 min before adding to the test system.

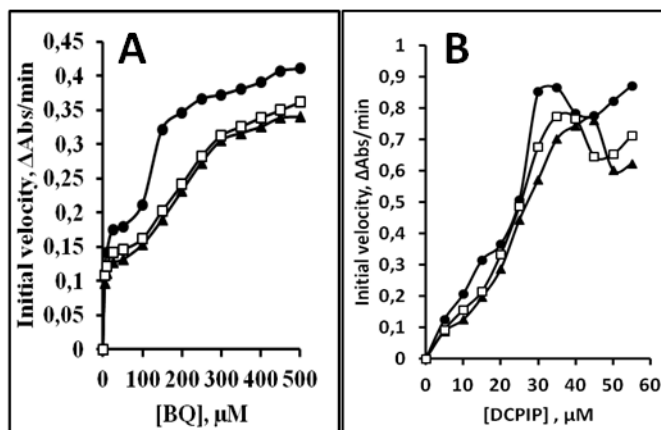
Surprisingly, the two plateau behavior was observed on concentration dependent plot for NADH and BQ. Probably, protein exists in tense state at optimal temperature of WrbA expression. This consideration imply that the equilibrium between dimer and tetramer is dependent on the temperature shift, thus at room temperature protein exist in a majority in one conformation state (either dimer or tetramer). At ice-cold temperature and at 37°C protein exists in two oligomeric states, the equilibrium is shifted either to dimers or tetramers with temperature change. Probably, extreme conditions shift the equilibrium to one of the oligomeric states.

#### 4.4. EFFECT OF DIFFERENT PHYSICAL-CHEMICAL FACTORS ON THE ACTIVITY RATE OF WRBA

To have a complete picture of kinetic properties of the WrbA, the kinetic assays of WrbA was monitored under influence of physical chemical factors such as pH, salt presence and adding of several modulators to the test system.

##### 4.4.1. Influence of pH and Salt on the Steady-State Kinetics of WrbA.

The study of influence of pH on the concentration dependent plot for each of the substrate in range 6.0-8.0 did not show the significant difference in kinetics. These experiments confirm the fact that the optimal range of pH for WrbA is quite wide. In contrast to pH influence, a salt presence in a test system demonstrates important difference on the concentration dependence plot for each of the substrate (Fig. III-18).



**Figure III-18.** Influence of NaCl on the concentration dependence plot for BQ (A) and DCPIP (B). Enzymatic assay were done at  $[NADH] = 50\mu M$ . **Rings** – WrbA protein was incubated at  $5^{\circ}C$  for 120 minutes. Salt was not added; **Squares** – protein was incubated with  $0.25M$  NaCl for 120 minutes at  $5^{\circ}C$ ; **Triangles** – WrbA was kept out with  $0.5M$  NaCl for 120 minutes at  $5^{\circ}C$ .

Figure III-18. shows the effect of salt on the concentration dependence plot for BQ and NADH with constant concentration of  $NADH=100\mu M$  and  $BQ= 50\mu M$  correspondingly. Experiments were done at  $5^{\circ}C$ . Plots demonstrate disappearing of the intermediate plateau with increasing of salt concentration. Also the initial velocity is decreasing with increasing the salt concentration in the solution. Dependence of reaction rate on DCPIP (substrate) concentrations in the absence and presence of different concentrations NaCl shows the deep on the curve shifts to the right side with increasing of NaCl concentration. These facts can be explained by effecting salt by ion fields and as the result the affinity changes of the substrate to the protein binding site. Furthermore hyperbolic shape of the curves presents on the all curves.

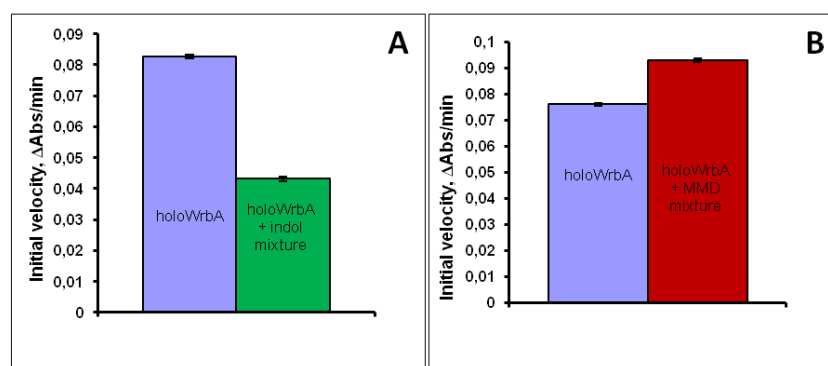
#### 4.4.2. Effect of Different Modulators on the WrbA Protein.

In the next series of experiments protein was incubated with different modulators for 120 minutes at  $5^{\circ}C$ . The initial rates of the protein were measured standard way. Table III-6 demonstrates the most interesting results of modulators effect on the protein activity.

Modulator	Effect
8-hydroquinone	Inhibition
Indol	Inhibition
Dicoumarol	Inhibition less than 10%
Tryptophan	Inhibition
Tryptophan repressor	Inhibition less than 10%
Tryptophan + Tryptophan repressor	No effect
BSA	Inhibition
Triton	Inhibition less than 10%
Membrane mimicking detector	Activation

**TABLE III-6.** Effect of different modulators on WrbA activity.

Figure III-19. shows the most interesting results. As can be seen on the picture indol inhibited the enzyme. Effect of the indol we can explain that probably the WrbA can be involved to signaling pathway. Indol is a well known signaling molecule in stationary phase (Lacour & Landini, 2004). Also it has been proposed that the function of WrbA homolog from *Arabidopsis thaliana* and *Schizosaccharomyces pombe* could be related with cell signaling (Daher *et al.*, 2005; Laskowski *et al.*, 2002).



**Figure III-19.** Effect of various modulators. **A** – influence of indol, demonstrates inhibition effect on the WrbA, activity of the protein is two times less in presence of indol; **B** – influence of the membrane mimicking detergent on WrbA activity. Protein preincubated with membrane-mimicking detergent (MMD) showed higher activity than the protein alone.

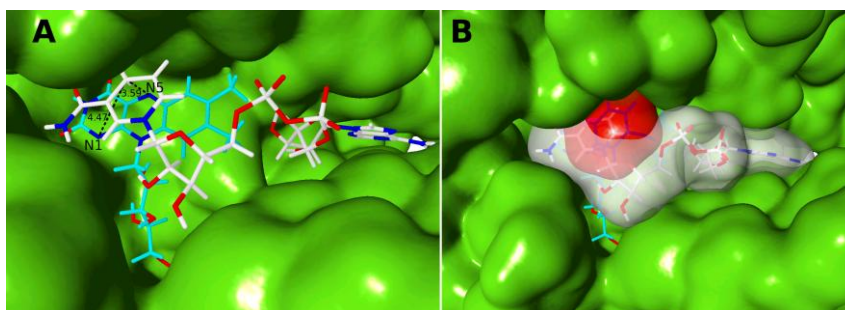
As WrbA kinetics is similar to one described for DT-diaphorase, it was expected similar influence of modulators on the WrbA activity. Dicoumarol has strong inhibition effect on the diaphorase (Hall *et al.*, 1972), but, surprisingly, this compound had no influence on WrbA activity.

Adding of the membrane-mimicking detergent and BSA to the WrbA solution induces the increasing of the activity rate of the protein similar as for DT-diphorase (Hall *et al.*, 1972). The membrane mimicking detergent is an activator of WrbA, what can be a result of the WrbA physiological role probably involves membrane binding. As the WrbA catalyzes the electron-transfer reactions, so it allows suggesting that the protein function close to the membrane surface in the cell, where is going the most of electron transfer reactions.

#### 4.5. KINETIC MECHANISM.

Closer studies of the WrbA active site by using docking analysis were performed in our group with the aim to find an appropriate position for substrates in the binding site based on the calculation of binding energies. The preferential position of NADH was (has been) found above the izoalloxazine ring of FMN. This location of NADH molecule permits electron transfer between this substrate and FMN (Kishko *et al.*, 2012).

The favorable location of NADH in binding site was compared with founded preferable position of NAD (oxidized substrate) in active site of reduced holoWrbA. The analysis displays that the docked positions were almost identical for both dinucleotides.

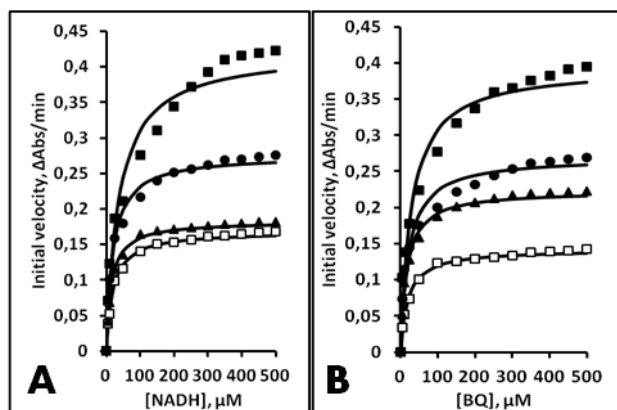


**Figure III-20.** A Active site of WrbA with found favored position of NADH there. B Analysis of positions of both of the substrates (NADH, BQ) in WrbA active site. (Picture taken from Kishko *et al.*, 2012)



Upon careful docking study of holo WrbA active site was evaluated the possibility of simultaneous binding both of the substrates in active site. The preferable found position of NADH was compared with the position of benzoquinone (BQ) (PDB ID 3B6K) published by Andrade *et al.*, 2007.

Figure III-20. presents the result of comparison of NADH and BQ binding positions. The docking analysis concludes that both of the substrates cannot occupy the active site simultaneously. That confirms theoretically the idea (hypothesis) that the possible kinetic mechanism for WrbA is a ping-pong one. To experimentally verify these results and evaluate the WrbA kinetic mechanism, a series of enzymatic assays were carried out. Enzyme was preincubated at 23°C to avoid the two plateau behavior and to use the single hyperbola for further calculations. The results of NADH titrations from 0 to 500  $\mu\text{M}$  at four fixed concentrations of BQ, 10, 20, 50, and 100  $\mu\text{M}$  are presented in figure III-21A. Figure III-21B shows the results of BQ titration in the range from 1 to 500  $\mu\text{M}$  at four constant concentrations of NADH, 10, 20, 50, and 100  $\mu\text{M}$ .



**Figure III-21.** Concentration-dependence plot for NADH (A) at fixed concentrations of BQ 10 (white squares), 20 (triangles), 50 (rings), 100 $\mu\text{M}$  (black squares); and for BQ (B) at fixed concentrations of NADH 10 (white squares), 20 (triangles), 50 (rings), 100 $\mu\text{M}$  (black squares). Enzymatic assays were carried out at 23°C.

All plots demonstrate single hyperbolas. Each of eight datasets were used for calculations of apparent kinetic constants  $K_{m,app}$  and  $V_{max,app}$ , which are presented in Table III-7. The ratio of apparent  $V_{max}$  to apparent  $K_m$  is constant with substrate concentration in case of ping-pong mechanism (Cleland, 1963). The ratio calculated for WrbA was approximately the same except of the lowest concentrations of the substrates. This fact supports a ping-pong mechanism for WrbA.

Concentration of fixed substrate ( $\mu\text{M}$ )	Apparent $V_{\text{max}}$ ( $\Delta\text{Abs}/\text{min}$ )	Apparent $K_m$ ( $\mu\text{M}$ )	App. $V_{\text{max}}/\text{App. } K_m$ ( $\text{min}^{-1} \mu\text{M}^{-1}$ )	Error ( $\text{min}^{-1} \mu\text{M}^{-1}$ )	
NADH	10	0.1421	19.0	0.00748	0.00027
	20	0.2231	16.2	0.01377	0.00043
	50	0.2691	20.7	0.01300	0.00048
	100	0.3946	28.2	0.01377	0.00075
BQ	10	0.1686	19.2	0.00878	0.00032
	20	0.1823	14.9	0.01223	0.00035
	50	0.2761	19.3	0.01431	0.00053
	100	0.4224	36.3	0.01163	0.00079

**Table III-7.** Kinetic constants of WrbA.

Additionally, the product inhibition pattern was analyzed for pairs NAD/BQ, NADH/BQH<sub>2</sub> and NAD/NADH, BQ/BQH<sub>2</sub> to further confirm the ping-pong mechanism and to evaluate the type of ping-pong as random or a sequential bi-bi mechanism.

Table III-8 presents the results of all product inhibition experiments. The bi-bi kinetic mechanism introduced by Cleland, 1963 was refused for WrbA. BQH<sub>2</sub> shows noncompetitive inhibition in all conditions, what means that it can bind to multiple enzyme forms or sites. NAD shows noncompetitive inhibition with either substrate when the other substrate is at low concentrations. At high NADH concentrations, NAD and BQ are competitive means they bind to a common site or sites. At high BQ concentrations, NAD and NADH are uncompetitive indicating they bind to different sites, and that at least one NAD binding site does not bind BQ. Thus, the inhibition experiments confirm the most probable kinetic mechanism for WrbA is a ping-pong mechanism with multiple enzyme forms or sites with different affinities for the different substrates and products.

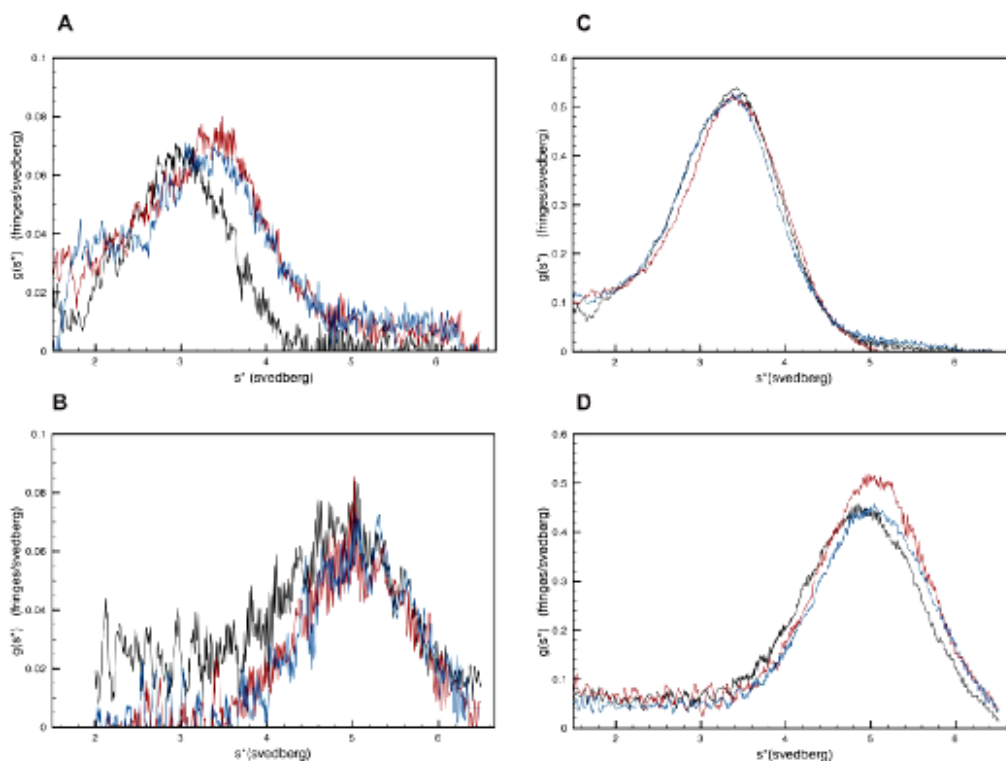
Varied substrate		Product	
		NAD	HQ
NADH	At 20 $\mu\text{M}$ BQ	Noncompetitive	Noncompetitive
	At 2mM BQ	Uncompetitive	Noncompetitive
BQ	At 20 $\mu\text{M}$ NADH	Noncompetitive	Noncompetitive
	At 2mM NADH	Competitive	Noncompetitive

**Table III-8.** Product inhibition.

The explanation of multiple enzyme forms can be the presence of two holoWrbA forms (dimeric and tetrameric holoWrbA) in the solution. The fact of dimer-tetramer equilibrium has been reported for apo WrbA (Grandori *et al.*, 1998). The preliminary ultracentrifugation (AUC) experiments for holo WrbA at the same condition as were used Grandori *et al.*, 1998 for apoWrbA, gave useless results, because of presence of

the natural co-factor FMN in the solution. As the high concentration of FMN gave high noise signal, the adsorption spectra were unreadable for chosen wavelengths. Further ultracentrifugation experiments for holo WrbA were done by member of our group with the respect to FMN limitation factor. The AUC results showed that the dissociation equilibrium constant for holoWrbA was at least ten times higher than for apo WrbA. Therefore, 99.9% of dimer form is present in the solution at 20nM (concentration used for enzymatic assays) holoWrbA (monomers).

The temperature effect also was studied for apo and holoWrbA using AUC in the collaborating group in Princeton. Interestingly, both apo and holoWrbA in presence and absence of NAD were sensitive to temperature change and the AUC results showed the shift to higher  $S$  values with temperature. (Fig. III-22.) This highlights that the WrbA presents in two forms (dimer and tetramer) in the solution and the ration of dimer-tetramer changes with the temperature. The AUC results clearly show that the dimers predominate in the solution at low temperature and the amount of tetramers is increasing with temperature.



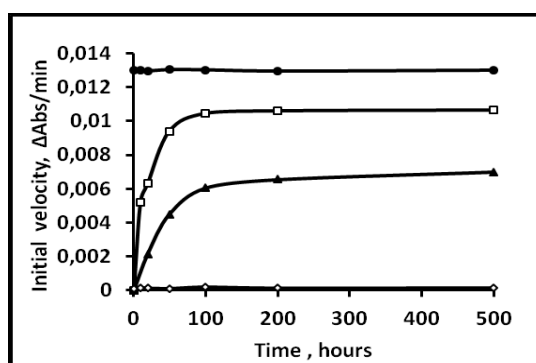
**Figure III-22.** Sedimentation velocity. Each panel shows the sedimentation velocity profile using the whole boundary  $g(s^*)$  approach of Stafford, 1992 for apoWrbA (black), WrbA+50  $\mu$ M FMN (red), and WrbA+50  $\mu$ M FMN+0.5 mM NAD (blue). A, 3  $\mu$ M total protein (monomer) at 5°C; B, 3  $\mu$ M total protein (monomer) at 20°C; C, 20  $\mu$ M total protein (monomer) at 5°C; D, 20  $\mu$ M total protein (monomer) at 20°C. (Picture taken from Kishko *et al.*, 2012)

Also the presence of several enzyme forms was confirmed by NMR experiments for WrbA premixed with NAD, which were done by our collaborator Harish Balasubramian. The comparison of NMR spectra of NAD alone with the spectra of WrbA-NAD mixture together with integration of NMR peaks result in the suggestion of existing more than one enzyme form in the solution. All these facts confirm the hypothesis about dependence of two plateau behavior on the presence of multiple forms of enzyme in the reaction mixture.

#### 4.6. STABILITY OF WRBA PROTEIN.

##### 4.6.1. Reactivation Temperature Inactivated Protein.

The stability of WrbA protein was studied at the next series of experiments, when the protein was inactivated by incubation at room temperature during 48 hours. Then the protein was reactivated by recooling of the WrbA. As can be seen on the figure III-23, in case of adding to the protein mixture the membrane-mimicking detergent before cooling, a reactivation of the enzyme goes faster and the initial rate of the WrbA is higher than in case of just recooling.



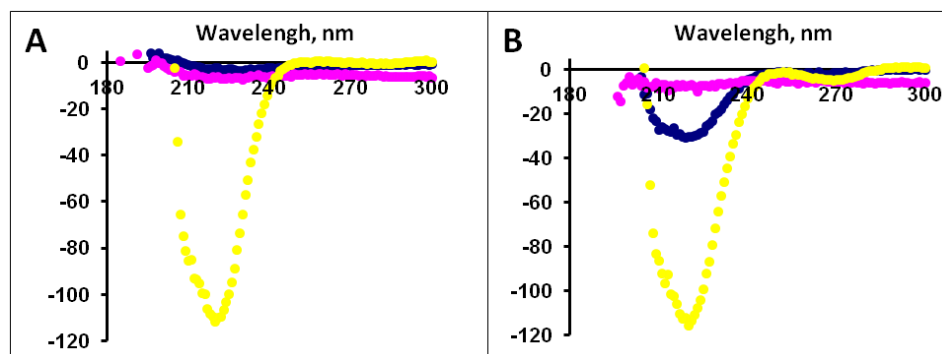
**Figure III-23.** Reactivation of previously inactivated protein. **Rings-** Activity of the enzyme stored at 5°C during the whole experiment. **Rhomb-** Protein was inactivated by incubation at 23°C for 60 hours and then enzyme was stored at 23°C during whole experiment. **Squares-** Protein was inactivated by incubation at 23°C for 60 hours and then enzyme was reactivated by incubation at 5°C during whole experiment. **Triangles-** Protein was inactivated by incubation at 23°C for 60 hours. Membrane-mimicking detergent was added to the enzyme before reactivation by incubation at 5°C during whole experiment.

Quinones are associated with the membrane in the living cells, most of electron transfer processes are going on the membrane surface, membrane mimicking detergent is the activator of WrbA; all these facts support the suggestion that the WrbA function might involve membrane binding. Furthermore, the WrbA tetramer

formed the hydrophobic channel, which can be potentially involved in membrane association.

#### 4.6.2. CD-Experiments.

The series of CD-experiment were done to evaluate the conformational changes of the secondary structure of WrbA under influence of temperature. Figure III-24. demonstrates the results of these experiments.



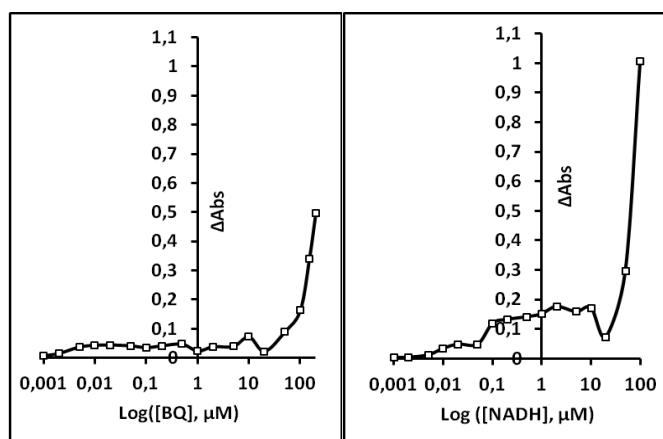
**Figure III-24.** Plots demonstrate CD spectra of apo and holoWrbA under influence of temperature. **A.** CD spectra of apoWrbA (5 $\mu$ M). **B.** CD spectra of holoWrbA (5 $\mu$ M). **Yellow** color – protein was kept at 5°C during the experiments; **Pink** – WrbA was incubated at 23°C for 48 hours; **Blue** – first enzyme was kept at room temperature for 48 hour and then cooled for 10 days.

The conformational changes of the secondary structure were registered for apo and holoWrbA after protein incubation at room temperature for 2 days. Surprisingly, it was observed significant differences on the CD-scans after 10 days incubation of previously inactivated sample (after 2 days at room temperature) at 5°C. Although the peak, which is characterizing the secondary structure, was not returned to initial value, but the dynamics of WrbA reactivation is clearly shown for holoprotein. In addition, the comparison of the apo and holo CD spectra results in the suggestion that the holo form of WrbA is more stable and compact than the apoWrbA, thus the FMN is one of the factors that provides the stability of WrbA. Therefore, the CD-experiments confirm the unusual property of WrbA reactivates by recooling after temperature provoked inactivation.

#### 4.7. SUBSTRATE AFFINITY.

A difference absorbance spectroscopy was used to determine the role of substrate affinity on the presence of double plateau on the Michaelis-Menten plots for WrbA.

These experiments were done only with apo form of WrbA, because of the spectral interference of FMN. It was supposed that if bi-phasic behavior will be presented for apo WrbA that will mean the same behavior for holo form too. Absorbance spectra were obtained for apo-protein with and without presence of NADH and BQ. From the difference spectra the wavelengths 265 nm and 256 nm were chosen for the titration of protein with NADH and BQ respectively (Fig. III-25).

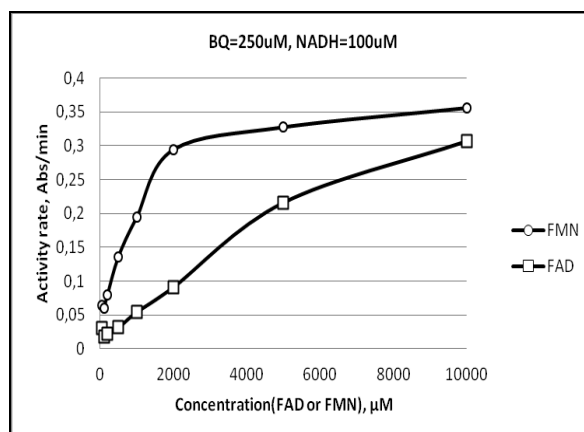


**Figure III-25.** Substrate affinity plots for BQ and NADH. Data are presented in logarithmic scale.

The high absorbance value of NADH and BQ at concentrations higher than 100 μM was the limiting factor for these experiments. Thus only partial binding curves could be obtained using difference spectroscopy. The limiting value of  $K_d$  consistent with the data is  $\geq 10 - 100 \mu\text{M}$ ; thus, the binding affinities for NADH and for BQ to apoWrbA are very weak, as it was expected.

#### **4.8. FMN vs. FAD. ACTIVITY OF THE HOLOWRBA RECONSTITUTED WITH TWO DIFFERENT CO-FACTORS.**

Present experiments were done to establish difference in activity of the WrbA protein depended on the co-factors used for reconstitution the holo protein. Dependence of enzyme activity on the concentration of flavin-cofactors is demonstrated on the figure III-26.



**Figure III-26.** Dependence of the initial activity on the concentration of co-factor in mixture. Squares- FAD was used as a cofactor. Rings- protein was reconstituted with FMN. Activity measurements were done at 5°C.

Activity of WrbA increases with co-factors concentration. WrbA shows higher activity in case of using FMN (natural cofactor), thus the affinity of WrbA to FMN is higher, than to FAD. The most important result of these experiments is the fact that the protein shows the activity not only with FMN but also with FAD cofactor. The most important result of these experiments is the fact that the protein shows the activity not only with FMN but also with FAD cofactor and the difference between activities demonstrated FMN-WrbA and FAD-WrbA is not big. These facts imply new considerations about the structural organization of WrbA molecule, its active site composition etc.

#### 4.9. EXPLANATION OF TWO PLATEAU KINETICS. ALLOSTERIC REGULATION OF WRBA.

Structurally and functionally FMN-dependent WrbA bridges monomeric bacterial FMN-dependent flavodoxins and dimeric eukaryotic FAD-dependent diaphorases. The comparison of the WrbA kinetic properties with kinetics published for DT-diaphorase (Hollander *et al.*, 1975) concludes significant similarities between enzymatic behaviors of these two proteins. Like DT-diaphorase, WrbA demonstrates the unusual two plateau kinetic behavior. The fact of biphasic kinetics of DT-diaphorase has been reported in attempt to fit the experimental data to complex kinetic models, but no molecular explanation has been proposed (Hollander *et al.*, 1975). Literature search directed on founding other examples of enzymes with two-plateau kinetic behavior was performed. Several enzymes with two plateau behavior were found (glyceraldehydes-3-phosphate dehydrogenase (Gelb *et al.*, 1970),

succinate dehydrogenase (Zeijlemaker *et al.*, 1969), glutamate dehydrogenase (LeJohn & Jackson, 1968), cytidine triphosphate synthetase (Levitzki & Koshland, 1969), phosphoenolpyruvate carboxylase (Corwin & Fanning, 1968), pyruvate kinase (Somero, 1969), lactate dehydrogenase (Somero & Hochachka, 1969), acetylcholinesterase (Kato *et al.*, 1972), L-threonine dehydratase (Kagan & Dorozhko, 1973)). Some of them was described as allosteric, some was characterized as izozymes, in sum, it means the presence of multiple forms of the protein in the solution and influence of this on enzyme kinetics.

Kinetic properties WrbA demonstrated under influence of different factors are similar to one DT-diaphorase displayed. Kinetic mechanism of DT-diaphorase is a ping-pong (Hall *et al.*, 1972). Investigation of WrbA kinetic mechanism results in multimeric sites ping-pong. This suggestion also was confirmed by structural analysis of binding site of WrbA based on the crystal structures published by Andrade *et al.*, 2007. The closer analysis of binding chamber demonstrated that although the WrbA active site is large, it is not large enough to bind two substrates (NADH and BQ) simultaneously. Thus, the most probable kinetic mechanism of WrbA is ping-pong one.

Experimental analysis of WrbA enzymatic behavior consistent with hypothesis about dependence of WrbA kinetic properties on the multimeric states of this enzyme in the solution. Existence of dimer-tetramer equilibrium for apoWrbA has been reported by Grandori *et al.*, 1998. AUC experiments for holo protein were carried out and confirmed the dimer-tetramer equilibrium for holo protein, too. It was clearly shown dependence of predominant multimeric WrbA form content on the temperature. AUC results demonstrated that 99.9% of dimers were obtained in the solution (3 $\mu$ M holoWrbA) at 5°C, but the percent of tetramers in the solution was increasing with temperature.

NMR experiments for WrbA premixed with NAD agreed to suggestion of existence several multimeric forms of WrbA in the solution. Comparison of NMR spectra for NAD-WrbA mixture with spectra of NAD alone showed the presence of at least two different forms of enzyme with bound NAD.

All these facts are consistent with WrbA subunit dissociation. It can be an explanation for WrbA biphasic kinetics. On the other hand, enzyme dissociation is one of the crucial indications of allosteric effect by Weber (Ruan & Weber, 1989). The suggestion about the allosteric regulation of WrbA allows a conjunction that the



physiological function of WrbA is more complicated than the quinone detoxication, because of dependence of enzyme kinetics behavior on the concentration of the substrates. In addition, the explanation of two-plateau behavior was used for WrbA could be actual for other enzymes, which demonstrate similar kinetic properties.

## 5. CONCLUSIONS.

Our attempts to crystallize WrbA not with the physiological co-factor FMN, but with FAD, which is used by the eucaryotic oxidoreductases, lead to very surprising results. Despite the fact that crystals were obtained from the drop containing a mixture of WrbA protein with FAD, in the crystal structure was uncovered the FMN instead of FAD. Luckily our crystal structure has a very high resolution of 1.2 Å, which allows a detailed structural interpretation. Interestingly the Met10 close to the phosphate oxygen (2.8 Å) was oxidized whereas Met42 that is located 4 Å away is not oxidized, which hints to the idea that FAD could have been cleaved in a chemical reaction that would have involved the methionine. This would be consistent with the fact that the FMN cofactor geometry showed that the FMN is not a planar and fully oxidized but partially reduced with the FMN isoalloxazine ring having a propeller twist along the length of the ring. Thus as the result our new structure does not only improve the resolution significantly compared to our older holo-structures at 2.0 and 2.6 Å, but also provides an alternative conformation of the active site, as in the older structures FMN was fully oxidized and no methionine oxidation was found.

Spectrophotometric method of kinetic activity measurement was successfully applied to study the kinetic mechanism and kinetic properties of E.coli WrbA. The kinetic features of WrbA were extensively investigated at both low and high concentrations of the substrates under the influence of different physical chemical factors in presence and absence of different modulators.

Interestingly, the WrbA steady-state kinetics demonstrated the presence of unusual intermediary plateau on the Michaelis –Menten plot. Alteration of physical chemical parameters such as pH, temperature and salt presence shows the significant changes on the protein steady-states kinetics. Similar two plateau kinetics and reversible temperature dependence has been reported for the closest structural homolog of WrbA the mammalian DT-diaphorase (Hollander *et al.*, 1975), but to date no molecular explanation has been proposed for that phenomenon. Therefore we designed additional studies to evaluate our hypothesis that a dimer-tetramer might be the underlying reason for the unusual two - plateau kinetics. The original idea came from the well known fact that the WrbA apo form exists in both dimer and tetramer states, so analysis of holoWrbA kinetic properties should allow us to study that these two states have different kinetics and if the equilibrium between them is affected by

temperature, which could potentially explain the presence of an intermediate plateau on the Michaelis-Menten plot.

In the first step we were able to confirm the ping-pong kinetic mechanism based on analysis of kinetic parameters  $K_m$  and  $V_{max}$  at steady state for NADH and BQ at four fixed concentrations of second substrates. Consistent evidence was obtained from product inhibition pattern analysis. Computational study of protein active site structure also supports the ping pong kinetic mechanism of WrbA, as the active site chamber is large, but is not large enough to bind both NADH and BQ at the same time, thus the only way of two substrate binding is in consecutive order, which corresponds to a ping pong kinetic mechanism.

The results obtained from the WrbA limited proteolysis experiments proposed subunit dissociation of WrbA and the existence of two forms of protein in the solution was confirmed by AUC and NMR techniques. Results of AUC experiments not only agreed with the fact of presence dimers and tetramers in the solution, but clearly demonstrated shift of equilibrium to the tetramers formation with temperature. Results obtained in NMR experiments with WrbA in presence  $NAD^+$  provided further evident for this conclusion. At least two different multimeric states of protein were observed in this experiment. Multimeric dissociation is one of factors corresponds to allosteric effects by Weber. Allosteric regulation can be a possible explanation of two-plateau kinetics, as it implies that the protein kinetic activity depends on physiological concentration of its substrates. This explanation could be applied for other proteins with similar kinetic properties such as mammalian DT-diaphorase.

## 6. REFERENCES.

- Akiyama K. T., Selhub J., Rosenberg I. H. (1982) FMN phosphatase and FAD pyrophosphatase in rat intestine brush border: role in intestinal absorption of dietary riboflavin. *J. Nutr.* **112**:263–268.
- Andrade SL, Patridge EV, Ferry JG, Einsle O (2007) Crystal structure of the NADH:quinone oxidoreductase WrbA from *Escherichia coli*. *J Bacteriol* **189**: 9101–9107.
- Bergmans HE, van Die IM, Hoekstra WP. (1981) Transformation in *Escherichia coli*: Stages in the process. *J Bacteriol.* May;146(2):564-70.
- Carey J (2000). A systematic and general proteolytic method for defining structural and functional domains of proteins. *Methods Enzymol* 328: 499-514
- Chappelle, E.W., Picciolo G.L. (1971) Assay of flavin mononucleotide (FMN) and flavin adenine dinucleotide (FAD) using the bacterial luciferase reaction. *Methods Enzymol* 18(B): 381- 385
- Cleland WW (1963) The kinetics of enzyme-catalyzed reactions with two or more substrates or products. I. Nomenclature and rate equations. *Biochim. Biophys. Acta* **67**, 104–137
- Corwin LM, Fanning GR (1968) Studies of parameters affecting the allosteric nature of phosphoenol pyruvate carboxylase of *E.coli*. *J Biol Chem* 243: 3517-25.
- Daher, B. S., E. J. Venancio, S. M. de Freitas, S. N. Bao, P. V. Vianney, R. V. Andrade, A. S. Dantas, C. M. Soares, I. Silva-Pereira, and M. S. Felipe. (2005) The highly expressed yeast gene pby20 from *Paracoccidioides brasiliensis* encodes a flavodoxin-like protein. *Fungal Genet. Biol.* 42:434-443.
- Ducruix, A. & Giege', R. (1999). *Crystallization of Nucleic Acids and Proteins: A Practical Approach*, 2nd ed. Oxford University Press.
- Frishman D, Argos P. (1995). Knowledge-based protein secondary structure assignment. *Proteins* 23(4):566-579

- Gelb WG, Oliver EJ, Brandts JF, Nordin JH (1970) Unusual kinetic transition in honeybee glyceraldehyde phosphate dehydrogenase. *Biochemistry* 9: 3228-3235.
- Grandori R, Khalifah P, Boice JA, Fairman R, Giovanielli K & Carey J (1998) Biochemical characterization of WrbA, founding member of a new family of multimeric flavodoxin-like proteins. *J Biol Chem.* **273**, 20960-20966.)
- Hall JM, Lind C, Golvano MP, Rase B, Ernster L (1972) DT Diaphorase- reaction mechanism and methabolic function. In Structure and Function of Oxidation-Reduction Enzymes (Akeson A., and Ehrenberg, A., eds) Pergamon Oxford 433-443.
- Hollander M, Bartfai T, Gatt S (1975) Studies on the reaction mechanism of DT diaphorase. Intermediary plateau and trough regions in the initial velocity vs substrate concentration curves. *Arch Biochem Biophys* 169: 568-576.
- Hutchinson, E. G. and Thornton, J. M. (1996). PROMOTIF--a program to identify and analyze structural motifs in proteins. *Protein Sci.* 5, 212-220.
- Kabsch W, Sander C (1983). "Dictionary of protein secondary structure: pattern recognition of hydrogen-bonded and geometrical features". *Biopolymers* **22** (12): 2577–637.
- Kagan ZS, Dorozhko AI (1973) pH-dependent intermediate plateaux in the kinetics of the reaction catalyzed by "biosynthetic" L-threonine dehydratase of Escherichia coli K-12. *Biochim Biophys Acta* 302: 110-128.
- Kato G, Tan E, Yung J (1972) Acetylcholinesterase. Kinetic studies on the mechanism of atropine inhibition. *J Biol Chem* 247: 3186-3189.
- Krissinel E. and Henrick K. (2004) Secondary-structure matching (SSM), a new tool for fast protein structure alignment in three dimensions *Acta Cryst.* D60, 2256-2268.
- Kumar, S., and Bansal M. (1996). Structure and sequences characteristics of long helices in globular proteins. *Biophys. J.* 71:1574 –1586.

- Lacour S, Landini P. (2004) SigmaS-dependent gene expression at the onset of stationary phase in *Escherichia coli*: function of sigmaS-dependent genes and identification of their promoter sequences. *J Bacteriol.* 186, 7186-95.
- Laskowski MJ, Dreher KA, Gehring MA, Abel S, Gensler AL, Sussex IM. (2002) FQR1, a novel primary auxin-response gene, encodes a flavin mononucleotide-binding quinone reductase. *Plant Physiol.* 128, 578-90.
- Laskowski RA, Swindells MB. (2011) LigPlot+: multiple ligand-protein interaction diagrams for drug discovery. *J Chem Inf Model.* 51(10):2778-86.
- LeJohn HB, Jackson S (1968) Allosteric interactions of a regulatory nicotinamide adenine dinucleotide-specific glutamate dehydrogenase from *Blastocladiella*. A molecular model for the enzyme. *J Biol Chem* 243: 3447-3457.
- Levitzki A, Koshland DE Jr (1969) Negative cooperativity in regulatory enzymes. *Proc Nat Acad Sci USA* 62: 1121-1128.
- Luo S, & Levine RL. 2009 Methionine in proteins defends against oxidative stress. *FASEB J.* (2):464-72.
- Røhr AK, Hersleth HP, Andersson KK. Tracking flavin conformations in protein crystal structures with Raman spectroscopy and QM/MM calculations. *Angew Chem Int Ed Engl.* 2010 Mar 22;49(13):2324-7.
- Ruan K, Weber G. (1989) Hysteresis and conformational drift of pressure-dissociated glyceraldehydephosphate dehydrogenase. *Biochemistry* 28 (5):2144-2153.
- Sancho, J. (2006). Flavodoxins: sequence, folding, binding, function and beyond. *Cell Mol Life Sci* 63, 855-864.
- Senda T, Senda M, Kimura S, Ishida T (2009) Redox control of protein conformation in flavoproteins. *Antioxid Redox Sign* 11:1741–1766
- Somero GN (1969) Pyruvate kinase variants of the Alaskan king-crab. Evidence for a temperature-dependent interconversion between two forms having distinct and adaptive kinetic properties. *Biochem J* 114: 237-241.

- Somero GN, Hochachka PW (1969) Isoenzymes and short-term temperature compensation in poikilotherms: activation of lactate dehydrogenase isoenzymes by temperature decreases. *Nature (London)* 223: 194-195.
- Stafford WF (1992) Boundary analysis in sedimentation transport experiments- a procedure for obtaining sedimentation coefficient distributions using the time derivative of the concentration profile. *Analytical Biochem.* 203: 295–301
- Stura, EA., Nemerow GR, and Wilson, IA. (1992). Strategies in the crystallization of glycoproteins and protein complexes. *J. Crystal Growth* 122:273-285
- Wolfova J, Kuta Smatanova I, Brynda J, Mesters JR, Lapkouski M et al. (2009) Structural organization of WrbA in apo- and holoprotein crystals. *Biochim Biophys Acta* 1794: 1288-1298.
- Zeijlemaker WP, Dervartanian DV, Veeger C, Slater EC (1969) Studies on succinate dehydrogenase. IV. Kinetics of the overall reaction catalysed by preparations of the purified enzyme. *Biochim Biophys Acta* 178: 213-224.



# Paper I

## **Biphasic Kinetic Behavior of *E. coli* WrbA, an FMN-Dependent NAD(P)H:Quinone Oxidoreductase**

KISHKO, I., HARISH, B., ZAYATS, V., REHA, D., TENNER, B., BERI, D., GUSTAVSSON, T., ETTRICH, R., AND CAREY, J.

*Published in:*

PLoS One. (2012) 7(8): e43902.

Published online 2012 August 29. doi: [10.1371/journal.pone.0043902](https://doi.org/10.1371/journal.pone.0043902)



## **Biphasic kinetic behavior of *E. coli* WrbA an FMN-dependent NAD(P)H:quinone oxidoreductase.**

Kishko, I., Harish, B., Zayats, V., Reha, D., Tenner, B., Beri, D., Gustavsson, T., Ettrich, R., Carey, J.

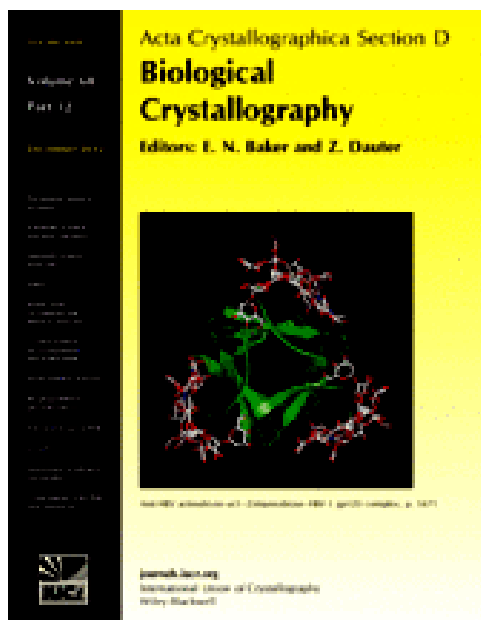
*Published in:*

PLoS One. (2012) 7(8): e43902.

Published online 2012 August 29. doi: 10.1371/journal.pone.0043902

### **Abstract**

The *E. coli* protein WrbA is an FMN-dependent NAD(P)H:quinone oxidoreductase that has been implicated in oxidative defense. Three subunits of the tetrameric enzyme contribute to each of four identical, cavernous active sites that appear to accommodate NAD(P)H or various quinones, but not simultaneously, suggesting an obligate tetramer with a ping-pong mechanism in which NAD departs before oxidized quinone binds. The present work was undertaken to evaluate these suggestions and to characterize the kinetic behavior of WrbA. Steady-state kinetics results reveal that WrbA conforms to a ping-pong mechanism with respect to the constancy of the apparent  $V_{max}$  to  $K_m$  ratio with substrate concentration. However, the competitive/non-competitive patterns of product inhibition, though consistent with the general class of bi-substrate reactions, do not exclude a minor contribution from additional forms of the enzyme. NMR results support the presence of additional enzyme forms. Docking and energy calculations find that electron-transfer-competent binding sites for NADH and benzoquinone present severe steric overlap, consistent with the ping-pong mechanism. Unexpectedly, plots of initial velocity as a function of either NADH or benzoquinone concentration present one or two Michaelis-Menten phases depending on the temperature at which the enzyme is held prior to assay. The effect of temperature is reversible, suggesting an intramolecular conformational process. WrbA shares these and other details of its kinetic behavior with mammalian DT-diaphorase, an FAD-dependent NAD(P)H:quinone oxidoreductase. An extensive literature review reveals several other enzymes with two-plateau kinetic plots, but in no case has a molecular explanation been elucidated. Preliminary sedimentation velocity analysis of WrbA indicates a large shift in size of the multimer with temperature, suggesting that subunit assembly coupled to substrate binding may underlie the two-plateau behavior. An additional aim of this report is to bring under wider attention the apparently widespread phenomenon of two-plateau Michaelis-Menten plots.



## Paper II

### **Crystallization and diffraction analysis of E.coli WrbA holoprotein with 1.2 Å resolution**

KISHKO, I., LAPKOUSKI M., BRYNDA J., KUTY M., CAREY J., KUTA  
SMATANOVA I., ETTRICH, R..

*prepared for submission to ACTA CRYST D*

---

## **Crystallization and diffraction analysis of E.coli WrbA holoprotein with 1.2 Å resolution.**

Kishko I, Lapkouski M, Brynda J, Kutý M, Carey J, Kuta Smatanova I, Ettrich R.

*prepared for submission to ACTA CRYST D*

### **Abstract**

The 21kDa flavoprotein WrbA from *Escherichia coli* was identified as a founding member of a new family of multimeric flavodoxin-like proteins that are implicated in cell protection against oxidative stress. WrbA hereby bridges bacterial flavodoxins and eukaryotic NAD(P)H: quinone oxidoreductase with its three-dimensional structure clearly revealing a close relationship to mammalian NAD(P)H: quinone oxidoreductase, Nqo1 (Carey et al., 2007). A closer analysis of apo and holo crystal structures with the physiological cofactor (FMN), together with flavodoxin structures, rationalizes functional similarities and differences of the WrbAs relative to flavodoxins, suggesting that WrbAs are not remote and unusual branch of the flavodoxin family as previously thought but rather a central member with unifying structural features (Wolfova et al., 2009). Here, we report the crystallization and diffraction analysis of holoprotein WrbA from *E. Coli* at high resolution. FAD was used for reconstitution of holoenzyme, but, surprisingly, in the final X-ray structure we find FMN in the binding pocket, indicating that FAD hydrolyzed to FMN during the crystallization experiment.